ENTANGLEMENT: QUANTIFICATION VIA UNCERTAINTIES AND SEARCH AMONG ULTRACOLD BOSONS IN OPTICAL LATTICES

A DISSERTATION SUBMITTED TO
THE DEPARTMENT OF PHYSICS
AND THE INSTITUTE OF ENGINEERING AND SCIENCE
OF BILKENT UNIVERSITY
IN PARTIAL FULFILLMENT OF THE REQUIREMENTS
FOR THE DEGREE OF
DOCTOR OF PHILOSOPHY

By
Barış Öztop
September, 2009

I certify that I have read this thesis and that in my opinion it is fully adequate, in scope and in quality, as a dissertation for the degree of Doctor of Philosophy.

Assoc. Prof. Dr. Mehmet Özgür Oktel (Advisor)

I certify that I have read this thesis and that in my opinion it is fully adequate, in scope and in quality, as a dissertation for the degree of Doctor of Philosophy.

Assoc. Dr. Prof. Oğuz Gülseren

I certify that I have read this thesis and that in my opinion it is fully adequate, in scope and in quality, as a dissertation for the degree of Doctor of Philosophy.

Assoc. Prof. Dr. Ceyhun Bulutay

I certify that I have read this thesis and that in my opinion it is fully adequate, in scope and in quality, as a dissertation for the degree of Doctor of Philosophy.

Assoc. Prof. Dr. Ergün Yalçın

I certify that I have read this thesis and that in my opinion it is fully adequate, in scope and in quality, as a dissertation for the degree of Doctor of Philosophy.

Assoc. Prof. Dr. Bayram Tekin

Approved for the Institute of Engineering and Science:

Prof. Dr. Mehmet Baray
Director of Institute of Engineering and Science

ABSTRACT

Entanglement: Quantification via Uncertainties and Search Among Ultracold Bosons in Optical Lattices

Barış Öztop
Ph.D. in Physics
Supervisor: Assoc. Prof. Mehmet Özgür Oktel
September, 2009

In the first part of the Thesis, the known measures of entanglement for finite dimensional systems are reviewed. Both the simplest case of pure states that belong to bipartite systems and more general case of mixed states are discussed. The multipartite extensions are also mentioned. In addition to the already existing ones, we propose a new measure of entanglement for pure states of bipartite systems. It is based on the dynamical symmetry group approach to quantum systems. The new measure is given in terms of the total uncertainty of basic observables for the corresponding state. Unlike conventional measures concurrence and 3-tangle, which measure the amount of entanglement of different groups of correlated parties, our measure gives the total amount of multipartite entanglement in a specific state.

In the second part of the Thesis, the trapping of bosonic atoms in optical lattices is reviewed. The band structure together with Bloch functions and Wannier basis are discussed for this system. In relation with that, the corresponding Bose-Hubbard model and by the use of this model, the resulting superfluid to Mott-insulator quantum phase transition is summarized. In this regard, the Bose-Hubbard Hamiltonian of a specific system, namely ultracold spin-1 atoms with coupled ground states in an optical lattice is considered. For this system we examine particle entanglement, that is characterized by pseudo-spin squeezing both for the superfluid and Mott-insulator phases in the case of ferromagnetic and antiferromagnetic interactions. The role of a small but nonzero angle between the polarization vectors of counterpropagating lasers forming the optical lattice on quantum correlations is investigated as well.

Keywords: Entanglement, quantum information, optical lattices, spin squeezing, quantum correlations, dynamic symmetry group, spinor Bose-Einstein condensates.

ÖZET

Dolanıklık: Belirsizlikler Aracılığıyla Nicelenmesi ve Optik Örgülerdeki Ultrasoğuk Bozonlar İçin Araştırılması

Barış Öztop
Fizik, Doktora
Tez Yöneticisi: Doç. Dr. Mehmet Özgür Oktel
Eylül, 2009

Tezin birinci kısmında sonlu sistemler için bilinen belli başlı kuvantum dolanıklık ölçütleri gözden geçiriliyor. İki parçalı sistemlerin saf durumları ve daha genel bir şekilde karışmış durumları ele alınıyor. Dolanıklık ölçütlerinin çok parçalı sistemlere genişletilmesinden de bahsediliyor. Var olan ölçütlere ek olarak iki parçalı sistemlerin saf durumları için yeni bir dolanıklık ölçütü öneriliyor. Bu ölçüt tanımlanırken, kuvantum sistemleri için dinamik simetri grubu yaklaşımı baz alınmaktadır. Bu yeni ölçüt, temel gözlenebilirlerdeki kuvantum dalgalanmaları cinsinden verilmektedir. İki ve üç parçalı sistemlerdeki geleneksel dolanıklık ölçütlerinin aksine bu ölçüt, herhangi bir sistemdeki çok parçalı toplam dolanıklık miktarını belirlemektedir.

Tezin ikinci kısmında öncelikle bozonik atomların optik örgülerde tuzaklanması gözden geçiriliyor. Bu sistem için tanımlanabilen bant yapısı ve bunlarla beraber Bloch ile Wannier fonksiyonları ele alınıyor. Bu sistem için yazılan Bose-Hubbard modeli ve bu modelden yola çıkarak incelenebilen süperakışkan–Mott yalıtkanı arasındaki faz geçişi özetlenmektedir. Bu bağlamda, özel bir sistem olan optik örgülere yüklenmiş, taban durumları eşleşmiş spin-1 atomların Bose-Hubbard Hamiltonyeni inceleniyor. Bu sistem için yalancı spin sıkıştırmasını kullanarak süperakışkan ve Mott yalıtkanı fazlarında feromanyetik ve antiferomanyetik etkileşimler için parçacık dolanıklığı gözden geçiriliyor. Optik örgüleri oluşturan karşılıklı yayılan lazer ışınlarının polarizasyon vektörleri arasındaki açının küçük fakat sıfırdan farklı olduğu durumlardaki kuvantum korelasyonları da bu tez içinde incelenmiştir.

Anahtar Sözcükler: Dolanıklık, kuvantum bilgi teknolojisi, optik örgüler, spin sıkıştırması, kuvantum korelasyonları, dinamik simetri grubu, spinör Bose-Einstein yoğuşukları.

“...bu tezde anlatılanların
gerçek kişilerle ve olaylarla
hiçbir ilişkisi yoktur.
onları ben,
büyük bir aynanın
içinde gördüm.
üstelik ayna dumanlıydı
ve olmayan bir şehirde
geziniyordu...”
Attila İlhan ve Alexander S. Shumovsky’nin anısına ithaf edilmiştir...

Acknowledgement

I would like to express my deepest gratitude to Prof. Alexander S. Shumovsky, whom may be too far away right now to hear, for somehow getting involved in my academic life even for the short term of two years and many thanks for his beautiful and legendary stories of science and history. I would like to thank Prof. M. Özgür Oktel and Prof. Özgür E. Müstecaplıoğlu from whom I have learned a lot, due to their supervision, suggestions, and support during my research, I owe them more than they can imagine.

I am also indebted to Prof. Alexander A. Klyachko for his invaluable contributions to my knowledge and for his collaboration.

I would like to thank my friends R. Onur Umucalılar, Barış Yalçın, A. Levent Subaşı, Kerim Savran, who are actually more than just being friends.

My last but of course not least thanks goes to my family, my mother, father, bro and my lovely little sweetheart Beliz Güney, for their endless support.

Contents

List of Figures

List of Tables

Chapter 1

A measure of entanglement

1.1 Introduction

It would be a hard work, for anybody, to search for a work that at least talks about entanglement and does not contain a reference to the famous EPR article [1]. The same is not true for Schrödinger's work [2] despite the fact that it is the first known place where the word *entanglement* is used. In the EPR article [1], it was used to show that quantum mechanics could not be a complete theory (i.e. locality and physical reality). As a result of the presented paradox, 'spooky action at a distance', *hidden variable* theories era was opened. Many years later John Bell proved that for any local hidden variable theory, existing correlations are upper bounded and they should obey a set of inequalities [3]. Later on, experiments showed that quantum mechanics violates those inequalities [4]. And now, entanglement is known to be one of the clear distinctions between classical and quantum physics together with the quantum superposition.

Since its first appearance in 1935, until mid 1990's, entanglement has been recognized as a curious phenomenon of no practical importance. But then with the birth and advance of quantum information science, it has started to be seen as a resource for quantum information processing and communications. Some of the applications of this indispensable resource are quantum cryptography [5], dense coding [6], teleportation of a quantum state [7] and quantum algorithms that are faster than their classical counterparts [8, 9, 10, 11].

In quantum information science, entanglement can be used to perform many tasks which would be impossible without it and also to improve the performance of other tasks. Entanglement is consumed to execute most of them, such that it is usually traded for something else. This is why entanglement is taken as a resource like energy. Since entanglement is now seen as a resource for quantum information and computation purposes, it is important

to quantify the entanglement in quantum states. This approach has become a large field of research following the first works on the subject [12, 13, 14, 15]. In the view of taking entanglement as a resource, the main question is when we are given a quantum state and a task that consumes entanglement, how much of it can be achieved? The answer is not clear since a given entangled state can achieve a certain task better than another entangled state, however the situation could be different for another task. There are many ways to quantify entanglement resource for a quantum state for this reason.

In the entanglement quantification industry, most of the work is done on bipartite systems where there are two parts of the whole system and the main focus is on systems where both parts have finite dimensional Hilbert spaces. In this first part of the Thesis, apart from the already existing ones, we give an alternative measure for bipartite entanglement of namely pure states, where the system can be described with a single state vector in the composite Hilbert space. In this task, our motivation is to *quantify* the degree *quantumness* of the state by investigating uncertainties (fluctuations) in the observables of the system. In this regard, the first part of the Thesis is organized as follows.

In the beginning, we introduce the basic constituents of the quantum information science, such as the qubit, pure states, mixed states etc. Then we briefly summarize some of the existing bipartite entanglement measures and give a list of multipartite entanglement measures.

In the third chapter, we discuss the dynamic symmetry group approach to quantum systems [16, 17, 18, 19] and introduce our entanglement measure according to this systematics. By the end of this chapter, we consider the generalization of this measure to multipartite systems and mixed states.

Finally, in the seventh chapter, we summarize the obtained results and conclude together with the results of the second part of the Thesis.

Chapter 2

Basic notions and existing measures of entanglement

In this chapter, some necessary basic concepts of the quantum information theory is introduced. Later on, some of the existing ways of quantifying entanglement are briefly reviewed.

2.1 The qubit

A bit is the most basic unit of classical informatics. It takes two values, either 0 or 1, TRUE or FALSE. All of the processes in conventional computation take place by manipulating a series of such bits (actually can be a huge number of them) with predefined operations. The quantum counterpart of this entity is called a *qubit*. It is defined as a two-level quantum system (simplest nontrivial), *i.e.* a vector in two-dimensional complex Hilbert space $\mathcal{H}_2$ with basis $\{|0\rangle, |1\rangle\}$. One of the most common physical realization of a qubit is a spin-1/2 system. Throughout this Thesis, I will the use spin of these systems to illustrate entanglement. If not mentioned otherwise, $|0\rangle$, $|+\rangle$, $|\uparrow\rangle$ and $|1\rangle$, $|-\rangle$, $|\downarrow\rangle$ will be used interchangeably denoting spin up and spin down (quantized along z-axis) respectively. These basis states can be written in the matrix representation

$$|\uparrow\rangle = \begin{pmatrix} 1 \\ 0 \end{pmatrix}, |\downarrow\rangle = \begin{pmatrix} 0 \\ 1 \end{pmatrix} \tag{2.1}$$

In these settings, a generic state of qubit can be written as

$$|\psi\rangle = \alpha|0\rangle + \beta|1\rangle \tag{2.2}$$

with the proper normalization $|\alpha|^2 + |\beta|^2$. It is seen immediately that, as opposed to the

classical bit, a qubit can take not only the values 0 and 1, but it can be in a continuum of superpositions of between the states $|0\rangle$ and $|1\rangle$ with probability amplitude given by the two parameters α and β. And this fact makes qubit a much richer structure for informatics. But still only one bit of information can be read from a single qubit due to the change of the state after a measurement, and we know the resulting (collapsed) state by the measurement. But then, no more information about the original state can be retrieved.

2.2 Bipartite systems, pure and mixed states

After introducing the simplest nontrivial quantum system, now we can turn to simplest composite quantum systems which consist of two qubits, say A and B. Thanks to superposition (or linearity) of quantum mechanics, for two qubits, we have tensor product of two-dimensional Hilbert spaces $\mathcal{H} = \mathcal{H}_2 \otimes \mathcal{H}_2$. In general, we can have n and m dimensional subsystems and the composite Hilbert space is $\mathcal{H}_m \otimes \mathcal{H}_n$. So the most general state that lives in this space can be written as

$$|\Psi\rangle = \sum_{ij} a_{ij} |\psi_i\rangle_A \otimes |\phi_j\rangle_B \tag{2.3}$$

where $\sum_{ij} |a_{ij}|^2 = 1$ and $\{|\psi_i\rangle\}, \{|\phi_i\rangle\}$ are orthonormal bases for subsystems A and B.

One of the basic axioms of the quantum mechanics tells us that representation of quantum system as a state vector in a Hilbert space is a complete description of its physical properties. In some occasions, however, it is not possible to represent the state of the system with a single vector, in cases that the state is not known precisely or the focus is on a subsystem of a larger system. For example this is the situation when we have an open quantum system, *i.e.* the system of interest is interacting with a larger one called environment. In this case, the subsystem cannot be represented by its own single state vector, but with a density operator (or matrix). For a pure state ψ, the density matrix can be defined as

$$\rho = |\psi\rangle\langle\psi| \tag{2.4}$$

with the normalization $\langle\psi|\psi\rangle = \mathrm{tr}\rho = 1$. Expectation value of any operator $\mathcal{O}$ acting in the space of the system becomes

$$\langle\mathcal{O}\rangle = \mathrm{tr}(\rho\mathcal{O}). \tag{2.5}$$

If it is known that the system is prepared with some statistical (classical) probability p_k in various states $|\psi_k\rangle$, then the density matrix becomes

$$\rho = \sum_k p_k |\psi_k\rangle\langle\psi_k| \tag{2.6}$$

where $\sum_k p_k = 1$ and in this case the expectation value of an operator is

$$\langle\mathcal{O}\rangle = \sum_k p_k \langle\psi_k|\mathcal{O}|\psi_k\rangle = \mathrm{tr}(\rho\mathcal{O}). \tag{2.7}$$

So, by definition, a state that may be represented by a unit vector is called a *pure state*. There are also states which are convex combinations of pure states as in Eq. (2.6), and they are called *mixed states*. For a pure state, we have maximal knowledge of the state. Whereas in the case of mixed states, when a state from an ensemble is described by its density operator, we discard the information about which ensemble the mixed state was made from. This is because different ensembles can have the same density operator and they are experimentally indistinguishable. For example if have a state $|0\rangle$ or $|1\rangle$, each with probability 1/2, then the density operator becomes $\rho = \frac{1}{2}(|0\rangle\langle 0| + |1\rangle\langle 1|)$. But the same density operator can be formed by mixing $\frac{1}{\sqrt{2}}(|0\rangle + |1\rangle)$ and $\frac{1}{\sqrt{2}}(|0\rangle - |1\rangle)$ with the same probabilities. Again the same density operator can be made by three states, $|\psi_1\rangle = |0\rangle$, $|\psi_2\rangle = \frac{1}{\sqrt{2}}(|0\rangle + |1\rangle)$ and $|\psi_3\rangle = \frac{1}{2}|0\rangle - \frac{\sqrt{3}}{2}|1\rangle$ with probabilities $p_1 = \frac{1}{2} - \frac{\sqrt{3}}{6}$, $p_2 = \frac{\sqrt{3}}{2} - \frac{1}{2}$ and $p_3 = 1 - \frac{\sqrt{3}}{3}$.

Some of the properties of density matrices are

- they are Hermitian, $\rho = \rho^\dagger$,
- they are positive semi-definite, for any vector ψ, $\langle\psi|\rho|\psi\rangle \geq 0$,
- $\mathrm{tr}\rho = 1$ and $\mathrm{tr}\rho^2 \leq 1$, equality holds for pure states.

Consider a bipartite composite system with subsystems A and B. In general, ignoring some degrees of freedom in such a composite system is done by tracing out the relevant degrees of freedom from the density operator, and this operation is called taking the *partial trace*. Assume that the orthonormal bases for subsystems A and B are $\{|a_i\rangle\}$ and $\{|b_k\rangle\}$ respectively. Any bipartite state of this composite system can be written as

$$\rho = \sum_{ijk\ell} c_{ijk\ell}|a_i\rangle\langle a_j| \otimes |b_k\rangle\langle b_\ell|. \tag{2.8}$$

The partial trace over the degrees of freedom of system B of this system is

$$\begin{aligned} \mathrm{tr_B}(\rho) &\equiv \sum_{ijk\ell} c_{ijk\ell}|a_i\rangle\langle a_j| \otimes \mathrm{tr}(|\mathrm{b_k}\rangle\langle \mathrm{b_\ell}|) \\ &= \sum_{ijk\ell} c_{ijk\ell}\langle b_\ell|b_k\rangle|a_i\rangle\langle a_j| \\ &= \sum_{ij} C_{ij}|a_i\rangle\langle a_j| \end{aligned} \tag{2.9}$$

where $C_{ij} = \sum_{k\ell} c_{ijk\ell}\langle b_\ell|b_k\rangle$. Here $\mathrm{tr}_B(\rho)$ is called *reduced density matrix*.

2.3 Bipartite entangled states

Consider the composite bipartite system of the previous section with parts labelled by A and B. Assume that these parts own two well separated observers, surprisingly named as Alice

and Bob. Generic states of each system that live in $\mathcal{H}_A$ and $\mathcal{H}_B$ respectively can be written as

$$|\psi\rangle_A = \sum_i a_i|\psi_i\rangle_A \quad |\phi\rangle_B = \sum_i b_i|\phi_i\rangle_B \tag{2.10}$$

with normalizations $\sum_i |a_i|^2 = \sum_i |b_i|^2 = 1$. Then the composite state of the two subsystems is

$$|\Psi_{\text{prod}}\rangle = |\psi\rangle_A \otimes |\phi\rangle_B \tag{2.11}$$

and such a state is called a *product* or *separable* state since it can be written as a tensor product of its constituents. But now if we let the two systems interact with each other, any superposition of separable states is realizable and we get the general composite state in Eq. (2.3). By definition, any state that is not separable is called an *entangled* state.

In the simplest case of two qubits, the most general state in composite Hilbert space $\mathcal{H}_2 \otimes \mathcal{H}_2$ is

$$|\psi\rangle = \psi_{00}|00\rangle + \psi_{11}|11\rangle + \psi_{01}|01\rangle + \psi_{10}|10\rangle \tag{2.12}$$

where $|ij\rangle$ is used as the shorthand notation of $|i\rangle \otimes |j\rangle$. Here, for example, if $\psi_{01} = \psi_{00} = 0$ then $|\psi = \psi_{11}|11\rangle + \psi_{10}|10\rangle$ which can be shown to be separable as $|\psi\rangle = |1\rangle\otimes(\psi_{10}|0\rangle + \psi_{11}|1\rangle)$. On the contrary, if $\psi_{00} = \psi_{11} = 0$, then $|\psi\rangle = \psi_{01}|01\rangle + \psi_{10}|10\rangle$ which cannot be written as a tensor product and so that it is an entangled state. Since the complex coefficients ψ_{ij} are only limited by the normalization condition, there are an infinite number of entangled states for the system of two qubits. For a bipartite system of qubits, four entangled states play a special role, which are first the singlet state

$$|\Psi^-\rangle \equiv \frac{1}{\sqrt{2}}(|01\rangle - |10\rangle), \tag{2.13}$$

and three triplet states

$$\begin{aligned} |\Psi^+\rangle &\equiv \frac{1}{\sqrt{2}}(|01\rangle + |10\rangle), \\ |\Phi^\pm\rangle &\equiv \frac{1}{\sqrt{2}}(|00\rangle \pm |11\rangle). \end{aligned} \tag{2.14}$$

These four states are called Bell states or EPR pairs and together they form an orthonormal basis for the composite Hilbert space $\mathcal{H}_2 \otimes \mathcal{H}_2$, which is called the Bell basis. All of these four states are *maximally entangled* and can be converted to each other by applying unitary transformations locally on any one of the subsystems.

When it comes to define separability for mixed states, the situation is a bit different from the pure states. In Section 2.2 it was shown that there different ensemble realizations of any mixed state, meaning different convex combinations of pure states. For example the mixed state $\rho = \frac{1}{2}|00\rangle\langle 00| + \frac{1}{2}|11\rangle\langle 11|$ can be written also as $\frac{1}{2}|\Phi^+\rangle\langle\Phi^+| + \frac{1}{2}|\Phi^-\rangle\langle\Phi^-|$. So the first realization is an ensemble of product states and the second one is ensemble of maximally entangled states. A mixed state is defined as separable if and only if it can be realized as

convex combination of product states such that

$$\rho_{\text{sep}} = \sum_i p_i \rho_i^{(A)} \otimes \rho_i^{(B)} \tag{2.15}$$

where p_i's form a probability distribution with $\sum_i p_i = 1$. In other words, any separable mixed state can be written as a mixture of pure product states such as

$$\rho_{\text{sep}} = \sum_{ij} p_{ij} |\psi_i^{(A)}\rangle\langle\psi_i^{(A)}| \otimes |\psi_j^{(B)}\rangle\langle\psi_j^{(B)}|. \tag{2.16}$$

And the above example tells us that, a convex combination of separable states is always separable whereas a mixture of entangled states need not to be entangled.

2.4 Generalized measurements and LOCC

Before we move to summarize some of the widely used entanglement measures, it is the right place to discuss the properties of entangled states and for this purpose we introduce generalized measurements and LOCC.

In introductory quantum mechanics courses, the concept of measurements are given in the projective measurement formalism, where measurements are represented by Hermitian operators and the result of the measurement is an eigenvalue of the observable. After the measurement, the new state of the system is the corresponding eigenstate (in the case of no degeneracy) and the probability of that outcome is square of the absolute value of the expansion coefficient when the initial state is expanded in the eigenspace.

Measurements can be described in a more general way [20]. Let us denote a measurement operator by A_i where i is the index that denotes a possible measurement result. When the system is described by the density operator ρ, the probability of finding measurement result i is $p_i = \text{tr}(\text{A}_\text{i}\rho\text{A}_\text{i}^\dagger)$ and the state of the system described by a density operator after obtaining measurement result i is

$$\rho' = \frac{A_i \rho A_i^\dagger}{\text{tr}(\text{A}_\text{i}\rho\text{A}_\text{i}^\dagger)}. \tag{2.17}$$

Measurement operators $\{A_i\}$ satisfy the completeness relation $\sum_i A_i^\dagger A_i = I$, which follows from the fact that probabilities sum to one. Projective measurement formalism is a special case of generalized measurements. The Hermitian operator $\mathcal{O}$, that is the observable, has the spectral decomposition

$$\mathcal{O} = \sum_i \lambda_i |u_i\rangle\langle u_i| \tag{2.18}$$

where $\{u_i\}$ are the eigenvectors and $\{\lambda_i\}$ are the corresponding eigenvalues of the observable. By taking $A_i = |u_i\rangle\langle u_i|$, the completeness relation is satisfied.

The general measurement scheme includes all possible operations that can be performed on a quantum system. Unitary transformations can be seen as special cases of single-outcome

measurements and so that the measurement operators have to be unitary to satisfy the completeness relation.

For composite quantum systems, either bipartite or multipartite, if the subsystems can be separated or well isolated from each other, then only local operations, acting on each subsystem, can be performed. So the global operators of the composite system can be written as $\mathcal{O} = \mathcal{O}_A \otimes \mathcal{O}_B \otimes \ldots$. Also in general, the parties (subsystems) are allowed to communicate classically such that they are free to perform different operations depending on the measurement results of the other parties. This combined set of operations are called *Local Operations and Classical Communication* (LOCC) and they are very special and important for quantum information purposes, especially for investigating entanglement. This importance comes from the fact that entanglement is usually defined as the *quantum correlations* present between the parties of a composite quantum system. This definition naturally leads to the question of differentiating quantum correlations form the classical counterparts. Even tough this crucial question is still open to debates, in quantum information settings and purposes, classical correlations are simply defined as those that can be generated by LOCC operations. So that entanglement is seen as the type of correlations that cannot be created by LOCC alone.

2.5 Properties of entangled states

In the case of having LOCC operations as the allowed class of operations for the composite systems, before mentioning the ways to quantify entanglement, we can discuss some basic properties of entangled states [21].

- *There is no entanglement in separable states.* We can generalize the separability definition of bipartite systems in Eq. (2.15) to multipartite systems. If $\rho_{ABC\ldots}$ is state of composite system of parties A, B, C, ..., then it is separable if

$$\rho_{ABC\ldots} = \sum_i p_i \rho_A^i \otimes \rho_B^i \otimes \rho_C^i \otimes \ldots . \tag{2.19}$$

  It can be shown that these separable states can trivially be created by LOCC operations [21] and so that all correlations present in these states can be described classically [22]. Thus, separable states contain no entanglement.

- *All nonseparable states are entangled.* It is possible to show that a quantum state may be generated perfectly (with probability 1) by using LOCC if and only if it is separable [21]. And also all nonseparable states can be used to perform some tasks better than by LOCC operations alone.

- *The amount of entanglement present in a state cannot be increased by LOCC operations.* Since the LOCC operations can only create separable (entangled) states, it is

obvious that LOCC cannot create entanglement form an unentangled state. In addition to this, it was shown that LOCC operations cannot increase the usefulness of quantum states in terms of performing certain tasks [14, 23, 24, 25].

- *Amount of entanglement in quantum state does not change under Local Unitary operations.* This property follows from the previous one such that if entanglement cannot be increased by local unitary operations, and since the unitary operations can be inverted by unitary operations, then entanglement remains same under Local Unitary operations.

- *There are maximally entangled states.* At least in bipartite systems with d-dimensional subsystems, there exist maximally entangled states that are more entangled than all other states. For such systems, pure states that are connected to

$$|\psi_{max}\rangle = \frac{|00\rangle + |11\rangle + \ldots + |(d-1)(d-1)\rangle}{\sqrt{d}} \tag{2.20}$$

with local unitary transformations turn out to be maximally entangled. It can also be shown that any pure or mixed state in this system with Hilbert space $\mathcal{H}_n \otimes \mathcal{H}_n$ can be prepared with certainty from the maximally entangled states by using only LOCC operations.

2.6 Review of some widely used bipartite entanglement measures

In this section, we will briefly review some of the most widely used entanglement measures in the literature. Some useful references are mentioned later on for further considerations of these measures.

There are a few axioms that were accepted widely over the years which any bipartite measure of entanglement should satisfy. These summarize the properties that a good measure of entanglement should possess. So a short list of postulates for entanglement measures, some of which are not satisfied by all proposed quantities is the following.

- An entanglement measure is a functional

$$E : \mathcal{D}(\mathcal{H}) \to \mathbb{R}^+ \tag{2.21}$$

which maps a density operator (quantum state) of the bipartite (in general multipartite) quantum system to a nonnegative real number, in general between 0 an 1. Here $\rho \in \mathcal{D}(\mathcal{H})$, $\mathcal{D}(\mathcal{H})$ is the set of density operators in Hilbert space $\mathcal{H} = \mathcal{H}_A \otimes \mathcal{H}_B$.

- If the state ρ is separable, then $E(\rho) = 0$.

- Under LOCC operations, the measure E should not increase. Mathematically

$$E(\rho) \geq \sum_i p_i E(\rho') \tag{2.22}$$

  where $\rho' = \frac{A_i \rho A_i^\dagger}{\mathrm{tr}(A_i \rho A_i^\dagger)}$ is the transformed state.

- For pure states $\rho = |\psi\rangle\langle\psi|$, the measure should reduce to the entropy of entanglement, which we discuss in the next section.

Any function E that satisfies the first three of the above conditions is called and *entanglement monotone*. Before we talk about the general case of mixed states, we discuss some measures for pure states.

2.6.1 Pure states

The investigation of entanglement present in pure states, in general, makes use of the fact that pure states do not contain any classical correlations. So any correlation present in a pure state, should be of quantum nature.

2.6.1.1 von Neumann entropy

In quantum mechanics, probability distributions are given by density operators. The entropy of a quantum probability distribution (or a density operator) is given by the von Neumann entropy, which is [26]

$$S_{vN}(\rho) \equiv -\mathrm{tr}(\rho \log_2 \rho). \tag{2.23}$$

In terms of the spectrum (eigenvalues λ_i) of density matrix, it can be written as

$$S_{vN}(\rho) = -\sum_i (\lambda_i \log_2 \lambda_i). \tag{2.24}$$

This entropy measure tells us how much information is extracted after a measurement or equivalently the amount of uncertainty about the measurement before we learn its value. In this sense, it is a measure of lack of knowledge about a system. For example, if the system is in a definite (pure) state (e.g. $\rho = |\psi\rangle\langle\psi|$), then $S_{vN} = 0$. On the other hand, if we know nothing about the system ($\rho = I/n$, n being the dimension of the Hilbert space), in other words if it is likely to find the system in any one of the possible states (completely random, or mixed), then S_{vN} is maximum.

Now we consider a bipartite system (A and B) and want to see what happens if we do the measurement only on one of the subsystems. For this purpose, we trace over the degrees of freedom of only one subsystem and calculate the von Neumann entropy of the reduced state. If the overall state is a separable one, the result is zero for both of reduced

matrices. For example, if the we have a bipartite system of qubits, and the state we consider is $|\psi\rangle = |00\rangle$, then $\rho = |00\rangle\langle 00|$. The reduced density matrix for subsystem A becomes $\rho_A = \mathrm{tr_B}(\rho) = |0\rangle\langle 0|$. Actually $\rho_B = \rho_A$ in this case. If we calculate the von Neumann entropy, $S_{vN}(\rho_A) = S_{vN}(\rho_B) = 0$. As we discussed previously, this result shows that there is no uncertainty in the system associated with the measurement of only one of the subsystems. Or equivalently, we do not reveal any information of the total system by doing a measurement only on one subsystem. So we can conclude that the subsystems are uncorrelated. In contrast to the separable case, if the state is inseparable (entangled), then the von Neumann entropy of the reduced states are finite. And it becomes maximum when the reduced state is completely mixed one. If we repeat the above calculation for a maximally entangled state like singlet Bell state $|\Phi^+\rangle$, then the reduced states become $\rho_A = \rho_B = I/2$ and $S_{vN}(\rho_A) = S_{vN}(\rho_B) = \log 2 = 1$. This time we have maximum uncertainty about the composite system when we do measurement on one of the subsystems. We should note here that for a pure state of a bipartite system, Schmidt decomposition [20] tells us the nonzero eigenvalues of the reduced density matrices ρ_A and ρ_B are same. By the use of Eq. (2.24), we immediately get $S_{vN}(\rho_A) = S_{vN}(\rho_B)$ for any pure state of bipartite systems. The reduced von Neumann entropy in Eq. (2.23) is also called the *entropy of entanglement* and usually labelled by E_E.

2.6.1.2 Entanglement cost and distillable entanglement

The discussions in this section mostly uses the fact given Section (2.5) that all pure states of a bipartite system can be created from maximally entangled states by only using LOCC operations. Two measures that are summarized in this section are defined in the so called asymptotic regime, meaning instead of asking whether for a single pair of particles the initial state $|\psi\rangle$ may be transformed to a final state $|\phi\rangle$ by LOCC operations, the question is whether for some large integers m and n, the transformation $|\psi\rangle^{\otimes n} \rightarrow |\phi\rangle^{\otimes m}$ can be implemented. For the purpose defining these two entanglement measures, in the limit $n \rightarrow \infty$, the transformation rate $r = m/n$ is fixed and this largest ratio that the transformation can be achieved gives the relative entanglement content of these two states.

Entanglement cost (E_C). For a given state $|\psi\rangle$, this measure calculates the value of the maximal possible rate r, at which blocks of maximally entangled states can be converted into output states that approximate many copies of $|\psi\rangle$, such that the approximations become vanishingly small in the limit of large block sizes [21]. In other words, for the given pure bipartite state $|\psi\rangle$, $E_C(|\psi\rangle)$ is the asymptotic number of maximally entangled states required to *locally* prepare a system in state $|\psi\rangle$ [15].

Distillable entanglement (E_D). One can ask about the reverse process of entanglement cost; what is the rate that the maximally entangled state can be obtained from input states of $|\psi\rangle$? In the quantum information community, this process is known as entanglement

distillation or entanglement concentration. The efficiency in the asymptotic regime is the distillable entanglement. The alternative definition is the asymptotic number of maximally entangled states that can be prepared from a system in state $|\psi\rangle$ by local operations [15].

In the asymptotic versions, both entanglement cost and distillable entanglement were shown to be equal to the entropy of entanglement [14]. For example, if the two states $|\psi_1\rangle$ and $|\psi_2\rangle$ have equal entropy of entanglement, then they can be converted to each other with efficiency approaching one for $n \to \infty$. In fact there is a uniqueness theorem for entanglement measures of pure states telling that if a measure of entanglement satisfies certain criteria, then it should be equal to the entropy of entanglement [27, 28, 29, 30].

2.6.2 Mixed states

As opposed to the case of pure states, there is no unique way to quantify entanglement for mixed states. This is because of the fact that, in the asymptotic limit, any pure state can be converted to any other one by LOCC regardless of the amount of entanglement in either. However for mixed states, there some that cannot be converted into another.

In this section we first consider the generalizations of pure state measures to the mixed state case. Later on we summarize some other measures.

2.6.2.1 Distillable entanglement and entanglement cost

These two measures for mixed states can be defined in the similar way as the case of pure states. Again in the asymptotic limit, distillable entanglement is the maximum number of maximally entangled states that can be generated by an optimal LOCC transformation from some state ρ. In mathematical language

$$E_D(\rho) = \sup\{r : \lim_{n\to\infty} \left[\inf_{\Psi} D(\Psi(\rho^{\otimes n}), \Phi(2^{rn}))\right] = 0\} \tag{2.25}$$

where Ψ denotes a general trace preserving LOCC operation and $\Phi(d) = |\psi_d^+\rangle\langle\psi_d^+|$ is the density operator corresponding to the maximally entangled state $|\psi_d^+\rangle$ in d dimensions. Here $D(\sigma, \eta)$ is a suitable measure of distance [31, 32] between states σ and η, e.g. $D(\sigma, \eta) = \mathrm{tr}|\sigma - \eta|$.

Entanglement cost is the minimum number of maximally entangled states needed to generate the desired state by using LOCC. Similar to distillable entanglement, it can be written as

$$E_C(\rho) = \inf\{r : \lim_{n\to\infty} \left[\inf_{\Psi} D(\rho^{\otimes n}, \Psi(\Phi(2^{rn})))\right] = 0\}. \tag{2.26}$$

2.6.2.2 Entanglement of formation

Entanglement of formation $E_F(\rho)$ for a mixed state ρ is defined as the least expected entanglement of any ensemble of pure states realizing ρ [15]. Remember from Section (2.2) that mixed states can have different pure state realizations, and the statement *least expected* proposes a minimization procedure over all such realizations. Entanglement of formation for a mixed state $\rho = \sum_i p_i |\psi_i\rangle\langle\psi_i|$ can be written as

$$E_F(\rho) = \inf\{\sum_i p_i E_E(|\psi_i\rangle)\} \tag{2.27}$$

where infimum is calculated over all pure state ensembles $\{p_i, |\psi_i\rangle\}$ and $E_E(|\psi_i\rangle)$ is the entropy of entanglement for pure state $|\psi_i\rangle$. So this measure represents the minimal possible average entanglement over all pure state decompositions. It was also proven that in the asymptotic limit, entanglement of formation is equal to the asymptotic entanglement cost [33].

The minimization problem to calculate E_F is generally very difficult to solve. Due to this difficulty, people either tried to use numerical techniques [34], or considered some states with high degree of symmetry [35, 36, 37]. It is quite interesting that for bipartite qubit states, the closed form of E_F is known and given in terms of a parameter called *concurrence* [38, 39, 40]. For a general state ρ of two qubits, the spin flipped state is

$$\tilde{\rho} = \sigma_y \otimes \sigma_y \rho^* \sigma_y \otimes \sigma_y \tag{2.28}$$

where ρ^* is the complex conjugate of ρ in the standard basis $\{|00\rangle, |01\rangle, |10\rangle, |11\rangle\}$ and σ_y is the Pauli y operator. Concurrence is defined as

$$C(\rho) \equiv \max\{0, \lambda_1 - \lambda_2 - \lambda_3 - \lambda_4\} \tag{2.29}$$

where $\{\lambda_i\}$ are square roots of the eigenvalues of $\sqrt{\rho}\tilde{\rho}\sqrt{\rho}$ in decreasing order. For a general two qubit state, entanglement of formation can be written in terms of concurrence as [15]

$$E_F(\rho) = h\left(\frac{1 + \sqrt{1 - C^2(\rho)}}{2}\right) \tag{2.30}$$

where h is the binary entropy function

$$h(x) = -x \log_2 x - (1 - x) \log_2 (1 - x). \tag{2.31}$$

Since the entanglement of formation is a monotonically increasing function of concurrence, concurrence itself is used as a measure of entanglement in the literature.

2.6.2.3 Relative entropy of entanglement

There is a whole class of entanglement measures that are based on some distance function on the set of density matrices. The measure becomes the distance from the state under

consideration to the nearest separable state. If $D(\rho, \sigma)$ is the distance function, then the entanglement measure becomes

$$E(\rho) \equiv \inf_{\sigma \in \mathcal{S}(\mathcal{H})} D(\rho, \sigma) \tag{2.32}$$

where $\mathcal{S}(\mathcal{H})$ is the set of separable states in Hilbert space $\mathcal{H}$. One of these distance functions, *quantum relative entropy* is defined as

$$S(\rho||\sigma) \equiv \mathrm{tr}(\rho \log \rho - \rho \log \sigma). \tag{2.33}$$

The relative entropy is not symmetric, it is nonnegative and zero only for identical density operators. If same unitary transformations are applied on both states, it is left invariant. Physically, it can be explained as a measure of distinguishability between the given quantum states. Through this interpretation, it is possible to show that $S(\sigma||\rho) = +\infty$ when ρ is a pure state. It is followed from the fact that for any pure state there can be found a complete measurement for which the outcome is certain. And by performing this measurement it is definitely possible to distinguish the pure state from any other state.

The entanglement measure given in terms of $S(\rho||\sigma)$ is

$$E_R(\rho) \equiv \inf_{\sigma \in \mathcal{S}(\mathcal{H})} S(\rho||\sigma) \tag{2.34}$$

that is called the *relative entropy of entanglement* and it was shown to be reduced to entropy of entanglement for pure states [25].

In addition to relative entropy of entanglement, even though it is the most used one, there some other distance based measures generated by other distance functions. One of those distance functions is the *Bures metric* [41, 42, 25]

$$D_B(\rho||\sigma) \equiv 2 - 2\sqrt{F(\rho, \sigma)} \tag{2.35}$$

where $F(\rho, \sigma) \equiv [\mathrm{tr}\{(\sqrt{\sigma}\rho\sqrt{\sigma})^{1/2}\}]^2$ is called the Uhlmann's transition probability [43]. Another distance is the trace norm distance $D_T(\rho, \sigma) \equiv \mathrm{tr}[\sqrt{(\rho - \sigma)^2}]$ for which the generated measure was shown to be an entanglement monotone [44].

2.6.2.4 Negativity

Consider the previous bipartite system of two parties A and B with bases $\{|a_i\rangle\}$ and $\{|b_k\rangle\}$ respectively. If we write the density matrix as in Eq. (2.8), the partial transposition with respect to party B is defined as

$$\rho^{T_B} \equiv \sum_{ijk\ell} c_{ijk\ell} |a_i\rangle\langle a_j| \otimes |b_\ell\rangle\langle b_k|. \tag{2.36}$$

The partial transposition of a density matrix has a spectrum that is independent of the choice of basis. In addition to this, the spectrum is same for partial transpositions over

A and B. The positive partial transpose (PPT) criterion (*Peres-Horodecki criterion*) tells us that if the state ρ is separable, then the partial transpose of the density operator with respect to one subsystem is positive [45, 46]. The entanglement measure called *negativity* $N(\rho)$ is than defined as [47, 48]

$$N(\rho) \equiv \frac{||\rho^{T_B}|| - 1}{2} \tag{2.37}$$

and it was shown to be an entanglement monotone [49]. Here $||P|| \equiv \mathrm{tr}\sqrt{\mathrm{P}^\dagger \mathrm{P}}$ is the trace norm. Another quantity that is an entanglement measure by itself is the *logarithmic negativity* and it is defined as

$$E_N(\rho) \equiv \log_2 ||\rho^{T_B}||. \tag{2.38}$$

It was proven that this measure is a monotone under probabilistic LOCC transformations [49].

2.6.2.5 Squashed entanglement

An interesting entanglement measure called *squashed entanglement* is defined as [50]

$$E_{sq}(\rho) \equiv \inf \left[\frac{1}{2} I(A;B|E) \mid \rho_{ABE} \text{ extensions of } \rho \text{ to } \mathcal{H}_\mathrm{E} \right] \tag{2.39}$$

where the infimum is taken over all extensions to a third subsystem E and $\rho = \rho_{AB} = \mathrm{tr_E}(\rho_{\mathrm{ABE}})$. Here

$$I(A;B|E) \equiv S_{vN}(\rho_{AE}) + S_{vN}(\rho_{BE}) - S_{vN}(\rho_{ABE}) - S_{vN}(\rho_E) \tag{2.40}$$

is the *quantum conditional mutual information*. The squashed entanglement vanishes for all separable states but it still is not known if it vanishes for some entangled states as well. For pure states, it coincides with entropy of entanglement. Similar to most of the other entanglement measures for mixed states, the optimization procedure contained in the definition of squashed entanglement makes it hard to compute.

2.6.2.6 Witnessed entropy of entanglement

Entanglement witnesses are tools introduced for the purpose of determining the separability of quantum states [46]. An entanglement witness, usually denoted by W, for an entangled state σ is a Hermitian operator for which $\mathrm{tr}(\mathrm{W}\sigma) < 0$ and for all separable states ρ, $\mathrm{tr}(\mathrm{W}\rho) \geq 0$. If

$$\mathrm{tr}(\mathrm{W}_\sigma \sigma) \leq \mathrm{tr}(\mathrm{W}\sigma) \tag{2.41}$$

for all entanglement witnesses W, then and entanglement witness W_σ is said to be optimal for state σ. The *witnessed entropy of entanglement* is defined as [51]

$$E_{wit}(\rho) \equiv \max[0, -\mathrm{tr}(\mathrm{W}_\rho \rho)] \tag{2.42}$$

and it is used as a measure of non-separability of a given state ρ. The main advantage of this measure is that it can be approximately calculated for all mixed states, however finding the exact optimal entanglement witness is a hard optimization problem.

2.6.2.7 Other bipartite measures

Although there are also some other measures proposed in the literature, they are less widely used. Some of them are *the distillable secret key* [52], *the Rains bound* (related to logarithmic negativity) [53], *robustness of entanglement* [54], *entanglement of assistance* [55, 56] and *localizable entanglement* [57].

2.6.3 Multipartite measures

Previously we talked about different ways to quantify entanglement in the bipartite systems. The measures differ from each other in the case of mixed states, since for pure states entropy of entanglement distinguished measure. When it comes to system with more than two parties, because the spectra of reduced density matrices are different in general, the von Neumann entropies are not equal. In the case of bipartite systems, all the correlations are between two parties. Once the number of parties is increased, e.g. to three, we have three pair relations in the system. But even investigating only those pairwise relations in the system is not enough since we may have three-party correlations. Let us consider the GHZ state as an example where

$$|GHZ\rangle \equiv \frac{1}{\sqrt{2}}(|000\rangle + |111\rangle). \tag{2.43}$$

If we calculate the reduced state by tracing out any one of the three subsystems, the reduced density matrix becomes

$$\rho_r = \frac{1}{2}(|00\rangle\langle 00| + |11\rangle\langle 11|), \tag{2.44}$$

which is separable. So there is no bipartite entanglement in the system, however tripartite entanglement is maximal.

When investigating multi partite entanglement, it is possible to borrow some notions from the bipartite case. A multipartite state ρ is separable if and only if it can be written as a convex combination of product states, i.e.

$$\rho = \sum_i p_i \rho_i^{(A)} \otimes \rho_i^{(B)} \otimes \rho_i^{(C)} \otimes \dots \tag{2.45}$$

with $p_i \geq 0$ and $\sum_i p_i = 1$.

In what follows, we very briefly summarize some entanglement measures for multipartite systems, some of which are simply the generalizations bipartite entanglement measures.

- *Entanglement cost and distillable entanglement.* The definition of entanglement cost and distillable entanglement is based on standard maximally entangled bipartite state (Bell state). It is not obvious how to extend these measures to multipartite systems since there is no unique target state to aim for. There are some attempts to solve this problem by generalizing the definition of Bell states to a definition in terms of qubits transferred in the case of entanglement cost [58].

- *Relative entropic measures.* Relative entropy of entanglement, as well as other distance based measure, do not have any reference to bipartite states in their definitions. In this case, the distance is defined with respect to set of multipartite separable states. And these measures are just as valid in the multipartite systems.

- *Robustness of entanglement, entanglement of assistance* and *localizable entanglement* are the measures, the definitions of which can be extended to the case of multipartite systems.

- *'Tangles' and related quantities.* The definition of *tangle* uses the property of bipartite entanglement that if two parties A and B are strongly entangled, a third party C can only be weakly entangled with A or B. For example if A and B produce a Bell state, then C cannot be entangled with any one of them. In the light of this property, the tangle $\tau(\rho)$ is defined as [59]

$$\tau(\rho) = \inf \sum_i p_i C^2(|\psi_i\rangle\langle\psi_i|) \tag{2.46}$$

  where $C^2(|\psi\rangle\langle\psi|)$ is the square of concurrence for pure state $|\psi\rangle$, and the infimum is calculated over all pure state decompositions of ρ. Tangle has been shown to satisfy the inequality [59, 60]

$$\tau(A:B) + \tau(A:C) + \tau(A:D) + \ldots \leq \tau(A:BCD\ldots), \tag{2.47}$$

  where $\tau(X : Y_1Y_2Y_3\ldots)$ means that tangle is calculated for the bipartite splitting between party X and parties $Y_1Y_2Y_3\ldots$ Eq. (2.47) shows that the amount of bipartite entanglement between party A and other individual parties B, C, D, ... bounded from above by the amount of bipartite entanglement between A and parties $BCD\ldots$ collectively.

  As an example, for the case of three qubit states, the *residual tangle* τ_3 is

$$\tau_3 = \tau(A:BC) - \tau(A:B) - \tau(A:C) \tag{2.48}$$

  which quantifies the amount of three party entanglement that is somehow isolated from the bipartite effects.

Chapter 3

Quantification of entanglement via uncertainties

In this chapter we discuss a method to investigate quantum entanglement based on dynamic symmetry group approach [16, 17, 18, 19, 61]. Later on we describe how one can develop a measure of entanglement for pure states of arbitrary dimensional bipartite systems by using this approach together with quantum uncertainties and the generalization to multipartite systems.

3.1 Dynamic symmetry group approach

When dealing with entanglement or entangled states, if we do not have a definite definition of entanglement, it is natural to start with the question 'what is *not* entanglement?'. It is somehow easier to answer this questions, immediately one can reply that it is *not* a phenomenon with a classical analogue, and it is a property inherit to quantum systems only. So, any attempt to explain entanglement requires the definition of a quantum system. For this purpose, a dynamic symmetry group approach has been developed and used for explaining quantum entanglement [16, 17, 18, 19, 61].

As well as any other quantum phenomenon, quantum entanglement manifests itself via measurement of physical observables [62]. Although in the von Neumann approach to quantum mechanics (based on the assumption that all Hermitian operators represent measurable quantities), all observables of a system are supposed to be equally accessible [63], the physical nature of the system introduces unavoidable constraints. This approach of von Neumann was first put into question by Wick, Wightman and Wigner [64]. Several of such examples for restrictions are the following [19].

Consider a bipartite system with parties A and B and Hilbert space $\mathcal{H}_{AB} = \mathcal{H}_A \otimes \mathcal{H}_B$. If the subsystems are separated spatially by long distances, then only local observations $\mathcal{O}_A$ on A and $\mathcal{O}_B$ on B are possible.

As another example, we can consider a system of N identical particles each with space $\mathcal{H}$ of their internal degrees of freedom. Due to Pauli principle, for fermions, the composite state space of this many-particle system reduces to *antisymmetric* subspace $\wedge^N\mathcal{H} \subset \mathcal{H}^{\otimes N}$ and for bosons to *symmetric* subspace $S^N\mathcal{H} \subset \mathcal{H}^{\otimes N}$.

The basis for dynamic symmetry group approach to quantum mechanics has been formulated by Eugene Paul Wigner [65, 66]. This formulation suggests that the general properties of a quantum system are determined by the symmetry of corresponding Hilbert space. Wigner's considerations, together with the restrictions on observables discussed above, made scientists to conclude that available observables should be included in description of any quantum system from the outset [67, 68]. This was stated by Hermann as follows [67]

" The basic principles of quantum mechanics seem to require the postulation of a Lie algebra of observables and a representation of this algebra by skew-Hermitian operators."

We denote this Lie algebra of observables by $\mathcal{L}$ which acts on the Hilbert space $\mathcal{H}$. The corresponding Lie group $G = \exp(i\mathcal{L})$ is called the *dynamic symmetry group* of the system and a unitary representation of the dynamical group G in the state space $\mathcal{H}$ is a *quantum dynamical system* [19]. The restrictions on observables discussed above are of fundamental importance for physics in general and for quantum information specifically. There is no place for entanglement in the von Neumann approach to quantum mechanics where full dynamical group $\mathrm{SU}(\mathcal{H})$ makes all states equivalent (with respect to LOCC operations). Entanglement can be seen as an effect caused by superselection rules or symmetry breaking which reduce the dynamical group to subgroup $G \subset \mathrm{SU}(\mathcal{H})$ that is small enough to create intrinsic differences between states. For example, in the case of bipartite system $\mathcal{H} = \mathcal{H}_A \otimes \mathcal{H}_B$, the parties may be spatially separated by a long distance where only local measurements are feasible and so that the dynamical group becomes $\mathrm{SU}(\mathcal{H}_A)\times\ \mathrm{SU}(\mathcal{H}_B) \subset \mathrm{SU}(\mathcal{H}_A \otimes \mathcal{H}_B)$. If there were full access to local degrees of freedom (without any restrictions on observables), the full dynamical group $\mathrm{SU}(\mathcal{H})$ would act transitively on pure states $\psi \in \mathcal{H}$ of the system, which makes them all equivalent. As a result, there would be no place for entanglement and other subtle phenomena based on intrinsic differences between quantum states.

3.2 Total variance

For calculations we choose an arbitrary orthonormal basis X_α of $\mathcal{L} = \mathrm{Lie}(G)$ and call its elements X_α *basic observables*.

Recall that uncertainty of an observable $X \in \mathcal{L}$ in state $\psi \in \mathcal{H}$ is given by the variance

$$V(X,\psi) = \langle\psi|X^2|\psi\rangle - \langle\psi|X|\psi\rangle^2. \tag{3.1}$$

Consider orthonormal basis X_α of the algebra of observables $\mathcal{L}$ with respect to its *Cartan-Killing form* $(X,Y)_K$ [69] and define *total variance* by equation

$$\mathbb{V}(\psi) = \sum_\alpha (\langle\psi|X_\alpha^2|\psi\rangle - \langle\psi|X_\alpha|\psi\rangle^2). \tag{3.2}$$

For example, for two-qubit system $\mathcal{H}_A \otimes \mathcal{H}_B$ one can take basis of $\mathcal{L} = \mathfrak{su}(\mathcal{H}_A) + \mathfrak{su}(\mathcal{H}_B)$, consisting of Pauli operators σ_i^A and σ_j^B that act in components A and B, respectively. For a general multipartite system, the sum (3.2) is extended over orthonormal bases of traceless local operators for all parties of the system.

The total variance (3.2) can be understood as trace of the quadratic form

$$Q(X) = \langle\psi|X^2|\psi\rangle - \langle\psi|X|\psi\rangle^2, \quad X \in \mathcal{L}$$

on Lie algebra $\mathcal{L}$, and therefore it is independent of the basis X_α. It measures overall level of quantum fluctuations of the system in state ψ.

The first sum in the total variance (3.2) contains *Casimir operator* $C = \sum_\alpha X_\alpha^2$, which acts as a scalar $C_\mathcal{H}$ in every irreducible representation $G : \mathcal{H}$. As a result we get

$$\mathbb{V}(\psi) = C_\mathcal{H} - \sum_\alpha \langle\psi|X_\alpha|\psi\rangle^2. \tag{3.3}$$

To clarify the second sum, consider the average of the basic observables X_α in state ψ

$$X_\psi = \sum_\alpha \langle\psi|X_\alpha|\psi\rangle X_\alpha. \tag{3.4}$$

It can be understood as the *center of quantum fluctuations* of the system in state ψ. For example, in spin system it is given by suitably scaled spin projection onto mean spin direction in state ψ. The operator X_ψ is also independent of the basis X_α. This can be seen from the following property

$$\langle\psi|X|\psi\rangle = (X, X_\psi)_K, \quad \forall X \in \mathcal{L}, \tag{3.5}$$

which holds for basic observables $X = X_\alpha$ by orthogonality $(X_\alpha, X_\beta)_K = \delta_{\alpha\beta}$, and hence by linearity for all $X \in \mathcal{L}$. Since Killing form is nondegenerate, equation (3.5) uniquely determines X_ψ and provides for it a coordinate free definition. We show in Appendix A that the operator X_ψ is closely related to orthogonal projection of $\rho = |\psi\rangle\langle\psi|$ into Lie algebra $\mathcal{L}$. The operator X_ψ allows to recast the total variance (3.2) into the form

$$\mathbb{V}(\psi) = C_\mathcal{H} - \langle\psi|X_\psi|\psi\rangle. \tag{3.6}$$

In Appendix A, we explain how the total variance can be calculated and give an explicit formula for multi-component system $\mathcal{H} = \bigotimes_A \mathcal{H}_A$ with full access to local degrees of freedom in terms of reduced states ρ_A

$$\mathbb{V}(\psi) = \sum_A \left[\dim \mathcal{H}_A - \mathrm{tr}_{\mathcal{H}_A}(\rho_A^2)\right]. \tag{3.7}$$

3.3 Completely entangled states

We can infer from (3.3) the inequality

$$\mathbb{V}(\psi) \leq C_{\mathcal{H}} \tag{3.8}$$

which turns into equation if and only if

$$\langle\psi|X|\psi\rangle = 0, \quad \forall X \in \mathcal{L}. \tag{3.9}$$

For multi-party systems $\mathcal{H} = \bigotimes_A \mathcal{H}_A$, the latter equation means that all one-party reduced states are completely disordered. In other words, there exists some local basis such that the reduced state is given by a diagonal matrix ρ_A, corresponding to uniform probability distribution (that is, ρ_A are scalar operators). This is a well known characterization of maximally entangled states. In general we refer to (3.9) as *entanglement equation* and call the corresponding state ψ *completely entangled.*

The completely entangled states are characterized by maximality of the total variance. Therefore one may be tempted to consider entanglement as a manifestation of quantum fluctuations in a state where they come to their extreme. Entanglement equation (3.9) just states that, in completely entangled state ψ, the quantum system is at the center of its quantum fluctuations, that is $X_\psi = 0$.

3.4 Measure of entanglement

States opposite to entangled ones, to wit those with minimal total level of quantum fluctuations $\mathbb{V}(\psi)$, for a long time were known as *coherent states* [70, 71, 16, 72]. For multi-component systems like $\mathcal{H}_A \otimes \mathcal{H}_B$ coherent states are just *separable* or *unentangled* states $\psi = \psi_A \otimes \psi_B$.

It is possible to show that concurrence (6.24) can be equivalently expressed in terms of the total uncertainty (3.2) in the case of bipartite systems [73]. Consider first the case of two qubits with the state

$$|\psi\rangle = \sum_{\ell,\ell'=0}^{1} \psi_{\ell\ell'}|\ell,\ell'\rangle, \quad \sum_{\ell,\ell'=0}^{1} |\psi_{\ell\ell'}|^2 = 1, \tag{3.10}$$

where $|\ell,\ell'\rangle \equiv |\ell\rangle \otimes |\ell'\rangle$ denotes a composite state. It can be easily seen that the concurrence (6.24) is then cast to the form

$$\begin{aligned} C(\psi) &= 2|\psi_{00}\psi_{11} - \psi_{01}\psi_{10}| \\ &= 2[|\psi_{00}|^2|\psi_{11}|^2 + |\psi_{01}|^2|\psi_{10}|^2 - 2Re(\psi_{00}\psi_{11}\psi_{01}^*\psi_{10}^*)]^{1/2}. \end{aligned} \tag{3.11}$$

On the other hand using Pauli operators

$$\begin{aligned} \sigma_x &= |0\rangle\langle 1| + |1\rangle\langle 0|, \\ \sigma_y &= -i(|0\rangle\langle 1| - |1\rangle\langle 0|), \\ \sigma_z &= |0\rangle\langle 0| - |1\rangle\langle 1| \end{aligned} \tag{3.12}$$

as the basic local observables X_i^A and X_j^B one gets

$$\begin{aligned} \mathbb{V}(\psi) &= 4 + 4[|\psi_{00}|^2|\psi_{11}|^2 + |\psi_{01}|^2|\psi_{10}|^2 \\ &- 2Re(\psi_{00}\psi_{11}\psi_{01}^*\psi_{10}^*)]. \end{aligned} \tag{3.13}$$

Comparing now Eqs. (3.11) and (3.13) and by taking into account that $\mathbb{V}_{\rm ent} = \mathbb{V}_{\rm max} = 6$ and $\mathbb{V}_{\rm coh} = \mathbb{V}_{\rm min} = 4$ are the total levels of quantum fluctuations in completely entangled and coherent states of two qubits, respectively, we get

$$C(\psi) = \sqrt{\frac{\mathbb{V}(\psi) - \mathbb{V}_{\rm min}}{\mathbb{V}_{\rm max} - \mathbb{V}_{\rm min}}} \tag{3.14}$$

in the case of the general two-qubit state (3.10). Thus, the amount of entanglement carried by a pure two-qubit state can be determined by measurement of mean values of the basic observables given by Pauli operators (3.12). These observables can be directly measured in experiments, say by the Stern-Gerlach apparatus in the case of spins, or by means of polarizers in the case of photons, etc.

The above observation clarifies physical meaning of the concurrence as a measure of overall quantum fluctuations in the system and leads us to the natural *measure of entanglement* of pure states [74]

$$\mu(\psi) = \sqrt{\frac{\mathbb{V}(\psi) - \mathbb{V}_{\rm coh}}{\mathbb{V}_{\rm ent} - \mathbb{V}_{\rm coh}}} \tag{3.15}$$

valid for an arbitrary quantum system (multicomponent, arbitrary finite dimensional systems). It coincides with the concurrence for two component systems, but we refrain to use this term in general, to avoid confusion with other multicomponent versions of this notion introduced in [75]. We explain how this measure can be calculated in Appendix A. For a multicomponent system $\mathcal{H} = \bigotimes_A \mathcal{H}_A$, it can be expressed via local data, encoded in reduced states ρ_A

$$\mu^2(\psi) = \frac{\sum_A \left(1 - \mathrm{tr}\,\rho_{\rm A}^2\right)}{\sum_A \left(1 - \frac{1}{\dim \mathcal{H}_A}\right)}. \tag{3.16}$$

For example, in two component system $\mathcal{H} = \mathcal{H}_A \otimes \mathcal{H}_B$ the reduced states ρ_A and ρ_B are isospectral. Hence $\mathrm{tr}\rho_{\rm A}^2 = \mathrm{tr}\rho_{\rm B}^2$ and for system of square format $d \times d$ we arrive at the familiar formula for concurrence [76]

$$C(\psi) = \sqrt{\frac{d}{d-1}(1 - \mathrm{tr}\,\rho_{\rm A}^2)}, \tag{3.17}$$

(in [76] the normalization factor is left adjustable). The isospectrality of single-party reduced states means that entanglement can be measured *locally*. For example, in the case of bipartite spin-s system, measurement of only three observables (spin operators for either party) completely specifies concurrence (see also discussion in [77]).

An important application for the case of two qubits is provided by the polarization of photon twins (biphotons) that are created by the type-II down-conversion [78]. The spin operators S_j can be associated with the Stokes operators

$$\begin{aligned} S_x &\sim (a_H^+ a_V + a_V^+ a_H)/\sqrt{2}, \\ S_y &\sim i(a_H^+ a_V - a_V^+ a_H)/\sqrt{2}, \\ S_z &\sim a_H^+ a_H - a_V^+ a_V, \end{aligned} \tag{3.18}$$

so that the measurement of concurrence (7.1) assumes measurement of three Stokes operators for either outgoing photon beam. Here a_H (a_V) denotes the photon annihilation operator with horizontal (vertical) polarization. The polarization of photons is known to be measured by means of either standard six-state or a minimal four-state ellipsometer [79].

Nevertheless, there is a certain problem with simultaneous measurement of polarization for one of the two photons created at once and forming an entangled couple. Because of the commutation relation

$$[S_j, S_k] = i\epsilon_{jkm} S_m, \quad j,k,m = x,y,z,$$

the three projections of spin (or three Stokes operators) cannot be measured independently. The minimal uncertainty relation by Schrödinger [80, 81] states

$$V(\psi; S_j)V(\psi; S_k) - (\mathrm{Cov}(\mathrm{S_j}, \mathrm{S_k}))^2 \geq \frac{1}{4}|\langle\psi|[\mathrm{S_j}, \mathrm{S_k}]|\psi\rangle|^2, \tag{3.19}$$

where $V(\psi; S_j)$ denotes variance (uncertainty) of observable S_j in the state ψ and covariance $\mathrm{Cov}(\mathrm{S_j}, \mathrm{S_k})$ has the form

$$\mathrm{Cov}(\mathrm{S_j}, \mathrm{S_k}) = \frac{1}{2}\langle\psi|\mathrm{S_j S_k} + \mathrm{S_k S_j}|\psi\rangle - \langle\psi|\mathrm{S_j}|\psi\rangle\langle\psi|\mathrm{S_k}|\psi\rangle.$$

It is a straightforward matter to see that the uncertainty relation is simply reduced to the following one

$$0 \leq \langle\psi|X_\psi|\psi\rangle \leq 1/4, \tag{3.20}$$

where X_ψ is defined by Eq. (3.4). Thus, the uncertainty relation (3.19) becomes an exact equality when $\psi = \psi_{\mathrm{coh}}$ with $\langle\psi|X_\psi|\psi\rangle = 1/4$. In other words, this is an unentangled biphoton state in which each photon has well-defined polarization.

In the case of completely entangled biphoton state, the quantity $\langle\psi|X_\psi|\psi\rangle$ has zero value (due to the condition (3.9)). In this case, the measurement performed on a single photon rises

an additional question: how to distinguish between entanglement and classical unpolarized state.

Since Eq. (3.20) is the only relation, connecting different components of the average spin vector in either party, the local quantity $\langle\psi|X_\psi|\psi\rangle$ cannot be detected by either single or even two measurements.

3.5 Measure $\mu(\psi)$ beyond two-partite states

Postponing consideration of the measure $\mu(\psi)$ in general settings till Appendix A, we now note that, in the case of multipartite system, it gives the total amount of entanglement carried by all types of inter-party correlations.

For example, the GHZ (Greenberger-Horne-Zeilinger) state of three qubits

$$|G\rangle = x|000\rangle + \sqrt{1-|x|^2}|111\rangle, \quad |x| \in [0,1], \tag{3.21}$$

carries only three-party entanglement as mentioned in Section 2.6.3. This means that any two parties are not entangled. The amount of three-partite entanglement in (3.21) is measured by *3-tangle* τ [59] or *Cayley hyperdeterminant* [82] (for definition of 3-tangle, see Appendix B). It is easily seen that

$$\tau(G) = \mu^2(G) = 4|x|^2(1-|x|^2).$$

Thus, the squared measure (7.1), calculated for the three-qubit state (3.21), gives the same result as 3-tangle.

Another interesting example is provided by the so-called W-state of three qubits

$$|W\rangle = \frac{1}{\sqrt{3}}(|011\rangle + |101\rangle + |110\rangle). \tag{3.22}$$

This is a nonseparable state in three-qubit Hilbert space. Nevertheless, it does not manifest three-party entanglement because the corresponding 3-tangle $\tau(W) = 0$ [82]. At the same time, the measure (7.1) gives

$$\mu(W) = \frac{2\sqrt{2}}{3} \approx 0.94 \tag{3.23}$$

because $\mathbb{V}(W) = 8 + 2/3$ and $\mathbb{V}_{\rm coh} = 6$ in this case. The point is that there is a two-qubit entanglement in the state (3.22). To justify that the difference $2 + 2/3$ is caused just by quantum pairwise correlations, let us calculate the total *covariance*

$$\mathrm{Cov(W)} = \sum_{\mathrm{i=x,y,z}} \sum_{\mathrm{J}\neq\mathrm{J'}} (\langle \mathrm{W}|\sigma_{\mathrm{i}}^{\mathrm{J}}\sigma_{\mathrm{i}}^{\mathrm{J'}}|\mathrm{W}\rangle - \langle \mathrm{W}|\sigma_{\mathrm{i}}^{\mathrm{J}}|\mathrm{W}\rangle\langle \mathrm{W}|\sigma_{\mathrm{i}}^{\mathrm{J'}}|\mathrm{W}\rangle). \tag{3.24}$$

Here $J, J' = A, B, C$ label the parties. It is a straightforward matter to see that $\mathbb{V}(W) - \mathbb{V}_{\rm coh} = \mathrm{Cov(W)}$. Similar results can be obtained for the so-called *biseparable* states of three

qubits

$$(|001\rangle + |010\rangle),\ (|001\rangle + |100\rangle),\ (|010\rangle + |100\rangle), \tag{3.25}$$

that also manifest entanglement of two qubits and no entanglement of all three parts.

Examining entanglement of multi-qubit systems in general (number of parts is greater than two), it is necessary first to determine classes of states with different types of entanglement (including the class of unentangled states). It is assumed that those classes are nonequivalent with respect to LOCC [83, 84]. The point as we mentioned earlier is that entanglement of a given type cannot be created or destroyed under action of LOCC. In the case of three qubits, such a classification has been considered in Refs. [82, 85]. In the case of four qubits, the number of classes is much higher [84]. A useful approach to classification is based on investigation of *geometrical invariants* for a given system [16].

For example, the class of four-qubit entangled states can be specified by the generic GHZ-type state

$$x|0000\rangle \pm \sqrt{1-|x|^2}|1111\rangle,\ |x| \in [0,1], \tag{3.26}$$

which becomes completely entangled at $|x| = 1/\sqrt{2}$. In general, four-qubit completely entangled states can be defined by means of the condition (3.9) (see Appendix C). For the state (3.26), the measure (7.1) gives the amount of entanglement $\mu = \sqrt{1-(2|x|^2-1)^2}$, which becomes complete entanglement at $|x| = 1/\sqrt{2}$ as expected.

At the same time, there is another class of pairwise separable four-qubit states

$$\frac{1}{\sqrt{2}}(|00\rangle + |11\rangle) \otimes \frac{1}{\sqrt{2}}(|01\rangle + |10\rangle), \tag{3.27}$$

in which the first two pairs and the last two pairs separately manifest complete two-party entanglement, while there is no four-qubit entanglement (compare with the biseparable states of three qubits (3.25)). In this case, the measure (7.1) again gives the total amount of entanglement carried by the parts of the system.

3.6 Mixed entanglement

The measure (7.1) cannot be directly applied to calculation of entanglement of mixed states because it is incapable of separation of classical and quantum contributions into the total variance (3.2). Therefore, $\mu(\rho)$ always gives estimation from above for the entanglement of mixed states. This can be easily checked for some characteristic states like Werner state [22] and the so-called maximally entangled mixed states [86].

As far as we know, nowadays there is no universally recognized protocol for separation of classical and quantum uncertainties in mixed states except the case of two qubits, i.e concurrence [38, 39]. A promising approach proposed in Refs. [75, 87] contains the representation

of concurrence of a mixed state ρ as $\inf \sum_{\mathrm{i}} \mathrm{C}(\psi_{\mathrm{i}})$ of all properly normalized states ψ such that $\rho = \sum_i |\psi_i\rangle\langle\psi_i|$. The measure introduced in Eq. (7.1) can be generalized in the similar way to mixed states as

$$\mu(\rho) = \inf \sum_i \mu(\psi_i) \tag{3.28}$$

when the states ψ_i are properly normalized. This can also be written as

$$\mu(\rho) = \inf \sum_i p_i \mu(\psi_i) \tag{3.29}$$

where infimum is calculated over all possible pure state decompositions $\{|\psi_i\rangle, p_i\}$ of density matrix $\rho = \sum_i p_i |\psi_i\rangle\langle\psi_i|$ [74].

Chapter 4

Quantum correlations of ultracold bosons in optical lattices

4.1 Introduction

The realization of Bose-Einstein condensation in ultracold dilute atomic gases [88, 89, 90] has opened a new era in atomic and molecular physics. In this era, the study of particle statistics and their interactions is the focus rather than the study of single atoms and photons. In this regard, the developments in this field of research has led to various fascinating experiments in which the fundamental topics in quantum mechanics is studied in a macroscopic and accessible system. Some of these are observation of interference of two overlapping condensates [91], long range phase coherence properties of matter waves [92], quantized vortices and vortex lattices [93, 94], molecular condensates with bound pairs of fermions [95, 96, 97]. In almost all of such experiments, Bose condensed atoms can be described by a single wave function, which shows the existence of a coherent, macroscopic matter wave in the interacting many-body system. This macroscopic wave function is directly connected with the microscopic degrees of freedom and thus provides a complete and quantitative description of both static and time-dependent phenomena as it is treated in the framework of the Gross Pitaevskii equation [98, 99] and Boguliubov theory [100].

In many-body physics, a system that can be explained by a single macroscopic wave function is the simplest case. In those systems, correlations due to interactions are neglected or as in the case of Boguliubov theory they are taken as a small perturbation. Thus it is natural to ask whether a dilute gas of bosons can be brought to a strongly correlated regime.

In this regime, correlations due to interactions play an important role and the system is too complex to be explained by a single macroscopic wave function. In order to study the rich structure that can be obtained in this strongly correlated regime, a novel quantum system, optical lattice, has been used where neutral atoms are trapped in the intensity maxima minima of a standing wave light field due to the optical dipole force. In this direction a rather remarkable idea was the proposal of realizing a zero temperature quantum phase transition from a superfluid to a Mott-insulating state by loading *Bose-Einstein condensates* (BECs) into an optical lattice and raising its depth [101]. This quantum phase transition has been observed experimentally together with the collapse and revival of the macroscopic matter wave field during the transition [102].

The quantum phase transition between two distinct phases, a superfluid and a Mott-insulator, that exists at sufficiently low temperatures has been revealed by the investigation of atomic bosons with short-range repulsive interactions in a periodic potential by using the Bose-Hubbard model [103]. The system of BECs trapped in an optical lattice potential is a nearly perfect experimental realization of the Bose-Hubbard model. Following the experimental realization of this phase transition with cold atoms in optical lattices [102], further theoretical examinations have provided more insight [104]. Continued progresses have focused on systems of multi-component BECs in an optical lattice [105], where diverse topics such as quantum phase transitions of spin-2 bosons [106], two-component condensates [107], and spin-1 bosons with coupled ground states [108] are studied.

An interesting feature characterizing a variety of lattice models mapped onto atomic gases is quantum entanglement. Additionally, cold atom based lattice models have been identified as ideal candidates for universal quantum emulation of strongly interacting many body systems. While a complete understanding of quantum entanglement and correlations in an atomic lattice model remains a significant challenge even in theoretical terms [109], much has been understood for an important type of correlation, the so-called spin squeezing, or pseudo spin squeezing. For those systems that undergo quantum phase transitions, the presence and the measure of entanglement is important not only at the transition point, but also for the different phases of the system. These systems show various behaviors, entanglement and disentanglement, coherent and squeezed spin states, mode and particle entanglement for different phases that can be controlled by interaction types and strengths as well as lattice configurations.

Squeezed spin states are states whose spin fluctuation in one of the transverse spin components is below the standard quantum limit. It was shown in Ref. [110] a spin-s squeezed spin state is a correlated state consisting of $2s$ spin-1/2 particles. This implies a potential connection between spin squeezing and entanglement, due to the existence of correlations affecting the separability of a system with many spin-1/2 particles [111]. Spin squeezing can occur in many models with a variety of atom-atom interactions [112, 113, 114], for atomic condensates inside external traps [111], and for atoms inside optical lattices [115].

In this second part of the Thesis, we investigate the quantum correlation properties in the system of ultracold spin-1 atoms in an optical lattice. These correlation properties are examined via using connection between pseudo-spin squeezing and entanglement. We are focused on the possibility and the condition for spin squeezing in the pseudo-spin of coupled ground states of the system. In this regard, the second part of the Thesis is organized as follows.

In the beginning, we briefly discuss the theory of a weakly interacting Bose gas and move to the description of the behavior of ultracold bosonic gases in optical lattice potentials. In relation with that, the Bose-Hubbard model and mean field theory are explained briefly. Later on, we discuss the superfluid–Mott-insulator phase transition in the model.

In the sixth chapter, we consider a system spin-1 atoms with coupled ground states in an optical lattice. We use mean field approximation to solve corresponding Bose-Hubbard Hamiltonian of the system and investigate the superfluid–Mott-insulator phase transition. We then introduce the measure of spin squeezing and entanglement that we employ and present the results of spin squeezing for different interaction regimes.

In the last chapter, we conclude both about this part and the previous part of the Thesis.

Chapter 5

Bose-Einstein condensates in optical lattices

This chapter is devoted to the brief summary of theory of BECs in optical lattices. We start with a short discussion of Bose-Einstein condensation in noninteracting and cold dilute gases, followed by periodic optical lattice potentials and resulting Bloch bands. It continues with the discussion of Bose-Hubbard model of interacting bosons in a lattice. Finally we consider the superfluid–Mott-insulator phase transition in this model.

5.1 Bose-Einstein condensation

In 1924, it was Einstein who predicted the Bose-Einstein condensation [116] for a gas of particles obeying the Bose statistics [117]. Although originally it was predicted for a noninteracting Bose gas, later on it was shown that Bose-Einstein condensation is the reason of superfluid properties for strongly interacting ^{4}He [118, 119].

In the case of a noninteracting Bose gas, at zero temperature, the gas is fully condensed and all N particles can be represented by identical single particle wave functions $\phi_i(\mathbf{r})$. Since all the bosons are in the same single particle state, the many-body wave function $\Psi_N(\mathbf{r}_1, \mathbf{r}_2, \ldots, \mathbf{r}_N)$ of the system then becomes simply the product of individual single particle wave functions, i. e.

$$\Psi_N(\mathbf{r}_1, \mathbf{r}_2, \ldots, \mathbf{r}_N) = \prod_{i=1}^{N} \phi(\mathbf{r}_i), \tag{5.1}$$

and the single particle wave function is normalized $\int d\mathbf{r}|\phi(\mathbf{r})|^2 = 1$. In this simple noninteracting case, the BEC can be described by a macroscopic wave function [120]

$$\psi(\mathbf{r}) = \sqrt{N}\phi(\mathbf{r}), \tag{5.2}$$

which is sometimes called the *order parameter* of the condensate. The particle density is then given by $n(\mathbf{r}) = |\psi(\mathbf{r})|^2$. In this case of noninteracting gas, single particle state is the single particle ground state of the confining potential. In the second quantization picture, the many particle state in general can be a superposition of states with different particle numbers. In those situations, the order parameter is defined as the expectation value of the single particle annihilation operator, such that $\psi(\mathbf{r}) = \langle\hat{\psi}(\mathbf{r})\rangle$.

In order to introduce the interactions in a cold dilute bosonic gas, it is important to mention that the atom-atom interactions in such gases are dominated by elastic binary collisions. In this case the actual inter-particle potential does not have an important role since the effective extension of the interaction potential is much smaller than the thermal de Broglie wavelength and so that the only significant scattering process is s-wave scattering. As a result, the inter-particle potential can be approximated by an effective contact potential

$$V_{int}(\mathbf{r}) = g\delta(\mathbf{r}) \tag{5.3}$$

where $\mathbf{r} = \mathbf{r}_i - \mathbf{r}_j$ is the vector connecting the two atoms i and j. Here $g = 4\pi\hbar^2 a_s/m$ is the coupling constant that is given in terms of the atom mass m and s-wave scattering length a_s.

In the case of a weakly interacting Bose gas, in the second quantized form, the many-body Hamiltonian for N interacting bosons in an external potential $V_{ext}(\mathbf{r})$ becomes

$$\begin{aligned} \hat{H} &= \int d\mathbf{r}\hat{\psi}^\dagger(\mathbf{r})\left(-\frac{\hbar^2}{2m}\nabla^2 + V_{ext}(\mathbf{r})\right)\hat{\psi}(\mathbf{r}) \\ &+ \frac{1}{2}\int d\mathbf{r}d\mathbf{r}'\hat{\psi}^\dagger(\mathbf{r})\hat{\psi}^\dagger(\mathbf{r}')V_{int}(\mathbf{r}-\mathbf{r}')\hat{\psi}(\mathbf{r}')\hat{\psi}(\mathbf{r}) \end{aligned} \tag{5.4}$$

where $\hat{\psi}(\mathbf{r})$ and $\hat{\psi}^\dagger(\mathbf{r})$ are the bosonic field operators that annihilate and create a particle at position $\mathbf{r}$ respectively. When we insert the contact potential from (5.3), the interaction part (second term) of the Hamiltonian (5.4) becomes

$$\frac{4\pi\hbar^2 a_s}{m}\int d\mathbf{r}\hat{\psi}^\dagger(\mathbf{r})\hat{\psi}^\dagger(\mathbf{r})\hat{\psi}(\mathbf{r})\hat{\psi}(\mathbf{r}). \tag{5.5}$$

According to Bogoliubov mean field approach [100], for a dilute gas of bosons, the bosonic field operator can be replaced by its expectation value $\psi(\mathbf{r},t) = \langle\hat{\psi}(\mathbf{r},t)\rangle$ with introducing small fluctuations around that value, i. e.

$$\hat{\psi}(\mathbf{r},t) = \psi(\mathbf{r},t) + \delta\hat{\psi}(\mathbf{r},t). \tag{5.6}$$

By neglecting the fluctuations, one can come up with the famous Gross-Pitaevskii equation [98, 99]

$$i\hbar\frac{\partial}{\partial t}\psi(\mathbf{r},t) = \left(-\frac{\hbar^2}{2m}\nabla^2 + V_{ext}(\mathbf{r}) + g|\psi(\mathbf{r},t)|^2\right)\psi(\mathbf{r},t). \tag{5.7}$$

5.2 Optical lattices

Ultracold atoms in a periodic trapping potential form an interesting system that similar to those in condensed matter physics. Such kind of periodic potentials are simply generated by overlapping two counterpropagating laser beams. An optical standing wave with period $\lambda/2$ is formed due to the the interference between the two laser beams, each with wavelength λ. When the neutral atoms are loaded in such kind of periodic interference patterns of laser beams, they interact with the light field in two ways, dissipative and conservative. The absorption of photons followed by subsequent spontaneous emissions results in a dissipative force on the atoms. This is because of the momentum transfer of the absorbed and spontaneously emitted photons. This dissipative interaction is used for laser cooling of atoms.

In contrast to the dissipative way, conservative interactions appear due to the interaction of the light induced dipole moment of the atom and the photon field. This dipole interaction results in a shift in potential energy, known as *ac Stark shift*. If the detuning is large, then the spontaneous emissions can be neglected and ac Stark shift can be used to trap atoms. We will discuss a semiclassical method to calculate ac Stark shift effect.

5.2.1 Semiclassical treatment

In this title, the word semiclassical means the electric field of light is treated classically and the energy levels of the atom is treated quantum mechanically. When a neutral atom with discrete spectrum is placed in an oscillating electric field $\mathbf{E}$, that oscillates with frequency $\omega = 2\pi f$, the electric field induces a dipole moment $\mathbf{d}$. The dipole moment oscillates at the same frequency with the complex amplitude d that is [121]

$$d = \alpha(\omega)E \tag{5.8}$$

where $\alpha(\omega)$ is the complex polarizability and it depends on the frequency ω. The energy of the atom in the electric field may be calculated by using perturbation theory. In the dipole approximation for the electric field, the interaction Hamiltonian becomes

$$H' = -\mathbf{d} \cdot \mathbf{E} \tag{5.9}$$

with dipole moment

$$\mathbf{d} = -e \sum_j \mathbf{r}_j \tag{5.10}$$

where $\mathbf{r}_j$ are the position operators of the electrons relative to the atomic nucleus and the sum is taken over all electrons. In the absence of external fields, most atomic states are eigenstates of the parity operator to a very good approximation.

Now we consider the electric field of a light field. The time dependent electric field with

frequency Ω can be written as

$$\mathbf{E}(\mathbf{r},t) = \mathbf{E}_0(\mathbf{r})\cos(\omega t) = \frac{\mathbf{E}_0(\mathbf{r})}{2}(e^{i\omega t} + e^{-i\omega t}). \tag{5.11}$$

Any state $|\psi\rangle$ of the atomic system can be expanded in terms of the unperturbed states $|n\rangle$ given as

$$|\psi\rangle = \sum_n a_n(t)e^{-iE_nt/\hbar}|n\rangle \tag{5.12}$$

since they form a complete set with eigenenergies E_n. The time dependent Schrödinger equation then becomes

$$i\hbar\dot{a}_n = \sum_k \langle n|H'|k\rangle a_k(t)e^{i\omega_{nk}t} \tag{5.13}$$

where $\omega_{nk} = (E_n - E_k)/\hbar$. We now assume that the atom is initially in an eigenstate $|m\rangle$ of the unperturbed Hamiltonian ($a_k(t=0) = \delta_{km}$) and the perturbation is turned on at time $t = 0$. If we use the electric field (5.11) in (5.13), we can write the first order time dependent perturbation result [122]

$$a_n^{(1)} = -\frac{1}{2i\hbar}\int_0^t dt' \langle n|\mathbf{d}\cdot\hat{\mathbf{e}}|m\rangle E_0[e^{i(\omega_{nm}+\omega)t'} + e^{i(\omega_{nm}-\omega)t'}] \tag{5.14}$$

where $\hat{\mathbf{e}}$ is the unit vector along the direction of the electric field and E_0 is the maximum value of the electric field. The integral can be calculated to give

$$a_n^{(1)} = \frac{E_0\langle n|\mathbf{d}\cdot\hat{\mathbf{e}}|m\rangle}{2\hbar}\left[\frac{e^{i(\omega_{nm}+\omega)t}-1}{\omega_{nm}+\omega} + \frac{e^{i(\omega_{nm}-\omega)t}-1}{\omega_{nm}-\omega}\right] \tag{5.15}$$

for $n \neq m$. By writing the complex coefficient a_m of the initial state as $a_m = e^{i\phi_m}$ and using the first order result (5.15) in Schrödinger equation of (5.13), one gets the second order equation [122]

$$\begin{aligned}\hbar\dot{\phi}_m &= \langle m|\mathbf{d}\cdot\hat{\mathbf{e}}|m\rangle E_0\cos(\omega t) \\ &+ \frac{E_0^2}{2\hbar}\sum_{n\neq m}|\langle n|\mathbf{d}\cdot\hat{\mathbf{e}}|m\rangle|^2 e^{-i\omega_{nm}t}\cos(\omega t)\left[\frac{e^{i(\omega_{nm}+\omega)t}-1}{\omega_{nm}+\omega} + \frac{e^{i(\omega_{nm}-\omega)t}-1}{\omega_{nm}-\omega}\right]\end{aligned} \tag{5.16}$$

where $e^{-i\phi_m}$ is taken as 1 on the right hand side, because perturbation is applied to second order in the amplitude of the electric field. The first order term $\hat{\mathbf{e}}\cdot\langle m|\mathbf{d}|m\rangle$ vanishes due to the parity symmetry since the unperturbed states are eigenstates of the parity operator as we mentioned above. The energy shift of the ground state of the atom due to perturbation can be calculated as the time averaged rate of decrease of the phase times $\hbar$ which becomes

$$\hbar\langle\dot{\phi}_m\rangle_t = \frac{E_0^2}{4\hbar}\sum_n |\langle n|\mathbf{d}\cdot\hat{\mathbf{e}}|m\rangle|^2\left(\frac{1}{\omega_{nm}+\omega} + \frac{1}{\omega_{nm}-\omega}\right) \tag{5.17}$$

where $\langle\ldots\rangle_t$ denotes time averaging over a period of the electric field. The time averaged energy shift in the ground state of the atom can be calculated as [122]

$$V_g = -\hbar\langle\dot{\phi}_m\rangle_t = -\frac{1}{2}\alpha(\omega)\langle\mathbf{E}^2(\mathbf{r},t)\rangle_t \tag{5.18}$$

by taking $m = g$ where g denotes the ground state and $\alpha(\omega)$ is the polarizability. So the frequency dependence of polarizability can be written as

$$\alpha(\omega) = \sum_e \frac{2(E_e - E_g)|\langle e|\mathbf{d}\cdot\hat{\mathbf{e}}|g\rangle|^2}{(E_e - E_g)^2 - (\hbar\omega)^2}. \tag{5.19}$$

where E_g and E_e are the ground and excited state energies respectively and the sum over n is replaced by sum over all exited states. In many situations of interest, the frequency of the light field is close to that of the atomic resonance $\omega_0 = (E_e - E_g)/\hbar$. In these cases, one can neglect all transitions except the resonant one. Also by neglecting the terms except the with the smallest energy contribution gives

$$\alpha(\omega) \approx \frac{|\langle e|\mathbf{d}\cdot\hat{\mathbf{e}}|g\rangle|^2}{E_e - E_g - \hbar\omega}. \tag{5.20}$$

In perturbation theory calculations, the excited state has been assumed to have an infinitely long lifetime [122]. In reality although it decays via spontaneous emission processes. This effect can be put into the picture by introducing a phenomenological complex excited state energy. If the excited state has a life time $1/\Gamma_e$ and if the amplitude of the excited state is to taken to decay as $\exp(-iE_e t/\hbar)$, then the imaginary contribution to the excited state energy is simply $-i\hbar\Gamma_e/2$. In this phenomenological approach, the polarizability becomes

$$\alpha(\omega) \approx \frac{|\langle e|\mathbf{d}\cdot\hat{\mathbf{e}}|g\rangle|^2}{E_e - i\hbar\Gamma_e/2 - E_g - \hbar\omega}. \tag{5.21}$$

Making the polarizability complex results in a complex energy shift in the ground state which is

$$\Delta E_g = V_g - i\hbar\Gamma_g/2 \tag{5.22}$$

and Γ_g is the rate of loss of atoms from the ground state. Eq. (5.22) shows the form of an effective potential acting on the atom where the real part corresponds to shift in the ground state energy and imaginary part corresponds to the finite life time of the ground state due to transitions to the excited state via the interaction with the radiation field. The shift in the ground state energy then becomes

$$V_g = -\frac{1}{2}\mathrm{Re}\{\alpha(\omega)\}\langle\mathbf{E}^2(\mathbf{r},\mathrm{t})\rangle_\mathrm{t}. \tag{5.23}$$

The *detuning* for this transition can be defined as $\Delta = w - w_0$. Positive Δ is called *blue detuning* and negative Δ is called *red detuning*. By using this definition Eq. (5.23) can be cast into

$$V_g = \frac{\hbar\Omega_R^2\Delta}{\Delta^2 + \Gamma_e^2/4} \tag{5.24}$$

where $\Omega_R = \langle e|\mathbf{d}\cdot\mathbf{E}_0|g\rangle/\hbar$ is the *Rabi frequency*. By using this definition, the rate Γ_g becomes

$$\Gamma_g = -\frac{2}{\hbar}\mathrm{Im}\{\Delta\mathrm{E_g}\} \approx \frac{\Omega_\mathrm{R}^2\Gamma_\mathrm{e}}{\Delta^2 + \Gamma_\mathrm{e}^2/4}. \tag{5.25}$$

It can be seen from Eq. (5.24) that the optical dipole potential is positive for blue detuning creating repulsive potential and negative for red detuning resulting in an attractive potential.

While adjusting the detuning, on one hand, small detunings allow to create larger trap depths since the potential scales as $1/\Delta$, on the other hand the rate of loss of atoms from the ground state in (5.25) scales quadratically with the detuning as $1/\Delta^2$. Actually, the decay rate of the ground state can be written as a function of the detuning and the trap depth as

$$\hbar\Gamma_g = \frac{\Gamma_e}{\Delta} V_g. \tag{5.26}$$

Thus, the detuning of the light field should be chosen as large as possible to minimize the losses from the ground state and create a conservative potential.

5.2.2 Trapping the atoms

The conservative potential discussed above can be used to trap the atoms. As mentioned before, a far detuned laser forms an attractive potential for the cold atoms. Since the intensity I of a light beam is given by [123]

$$I(\mathbf{r}) = \frac{1}{2} c\epsilon_0 \langle \mathbf{E}^2(\mathbf{r}, t) \rangle_t, \tag{5.27}$$

the trap potential for ground state (5.24) can be written as

$$V_g = \frac{|\langle e|\mathbf{d}\cdot\hat{\mathbf{e}}|g\rangle|^2}{\hbar c\epsilon_0} \frac{\Delta}{\Delta^2 + \Gamma_e^2/4} I(\mathbf{r}). \tag{5.28}$$

As an example, in the case of a tightly focused Gaussian laser beam travelling along the z direction, the electric field is [125]

$$E(r, z) \simeq E_0 \frac{w_0}{w(z)} e^{i(kz-\omega t)} e^{-r^2/w^2(z)} \tag{5.29}$$

where E_0 is the maximum amplitude of the electric field (on axis at waist), $w(z) = w_0(1 + (z/z_R)^2)^{1/2}$, $z_R = \pi w^2/\lambda$ is the Rayleigh length (the distance along the propagation of a beam from the waist to the place for which the cross sectional area is doubled), w_0 is the radius of the cross sectional area at the *beam waist*. The corresponding intensity profile is

$$I(r, z) = \frac{2P}{\pi w^2(z)} e^{-2r^2/w^2(z)} \tag{5.30}$$

where P is the total power of the laser light. Such a Gaussian beam produces a cylindrically symmetric dipole trap and by expanding the exponential term of Eq. (5.30) the trapping potential in the center of the trap approximately becomes

$$V(r, z) \simeq -V_0 \left[1 - 2\left(\frac{r}{w_0}\right)^2 - \left(\frac{z}{z_R}\right)^2 \right]. \tag{5.31}$$

The above investigation of the Gaussian beam can be used to generate periodic lattice potentials with tightly confining potential wells. The way to do that is creating a dipole trap with superimposed counterpropagating laser beams. An example in one dimension

can be given by the standing wave interference pattern of a retroreflecting Gaussian laser beam [124]. In this case, by using Eq. (5.29), the trapping potential becomes

$$V(r,z) = -V_{lat}e^{-2r^2/w_0^2}\sin^2(kz) \simeq -V_{lat}\left(1-2\frac{r^2}{w_0^2}\right)\sin^2(kz) \tag{5.32}$$

where $k = 2\pi/\lambda$ is the wave number and V_{lat} is the depth of the optical lattice potential.

In a similar manner to one-dimensional case, higher dimensional periodic optical potentials can be created by superimposing standing waves from different directions. In order to form a two-dimensional lattice, two standing waves (two orthogonal conterpropagating beam pairs) that are orthogonal two each other can be superimposed. Similarly, three orthogonal standing waves (three orthogonal counterpropagating beam pairs) form a three-dimensional periodic lattice potential.

In the case of large detunings of the laser fields that are forming the optical lattices (large compared to the fine structure splitting of the typical alkali atom), the potential profile is almost the same for all magnetic sublevels in the ground state manifold of the atom. For smaller detunings, however, different magnetic sublevels can be subject to very different optical potential profiles [127]. Such spin dependent lattice potentials can be created by the standing wave configuration of two counterpropagating laser beams with an angle θ between their linear polarization vectors (lin-θ-lin configuration) [127, 128, 129, 130]. Such a standing wave formed by two linearly polarized laser beam can be written as a superposition of a σ^+ and σ^- polarized standing wave laser field. The corresponding lattice potentials are

$$\begin{aligned} V_+(z,\theta) &= V_0\cos^2(kz+\theta/2), \\ V_-(z,\theta) &= V_0\cos^2(kz-\theta/2) \end{aligned} \tag{5.33}$$

for which by changing the polarization angle θ the relative separation between the potentials can be controlled. By using such spin dependent optical potentials it is possible to tune the interactions between two atoms in different spin states. This is done by shifting the spin dependent lattices relative to each other in order to tune the overlap of the on-site wave function between zero and its maximum value. This is how one can control the interaction strength between the atoms with different spins in a restricted range.

5.2.3 Emergence of Bloch bands and Wannier functions

If a quantum particle is subject to a periodic potential, then the solution of the Schrödinger equation results in the emergence of a band structure [126]. When we consider the ideal situation of vanishing interactions and no additional confining potential other than the intensity profile, the atoms experience the lattice potential in Eq. (5.32) with a tunable amplitude V_{lat}. In a deep optical lattice with $V_{lat} \gg E_R$ ($E_R = \hbar^2k^2/(2m)$ being the *recoil energy*), the energy of local oscillations is much larger than the recoil energy and provided that all

atoms are in the lowest vibrational level at each site, their kinetic energy is frozen except for the small tunnelling amplitude to the neighboring sites. The corresponding single particle eigenstates in the lowest band are the *Bloch wave functions*. The analysis is as follows. For a particle moving in a one dimensional potential $V(x)$, the Schrödinger equation is

$$H\phi_q^{(n)}(x) = E_q^{(n)}\phi_q^{(n)}(x) \tag{5.34}$$

with Hamiltonian

$$H = \frac{\hat{p}^2}{2m} + V(x) \tag{5.35}$$

and the solutions $\phi_q^{(n)}(x)$ are called Bloch wave functions. Here q is the quasi momentum and within the first Brillouin zone $-\hbar k \leq q \leq \hbar k$. Eigenvalues $E_q^{(n)}$ are the eigenenergies for the n^{th} energy band for a given value of q. These Bloch wave functions can be written as

$$\phi_q^{(n)}(x) = e^{iqx/\hbar}u_q^{(n)}(x) \tag{5.36}$$

where $u_q^{(n)}(x)$ are some functions having the same period as the potential. If we use the relation (5.36) in the Schrödinger equation, we get

$$H'u_q^{(n)}(x) = E_q^{(n)}u_q^{(n)}(x) \tag{5.37}$$

which is the Schrödinger equation for $u_q^{(n)}(x)$ with the Hamiltonian

$$H' = \frac{(\hat{p}+q)^2}{2m} + V(x). \tag{5.38}$$

The discrete Fourier transforms

$$u_q^{(n)}(x) = \sum_\ell a_\ell^{(n,q)}e^{i2\ell kx} \quad \text{and} \quad V(x) = \sum_m V_m e^{i2mkx} \tag{5.39}$$

where m and ℓ are integers, can be defined since both the potential and $u_q^{(n)}(x)$ has the same period. If we use these Fourier expansions in Eq. (5.37), the kinetic energy term becomes ($\hat{p} = -i\hbar\partial/\partial x$)

$$\frac{(\hat{p}+q)^2}{2m}u_q^{(n)}(x) = \sum_\ell \frac{(2\hbar k\ell + q)^2}{2m}a_\ell^{(n,q)}e^{i2\ell kx}, \tag{5.40}$$

and the potential energy becomes

$$V(x)u_q^{(n)}(x) = \sum_\ell \sum_m V_m e^{i2(m+\ell)kx}a_\ell^{(n,q)}. \tag{5.41}$$

For example, if we have the lattice potential of a retroreflected Gaussian laser beam such as the one in Eq. (5.32), it can be written as

$$V(x) = -V_{lat}\cos^2(kx) = -\frac{V_{lat}}{2}[\cos(2kx)+1] = -\frac{1}{4}V_{lat}(e^{2ikx} + e^{-2ikx} + 2) \tag{5.42}$$

for which $V_{m=-1} = V_{m=1} = -(1/4)V_{lat}$ and V_0 can be taken zero. If the Fourier transforms (5.40) and (5.41) together with the optical lattice potential (5.42) are used in the Schrödinger equation of (5.37), one gets

$$\sum_{\ell'} H'_{\ell,\ell'}a_{\ell'}^{(n,q)} = E_q^{(n)}a_\ell^{(n,q)} \tag{5.43}$$

where

$$H'_{\ell,\ell'} = \begin{cases} (2\hbar k\ell + q)^2/2m, & \text{if } \ell = \ell'; \\ -V_0/4, & \text{if } |\ell - \ell'| = 1; \\ 0, & \text{else.} \end{cases} \tag{5.44}$$

The eigenvectors $a_\ell^{(n,q)}$ corresponding to energies $E_q^{(n)}$ defines the proper Bloch wave function.

Bloch functions given in Eq. (5.36) are extended over the whole lattice since they are complete delocalized energy eigenstates with a given quasi momentum q and energy band n. An alternative single particle basis is given by the Wannier functions $w_n(x - x_i)$ [131]. They can be written in terms of Bloch functions by

$$w_n(x - x_i) = \sum_q e^{-iqx_i/\hbar} \phi_q^{(n)}(x). \tag{5.45}$$

As opposed to Bloch states, Wannier functions from an orthonormal set where each one is maximally localized to an individual lattice site. In Eq. (5.45), it is the Wannier function for a localized particle in the n^{th} energy band and i^{th} lattice site with position x_i. The orthonormality condition for proper normalization is

$$\int dx w_n^*(x - x_i) w_m(x - x_j) = \delta_{n,m}\delta_{i,j}. \tag{5.46}$$

The Wannier picture becomes useful in those cases for which the interaction between the particles are present. For the local interactions between the particles on particular lattice site, the best description is given by the localized Wannier functions.

5.3 Bose-Hubbard model and superfluid–Mott-insulator phase transition

5.3.1 Bose-Hubbard Hamiltonian

Ultracold bosons with short-range repulsive interactions in a periodic optical potential discussed in the previous sections are best described by using the Bose-Hubbard model [103]. Apart from being the simplest nontrivial model describing a bosonic many-body system on a periodic lattice that cannot be mapped onto a single particle problem, it is as rich when the effects like superfluid–Mott-insulator quantum phase transition are considered. It was also experimentally realized for ultracold bosonic atoms [102].

Bose-Hubbard model is obtained from the general many-body Hamiltonian of Eq. (5.4) and (5.5) which can be written as

$$\hat{H} = \int d^3x \hat{\psi}^\dagger(\mathbf{x}) \left(-\frac{\hbar^2}{2m}\nabla^2 + V(\mathbf{x}) \right) \hat{\psi}(\mathbf{x}) + \frac{1}{2}\frac{4\pi a_s \hbar^2}{m} \int d^3x \hat{\psi}^\dagger(\mathbf{x})\hat{\psi}^\dagger(\mathbf{x})\hat{\psi}(\mathbf{x})\hat{\psi}(\mathbf{x}), \tag{5.47}$$

where $\hat{\psi}(\mathbf{x})$ is the bosonic field operator and in the optical system that we consider, the trapping potential $V(\mathbf{x})$ is the sum of the periodic lattice potential $V_{lat}(\mathbf{x})$ and any other external confinement potential $V_{ext}(\mathbf{x})$ present. As mentioned previously, a_s is the scattering length and m is the mass of an atom.

In the view of two assumptions,

- thermal and mean interaction energies at a single lattice site are much smaller than the separation from the first excited band,
- the Wannier functions decay within a neighboring lattice site separation,

only the lowest band is taken into account and the lattice potential is deep enough to consider the hopping only to the nearest neighbor sites. Since the Wannier functions $w(\mathbf{x}-\mathbf{x}_i)$ of the lowest band form a complete set, then the field operators can be expanded as

$$\hat{\psi}(\mathbf{x}) = \sum_i \hat{a}_i w(\mathbf{x} - \mathbf{x}_i) \tag{5.48}$$

where $\hat{a}_i$ is the particle annihilation and $\hat{a}_i^\dagger$ is the particle creation operators for the i^{th} lattice site with the bosonic commutation relation $[\hat{a}_i, \hat{a}_j^\dagger] = \delta_{ij}$. Plugging this expansion into Eq. (5.47) together with imposing tunnelling only between the nearest neighbors, we get the Bose-Hubbard Hamiltonian

$$\hat{H} = -J \sum_{<i,j>} \hat{a}_i^\dagger \hat{a}_j + \frac{U}{2} \sum_i \hat{n}_i(\hat{n}_i - 1) + \sum_i (\epsilon_i - \mu)\hat{n}_i \tag{5.49}$$

where $\hat{n}_i = \hat{a}_i^\dagger \hat{a}_i$ is number of bosons on the i^{th} lattice site and $< i, j >$ denotes all nearest neighbor sites i and j. The first term in the Bose-Hubbard Hamiltonian is tunnelling of bosons between neighboring potential wells and it is called the *hopping term*. The strength of the coupling is given by $J = -\int d^3x w(\mathbf{x} - \mathbf{x}_i)(\hbar^2\nabla^2/2m + V_{lat}(\mathbf{x}))w(\mathbf{x} - \mathbf{x}_j)$. The parameter $U = (4\pi\hbar^2 a_s/m) \int d^3x |w(\mathbf{x})|^4$ corresponds to the strength of the on-site repulsion of two atoms on the lattice site i which disfavors more than one boson at a given site. The last term $\epsilon_i = \int d^3x V_{ext}(\mathbf{x})|w(\mathbf{x}-\mathbf{x}_i)| \approx V_{ext}(\mathbf{x}_i)$ describes the effect of the external trapping potential and gives rise to an energy offset on the i^{th} lattice site. For a homogenous system ϵ_i is zero. Finally μ is the chemical potential which acts as a Lagrange multiplier for the constraint of fixed number of particles in a grand canonical ensemble.

The Bose-Hubbard model describes the competition between the repulsive on-site interaction U and the kinetic energy J that is gained by delocalizing particles over the sites. When the depth of the optical lattice potential is increased, the tunnelling barrier increases and hence the hopping parameter J decreases exponentially [132]. On the contrary, due to tighter confinement in a deeper lattice, on-site interaction U increases slightly. Thus U/J can be changed continuously by changing the depth of the lattice potential.

5.3.2 Superfluid–Mott-insulator phase transition

Although the Bose-Hubbard Hamiltonian (5.49) is not an exactly solvable one even in one-dimensional case, the underlying physics and properties of the existing quantum phase transition is well understood [103]. Two distinct ground states of the Hamiltonian of Eq. (5.49) can be identified depending on tunnelling strength J relative to the strength of interactions U. The classification is as follows.

- *Superfluid ground state.* In the limit for which the tunnelling term J is much larger than the strength of the inter-atomic interactions, $U/J \to 0$ and the many-body ground state is simply a BEC. All bosonic atoms are in the $q = 0$ Bloch state of the lowest band, in other words each atom is delocalized over the entire lattice. The resulting many-body state then can be written as a product of identical single-particle Bloch states such as

$$|\Psi_{SF}\rangle_{U/J\to 0} = \frac{1}{\sqrt{N!}}\left(\frac{1}{\sqrt{M!}}\sum_{i=1}^{M}\hat{a}_i^{\dagger}\right)^{N}|0\rangle \tag{5.50}$$

  where there are N atoms on a lattice with M sites. The existence of a macroscopic wave function for the superfluid state shows that a macroscopic phase is well defined on each lattice site. Depending on this situation, on the contrary, the number of atoms on a site is uncertain, meaning a measurement of number of atoms would give a random result. Indeed for a sufficiently large system ($M, N \to \infty$) at fixed density (N/M finite), the perfect condensate becomes a product of local coherent states [132] and so that the particle number per site has a Poissonian distribution with variance $\mathrm{Var}(n_i) = \bar{n}_i$. The phase coherent matter field on i^{th} lattice site is therefore shown by the nonzero expectation value of the particle annihilation operator $\hat{a}_i$ (or equivalently field operator $\hat{\psi}_i$) $\psi_i = \langle\Psi_{SF}|\hat{a}_i|\Psi_{SF}\rangle$ since the local coherent states are eigenstates of the operator $\hat{a}_i$.

- *Mott-insulator ground state.* In the opposite limit of the superfluid regime, where the on-site atomic interactions becomes much larger than the hopping strength, *i.e.* $U/J \gg 1$, *the energetic cost of atom number per site fluctuations becomes large and the system prefers to have localized atomic wave functions to minimize the interaction energy. In the limit* $J \to 0$ *the many-body ground state then becomes a product of local Fock number states in atom numbers per site and it can be written as*

$$|\Psi_{MI}(n)\rangle_{J\approx 0} \propto \prod_{i=1}^{M}(\hat{a}_i)^n|0\rangle \tag{5.51}$$

  with commensurate filling of n atoms per lattice site. Since the atoms are localized at each lattice site, the number of atoms at each site is definite but this time the phase of the coherent matter wave field on a site is uncertain. This is shown by the vanishing expectation value $\psi_i = \langle\Psi_{MI}(n)|\hat{a}_i|\Psi_{MI}(n)\rangle = 0$.

By changing strength of the interactions U relative to the hopping term J, the system arrives to a critical point for the ratio U/J. At this critical point, the system undergoes a quantum phase transition between the superfluid and Mott-insulator ground states. In the limit $U/J \to 0$, the dominance of kinetic energy results in a completely delocalized superfluid ground state. On the other limit, when interaction are dominant, for large U/J values, the ground state has fixed number of particles per site and is in the Mott-insulator phase. This time the state are *incompressible* meaning that the density remains same if the chemical potential is varied, i. e. $\partial n/\partial \mu = 0$. The quantum nature of this phase transition comes from the fact that it is driven by quantum fluctuations and hence it exists even at zero temperature where thermal fluctuations completely die away.

It is possible to treat the above quantum phase transition by the use of mean field approach and the help of the Gutzwiller approximation [133]. In this approximation, the many-body state is assumed to be written as the product of localized states at each site

$$|\Psi_{MF}\rangle = \prod_{i}^{M} |\phi_i\rangle \tag{5.52}$$

where the localized states $|\phi_i\rangle$ are written as a superposition of Fock states with different number of atoms

$$|\phi_i\rangle = \sum_{n=0}^{\infty} a_n^{(i)} |n\rangle. \tag{5.53}$$

Here $a_n^{(i)}$ are complex coefficients denoting the amplitude of finding n particle on lattice site i. Both superfluid and Mott-insulator phases can be written by using Gutzwiller ansatz and the coefficients $a_n^{(i)}$ are calculated by minimizing $\langle \Psi_{MF}|\hat{H}|\Psi_{MF}\rangle$ where $\hat{H}$ is the Bose-Hubbard Hamiltonian given in Eq. (5.49). We should note here that the Gutzwiller approach is not exact and it fails to describe the nontrivial correlations between different lattice sites which are possible for finite hopping J [134]. Therefore local number fluctuations on a lattice site completely vanishes when the transition point is passed and there remains no long range phase coherence, however in the exact case there remains short range phase correlations and number fluctuations do not completely die away when the Mott-insulator phase is entered.

Chapter 6

Entanglement of ultracold spin-1 atoms in optical lattices

In this chapter, we are interested in the possibility and the condition for spin squeezing in the pseudo-spin of coupled ground states in an optical lattice model with spin-1 bosons. We hope to explore spin squeezing properties of the system carefully studied in Ref. [108]. For this aim, first we review the model system [108, 135] and describe the mapped Bose-Hubbard Hamiltonian in the mean-field approximation. Later on, the measure of spin squeezing and quantum entanglement that we employ is introduced. Then, in the end of the chapter, the results of spin squeezing for different interaction regimes are presented.

6.1 Bose-Hubbard model for spin-1 atoms with coupled ground states in an optical lattice

6.1.1 System and the Hamiltonian

The system we study consists of neutral bosonic atoms with hyperfine spin $F = 1$ in an optical lattice. The optical lattice results from the ac Stark shifts of standing wave laser fields, which are dipole coupled to atomic electronic transitions. The off-resonant coupling induces virtual transitions to electronic excited states, which upon adiabatic elimination give rise to level shifts (ac Stark shifts) in the ground state manifold. These shifts are proportional to the intensity distribution of the laser light, as mentioned in Section 5.2. Additionally two-photon Raman like transitions can couple any two Zeeman states within the spin-1 ground state manifold, subject to appropriate polarization selections. In a lattice of ac Stark shifts from standing waves, the periodic level shift gives rise to band structures. When the lasers

are linearly polarized, the Zeeman ground state manifold of ($M_F = -1, 0, +1$) remains degenerate in the lattice. For more general cases of coupling referred to as the Λ or V scheme with suitable polarizations, two alternate ground states become coupled and will be denoted as the electronic modes with $\sigma = 0$ and $\sigma = \Lambda$ [108].

The optical lattice in the model is assumed to be created by two counterpropagating linearly polarized laser beams. The two beams have equal amplitudes and frequencies. As discussed in Section 5.2.2, lin-θ-lin configuration (θ being the angle between the polarization vectors) is used to form a spin dependent optical potential. The magnitude of detuning $|\Delta|$ is chosen to be much larger than the spontaneous emission rate to avoid decoherence (see Section 5.2.1) and due to this choice, the excited state can be adiabatically eliminated. The two counterpropagating laser beams form left and right polarized standing waves with Rabi frequencies [108]

$$\Omega_{\pm}(z) = \tilde{\Omega}_0 \cos(k_L z \pm \theta/2) \tag{6.1}$$

where k_L is the wave number of the laser waves. These standing waves couples the ground and excited states as discussed above via V and Λ type transitions.

As in the case of spinless BECs discussed in Section 5.1, the low energy dynamics of spinor BECs is also described by a pairwise interaction that is rotationally invariant in the hyperfine spin space and the hyperfine spin of the individual atoms are conserved [136]. The interaction potential between two atoms in Eq. (5.4) becomes

$$\hat{V}(\mathbf{r}_1 - \mathbf{r}_2) = \delta(\mathbf{r}_1 - \mathbf{r}_2) \sum_{F=0}^{2f} g_F \mathcal{P}_F \tag{6.2}$$

where $g_F = 4\pi\hbar^2 a_F/m$ and $\mathcal{P}_F = \sum_{M_F} |F, M_F\rangle\langle F, M_F|$ is the projection operator for projecting atom 1 and atom 2 into a total hyperfine spin F. Due to symmetry, only even F terms appear for bosons. a_F is the s-wave scattering length in the total spin F channel and f is the hyperfine spin of each atom. It is a straightforward matter to see that $\mathbf{F}_1 \cdot \mathbf{F}_2 = \sum_F (1/2)[F(F+1) - 2f(f+1)]\mathcal{P}_F$ where $\mathbf{F}_1$ and $\mathbf{F}_2$ are the hyperfine spin vectors of the two interacting atoms.

In the case of $f = 1$ atoms, $V = g_0\mathcal{P}_0 + g_2\mathcal{P}_2$ and $\mathbf{F}_1 \cdot \mathbf{F}_2 = \mathcal{P}_2 - 2\mathcal{P}_0$ together with completeness relation $\mathcal{P}_0 + \mathcal{P}_2 = 1$. If we take $g_s = (g_0 + 2g_2)/3$ and $g_a = (g_2 - g_0)/3$, the potential becomes

$$\hat{V} = (g_s + g_a \mathbf{F}_1 \cdot \mathbf{F}_2)\delta(\mathbf{r}_1 - \mathbf{r}_2). \tag{6.3}$$

Using this potential in the second quantized Hamiltonian of (5.4), we get

$$\hat{H} = \int d\mathbf{r} \left(\frac{\hbar^2}{2m} \nabla\hat{\psi}_\alpha^\dagger \cdot \nabla\hat{\psi}_\alpha + \hat{\psi}_\alpha^\dagger V(\mathbf{r})\hat{\psi}_\alpha + \frac{g_s}{2}\hat{\psi}_\alpha^\dagger\hat{\psi}_\beta^\dagger\hat{\psi}_\beta\hat{\psi}_\alpha + \frac{g_a}{2}\hat{\psi}_\alpha^\dagger\hat{\psi}_{\alpha'}^\dagger \mathbf{F}_{\alpha\beta} \cdot \mathbf{F}_{\alpha'\beta'}\hat{\psi}_{\beta'}\hat{\psi}_\beta \right), \tag{6.4}$$

where $\hat{\psi}_\alpha$ is the bosonic field annihilation operator for the atom in the hyperfine ground state $|F = 1, \alpha\rangle$ ($\alpha = -1, 0, 1$) at point $\mathbf{r}$ and $V(\mathbf{r})$ is the trapping potential. There is summation over the repeated indices α, β and $\mathbf{F}_{\alpha\beta}$ is the vector of (3×3) $F = 1$ spin matrices, i.e

$\mathbf{F} = F_1\hat{\imath} + F_2\hat{\jmath} + F_3\hat{k}$ with

$$F_1 = \frac{1}{\sqrt{2}}\begin{pmatrix} 0 & 1 & 0 \\ 1 & 0 & 1 \\ 0 & 1 & 0 \end{pmatrix}, \quad F_2 = \frac{1}{\sqrt{2}}\begin{pmatrix} 0 & -i & 0 \\ i & 0 & -i \\ 0 & i & 0 \end{pmatrix}, \quad F_3 = \begin{pmatrix} 1 & 0 & 0 \\ 0 & 0 & 0 \\ 0 & 0 & -1 \end{pmatrix}. \quad (6.5)$$

In the case of coupled ground state, via V or Λ type transitions mentioned earlier, second quantized Hamiltonian for a one-dimensional lattice can be written as [108]

$$\hat{H} = \int dz \left(\frac{\hbar^2}{2m}\nabla\hat{\psi}^\dagger_\alpha \cdot \nabla\hat{\psi}_\alpha + \frac{\hbar}{\Delta}\hat{\psi}^\dagger_\alpha \hat{\Omega}^2_{\alpha\beta}\hat{\psi}_\beta + \frac{g_s}{2}\hat{\psi}^\dagger_\alpha\hat{\psi}^\dagger_\beta\hat{\psi}_\beta\hat{\psi}_\alpha + \frac{g_a}{2}\hat{\psi}^\dagger_\alpha\hat{\psi}^\dagger_{\alpha'}\mathbf{F}_{\alpha\beta}\cdot\mathbf{F}_{\alpha'\beta'}\hat{\psi}_{\beta'}\hat{\psi}_\beta \right), \quad (6.6)$$

where the matrix

$$\hat{\Omega}^2 = \begin{pmatrix} \Omega_+^2 & 0 & \Omega_+\Omega_- \\ 0 & \Omega_0^2 & 0 \\ \Omega_+\Omega_- & 0 & \Omega_-^2 \end{pmatrix} \quad (6.7)$$

with $\Omega_0^2 = \Omega_+^2 + \Omega_-^2 = \tilde{\Omega}_0^2(1+\cos\theta\cos 2k_L z)$ describes the periodic (with period π/k_L) lattice potential while coupling the ground states with $M_F = \pm 1$.

Previously mentioned coupled ground states that are coupled via V and Λ type transitions result in two orthogonal Bloch eigenmodes denoted by 0 and Λ indices respectively. Further investigations of this system are done for $\Delta < 0$ and $\theta \approx 0$ where we can safely assume that atoms will remain in the lowest Bloch bands as a result of the relatively large band gap in comparison to their kinetic energies. Within this approximation, the atomic field operator can be expanded in terms of the site localized Wannier basis as it was investigated in Section 5.2.3. This expansion can be written as

$$\hat{\mathbf{\Psi}}(z) = \sum_i \sum_{\sigma=0,\Lambda} e^{i\varphi_{\sigma i}}\mathbf{W}_{\sigma i}(z)\hat{a}_{\sigma i} \quad (6.8)$$

where $\mathbf{W}_{\sigma i}(z) = \mathbf{W}_\sigma(z - z_i)$ are three-component Wannier spinors of the lowest band and i, j label the sites of the one-dimensional periodic lattice. Here $\hat{a}_{\sigma i}$ is the Bose annihilation operator for the σ mode at the i^{th} site. The phases $\varphi_{\sigma i}$ are determined by the minimal energy requirement of the Bose-Hubbard Hamiltonian and we will give them later in this section. The Wannier spinors satisfy the orthonormality condition

$$\int dz \mathbf{W}^\dagger_{\sigma i}(z)\cdot\mathbf{W}_{\sigma j}(z) = \delta_{ij}\delta_{\sigma\sigma'} \quad (6.9)$$

and they can be calculated by solving the Schrödinger equation with the Hamiltonian in Eq. (6.6) with adjusting the inter-atomic interactions to zero ($g_{a,s} = 0$). These Wannier spinors are in the form

$$\mathbf{W}_{0i} = \begin{pmatrix} 0 \\ W_{0i} \\ 0 \end{pmatrix}, \quad \mathbf{W}_{\Lambda i} = \begin{pmatrix} W_{+i} \\ 0 \\ W_{-i} \end{pmatrix}. \quad (6.10)$$

As was done in the previous chapter, with assuming hopping only between the nearest lattice sites and taking into account only the on-site interactions, if we put the Wannier expansion of Eq. (6.8) into the Hamiltonian (6.6), we arrive at the Bose-Hubbard Hamiltonian

$$\begin{aligned}\hat{H}_{BH} &= -\sum_{\sigma=0,\Lambda}|J_\sigma|\sum_{\langle i,j\rangle}\hat{a}^\dagger_{\sigma i}\hat{a}_{\sigma j}+\sum_{\sigma=0,\Lambda}\frac{U_\sigma}{2}\sum_i\hat{n}_{\sigma i}(\hat{n}_{\sigma i}-1)+K\sum_i\hat{n}_{0i}\hat{n}_{\Lambda i}\\ &-\frac{|P|}{2}\sum_i(\hat{a}^\dagger_{0i}\hat{a}^\dagger_{0i}\hat{a}_{\Lambda i}\hat{a}_{\Lambda i}+\hat{a}^\dagger_{\Lambda i}\hat{a}^\dagger_{\Lambda i}\hat{a}_{0i}\hat{a}_{0i})-\delta\sum_i\hat{n}_{0i}-\mu\sum_{\sigma=0,\Lambda}\sum_i\hat{n}_{\sigma i},\end{aligned}\tag{6.11}$$

where

$$J_\sigma=-\int dz\mathbf{W}^\dagger_{\sigma,i+1}(z)\cdot\left(-\frac{\hbar^2}{2m}\frac{\partial^2}{\partial z^2}+\frac{\hbar}{\Delta}\hat{\Omega}^2\right)\cdot\mathbf{W}_{\sigma,i}(z)\tag{6.12}$$

is the tunnelling parameter,

$$U_0=g_s\int dz|W_{0i}|^4,$$

$$U_\Lambda=\int dz[(g_s+g_a)(|W_{+i}|^2+|W_{-i}|^2)^2-4g_a|W_{+i}|^2|W_{-i}|^2],$$

$$K=(g_s+g_a)\int dz|W_{0i}|^2(|W_{+i}|^2+|W_{-i}|^2),$$

$$P=2g_a\int dz(W^*_{0i})^2W_{+i}W_{-i}\tag{6.13}$$

are parameters from the repulsive density-density interaction of condensed atoms and the spin-exchange interaction. In addition,

$$\begin{aligned}\delta &= \int dz\mathbf{W}^\dagger_{\Lambda,i}(z)\cdot\left(-\frac{\hbar^2}{2m}\frac{\partial^2}{\partial z^2}+\frac{\hbar}{\Delta}\hat{\Omega}^2\right)\cdot\mathbf{W}_{\Lambda,i}(z)\\ &-\int dz\mathbf{W}^\dagger_{0,i}(z)\cdot\left(-\frac{\hbar^2}{2m}\frac{\partial^2}{\partial z^2}+\frac{\hbar}{\Delta}\hat{\Omega}^2\right)\cdot\mathbf{W}_{0,i}(z)\end{aligned}\tag{6.14}$$

parameterizes the energy difference between the electronic internal states $\sigma=0$ and $\sigma=\Lambda$. μ is the chemical potential and $\hat{n}_{\sigma i}=\hat{a}^\dagger_{\sigma i}\hat{a}_{\sigma i}$ is the number operator for the i^{th} site. In addition, the parameters J_σ, U_σ, K and P can be changed by varying the laser intensity that is proportional to $\tilde{\Omega}_0^2$ or angle θ. The dependence of the these parameters on angle θ is given in Figure 6.1. The parameter P becomes for positive or negative depending on g_a.

As we mentioned earlier, the phases $\varphi_{\sigma i}$ are determined by the minimal energy requirement of the Hamiltonian (6.11). They become [108]

$$\varphi_{\sigma i+1}=\begin{cases}\varphi_{\sigma i}, & \text{if } J_\sigma>0\\ \varphi_{\sigma i}\pm\pi, & \text{if } J_\sigma<0\end{cases},\quad \varphi_{0i}=\begin{cases}\varphi_{\Lambda i}, & \text{if } g_a<0\\ \varphi_{\Lambda i}\pm\pi/2, & \text{if } g_a>0\end{cases}\tag{6.15}$$

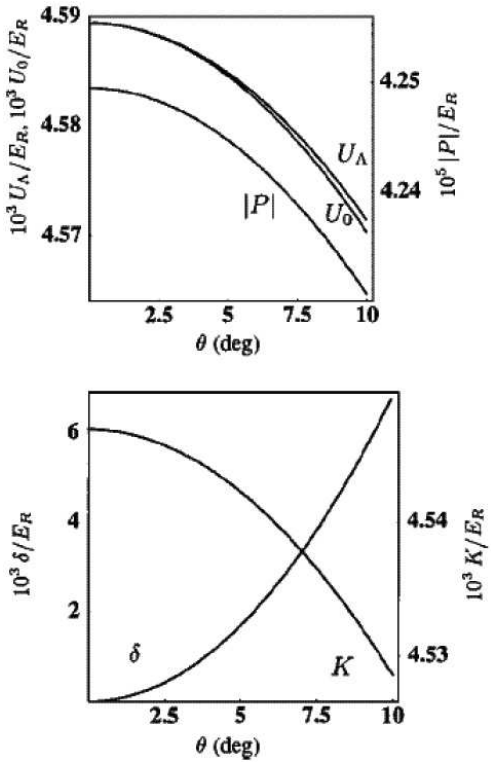

Figure 6.1: Dependence of the parameters in the Bose-Hubbard Hamiltonian (6.11) on θ. The parameters are given in units of recoil energy E_R. The figure is taken from Ref. [108]

6.1.2 Mean field approximation

In the mean-field approximation [133] with $\psi_\sigma = \langle \hat{a}_{\sigma j} \rangle$ assumed real [108], we substitute

$$\hat{a}^\dagger_{\sigma i}\hat{a}_{\sigma j} \approx \psi_\sigma(\hat{a}_{\sigma j} + \hat{a}^\dagger_{\sigma i}) - \psi^2_\sigma, \tag{6.16}$$

into the Hamiltonian (6.11), and arrive at

$$\begin{aligned}\hat{H}^{\rm MF}_{BH} &= -2\sum_{\sigma=0,\Lambda} J_\sigma[(\hat{a}_\sigma + \hat{a}^\dagger_\sigma)\psi_\sigma - \psi^2_\sigma] + \sum_{\sigma=0,\Lambda}\frac{U_\sigma}{2}\hat{n}_\sigma(\hat{n}_\sigma - 1) + K\hat{n}_0\hat{n}_\Lambda \\ &\quad -\frac{|P|}{2}(\hat{a}^\dagger_0\hat{a}^\dagger_0\hat{a}_\Lambda\hat{a}_\Lambda + \hat{a}^\dagger_\Lambda\hat{a}^\dagger_\Lambda\hat{a}_0\hat{a}_0) - \delta\hat{n}_0 - \mu\sum_{\sigma=0,\Lambda}\hat{n}_\sigma,\end{aligned} \tag{6.17}$$

a system of many independent sites. In the above, we have omitted the site index i so that effectively, the optical lattice model is reduced to a collection of single site problems. Although mean-field theory (MFT) is believed to be not well suited to examine quantum correlations in many body systems, we shall nevertheless use it here. The cost is that MFT would wipe away quantum correlations between the sites. On the other hand, in the case of spinor BEC, quantum correlations among the particles survive even within the MFT, due to the fact that MFT still respects the quantum nature of spin components in a single lattice site and thus, mean field ground state can still be found to be entangled. The question

we address here is how the type and amount of the entanglement among the particles in a single lattice site would change when the whole lattice system undergoes quantum phase transitions and the use of MFT is sufficient for this question.

In order to test the validity of MFT that we use in our model, we studied a simple lattice model having two sites. We used the Bose-Hubbard Hamiltonian in (6.11) and i runs from 1 to 2 with the periodic boundary conditions. The purpose of this calculation is to investigate the effect of inter-site interaction on the single-site state. The exact ground state calculations were done by using those parameter values corresponding to $n = 1$ and $n = 2$ Mott phases in the phase diagrams for different parameter regimes ($P > 0$ and $P < 0$) in the case of $\theta = 0$ and for a small θ value. Once the exact two-site ground state is determined, we calculate the one-site density matrix by tracing out the other site. Following this procedure, the overlap of ground states from MFT and exact two-site model can be computed. Our results show that most of these overlap values are above 0.95, confirming the success of MFT in calculating one-site ground states and so that using it to quantify correlations among particles in a single site.

In general, many-body wave functions are too complicated to express explicitly, but MFT allows for writing down analytical wave functions of the ground states and hence one can gain valuable insights into the quantum correlations in such complex many-body systems such as spinor condensates in optical lattices. This insight should serve as a guide even for comprehending quantum correlations among the lattice sites which require beyond MFT calculations.

6.1.3 Pseudo-spin algebra

A general spin-1 system is described by the symmetry group SU(3). In the model considered here, a reduced two-mode description for the two coupled ground states is represented by a pseudo-spin-1/2 algebra, effectively the isospin subgroup of SU(3) [108]. The corresponding generators of the SU(2) isospin algebra are given by [108]

$$\begin{aligned}
\hat{T}_1 &= \frac{1}{2}(\hat{a}_\Lambda^\dagger \hat{a}_0 + \hat{a}_0^\dagger \hat{a}_\Lambda), \\
\hat{T}_2 &= \frac{\mathrm{i}}{2}(\hat{a}_\Lambda^\dagger \hat{a}_0 - \hat{a}_0^\dagger \hat{a}_\Lambda), \\
\hat{T}_3 &= \frac{1}{2}(\hat{a}_0^\dagger \hat{a}_0 - \hat{a}_\Lambda^\dagger \hat{a}_\Lambda),
\end{aligned} \tag{6.18}$$

in terms of which the mean-field Hamiltonian (6.17) can be expressed as [137]

$$\hat{H}_{BH}^{\mathrm{MF}} = -2 \sum_{\sigma=0,\Lambda} J_\sigma[(\hat{a}_\sigma + \hat{a}_\sigma^\dagger)\psi_\sigma - \psi_\sigma^2] + \frac{U_\Sigma}{2}\hat{T}_3^2 + (K - |P|)\hat{T}_1^2 + (K + |P|)\hat{T}_2^2$$

$$+\frac{U_\Sigma}{8}\hat{n}^2-\left(\frac{K}{2}+\mu+\frac{U_\Sigma}{4}+\frac{\delta}{2}\right)\hat{n}-\left(\frac{\Delta U}{2}+\delta\right)\hat{T}_3+\frac{\Delta U}{2}\hat{n}\hat{T}_3, \tag{6.19}$$

where $\Delta U = U_0 - U_\Lambda$, $U_\Sigma = U_0 + U_\Lambda$, and $\hat{n} = \hat{n}_0 + \hat{n}_\Lambda$. Spin dependent interaction terms in this Hamiltonian emulates that of the generalized Lipkin-Meshkov-Glick (LMG) model [138, 139], or its special case of the two-axis twisting model [110]. Such models are capable of generating spin squeezing [110] and multiparticle entanglement [140, 141, 139]. Our model above, includes tunnelling and collision effects in addition to the generalized LMG interaction terms.

When the lattice parameter $\theta = 0$, the two modes have the same energy and $J_0 = J_\Lambda = J$, $U_0 = U_\Lambda = U$, $K = U + P$, and $\delta = 0$ [108]. The simplified Hamiltonian (6.17) takes the following form [137]

$$\hat{\mathcal{H}}_{\mathrm{af(f)}} = -2J\sum_{\sigma=0,\Lambda}[(\hat{a}_\sigma^\dagger+\hat{a}_\sigma)\psi_\sigma-\psi_\sigma^2]+2\left(U\hat{T}^2+P\hat{T}_{2(1)}^2\right)+\alpha\hat{n}, \tag{6.20}$$

for both antiferromagnetic ($P > 0$) and ferromagnetic ($P < 0$) interactions [135], where we have used $\hat{T}^2 = \hat{n}^2/4 + \hat{n}/2$ for the collision interaction in terms of the total isospin operator $\hat{T}^2$ with $\alpha = -3U/2 - P/2 - \mu$. The spin interaction now reduces to that of a single-axis twisting type [110].

The above considerations show that our model allows for the investigation of effects due to tunnelling and collision on spin squeezing induced by either the two-axis twisting interaction as in the generalized LMG model or the single-axis twisting interaction in the simplified case. In the general case of the LMG model, particle entanglement thus exists for atoms in the non-degenerate ground state modes, which become degenerate for the special case of a lattice with $\theta = 0$.

6.2 Spin Squeezing and Quantum Entanglement

Squeezed spin states defined by Kitagawa and Ueda [110] is widely used in atomic physics, especially in the context of particle correlation and entanglement. A criterion was found recently connecting many atom entanglement and correlation originally from atoms in a Bose-Einstein condensate (BEC) [111]. If the squeezing parameter

$$\xi_\alpha^2 = \frac{N(\Delta J_\alpha)^2}{\langle J_\beta\rangle^2+\langle J_\gamma\rangle^2}, \tag{6.21}$$

is smaller than 1, the two mode bosonic many atom state under consideration is spin squeezed along the direction of α. $\vec{J}$ is the total pseudo spin operator, while α, β, and γ denote three orthogonal axes. The condition for $\xi_\alpha^2 < 1$ coincides with the non-separability criterion of a density matrix for N two state boson [111]. Thus ξ_α^2 can be used to measure quantum entanglement in the two state atomic system discussed above. In our study outlined below, we examine spin squeezing for the on-site isospin algebra by calculating the variance and

expectation values of the corresponding generators T_i defined in (6.18). Our results show clearly the existence of quantum correlations between atoms on the same lattice site.

To identify pairwise entanglement in our many-body system, we can make use of a direct relationship between concurrence [38, 39] that we discussed in Section 2.6.2.2, which is well-known and represents a widely accepted measure of bipartite entanglement, and spin squeezing criterion [142, 143]. Thus, we take (6.21) as an indicator for two-particle entanglement. We will in addition also calculate the concurrence and compare the results with the squeezing parameter (6.21).

In view of the significant difficulties of measuring spin squeezing along any arbitrary direction α, our investigation will focus on the simplest case of a single orthogonal configuration with three fixed axes. Other orthogonal axes configurations may be sequentially searched for if the optimal squeezing is to be found. For this aim we only need to rotate the coordinate system about each of the axes by an angle ϕ. For example if the rotation is about the axis-3, ξ_3^2 remains the same, while the squeezing parameters for the new axis-1 and axis-2 become

$$\begin{aligned} \xi_{1'}^2 &= N\frac{\Delta T_1^2\cos^2\phi+\Delta T_2^2\sin^2\phi-\sin\phi\cos\phi\langle T_1,T_2\rangle}{\langle T_3\rangle^2+(\langle T_1\rangle\sin\phi+\langle T_2\rangle\cos\phi)^2}, \\ \xi_{2'}^2 &= N\frac{\Delta T_1^2\sin^2\phi+\Delta T_2^2\cos^2\phi+\sin\phi\cos\phi\langle T_1,T_2\rangle}{\langle T_3\rangle^2+(\langle T_1\rangle\cos\phi-\langle T_2\rangle\sin\phi)^2}, \end{aligned} \tag{6.22}$$

where $\langle T_i,T_j\rangle=\langle T_iT_j+T_jT_i\rangle-2\langle T_i\rangle\langle T_j\rangle$.

6.3 Results

6.3.1 Numerical method

The mean-field Bose-Hubbard Hamiltonian in (6.17) has been used to examine the phase transition between the superfluid and Mott-insulator phases [108], with ψ_σ denoting the order parameter for the σ mode. The superfluid phase for the σ component is identified with $\psi_\sigma\neq 0$. As we discussed in Section 5.3.2, in the superfluid state the tunnelling term J_σ is large and dominates the Hamiltonian. As a result the ground state corresponds to the single particle wave function of all σ-type atoms extended over the whole lattice, with each site being a coherent superposition of Fock number states [102]. In the Mott phase, on the other hand, the interaction term dominates so that the ground state exhibits minimal number fluctuation and corresponds to a product of atom Fock number states at each lattice site, which in turn gives $\psi_\sigma=0$ [102].

We have performed numerical diagonalization of the mean-field Hamiltonian (6.17) by

using a set of states expanded in terms of the product of individual atom number states

$$|\Omega\rangle = \sum_{n_0=0}^{N} \sum_{n_\Lambda=0}^{N} c_{n_0 n_\Lambda} |n_0\rangle |n_\Lambda\rangle. \tag{6.23}$$

While performing this diagonalization, two different regimes with respect to the same parameter P must be carried out. One is for a positive antisymmetric coupling ($g_a > 0$), with a corresponding antiferromagnetic ground state, where individual spins are anti-aligned due to spin-exchange interaction. The other case is ferromagnetic for a negative spin exchange interaction ($g_a < 0$). In addition, we explore the dependence of our results on the small, but non-vanishing lattice parameter θ, which introduces a spin dependent lattice potential.

We study the parameter regions corresponding to those considered in Ref. [108]. The values of the parameters in Hamiltonian (6.17), which are needed for numerical computation, are thus read from the Figure 6.1, with J/U picked to ensure the system have full access to the $n = 2$ Mott regime, but barely enters the $n = 3$ Mott phase. θ is taken to be small and δ values used are for the range of $0 \leq \theta \leq 1$. We study the degenerate ($\theta = 0$) and non-degenerate cases ($\theta \neq 0$) separately. From the initial values of the order parameters ψ_0 and ψ_Λ we compute the diagonal basis and the corresponding ground state. This ground state then allows us to calculate the new order parameters and to compare with the initial values. This procedure is iterated to reach a self-consistent solution, with which it becomes straightforward to calculate the expectation values and the second moments of the operators in (6.18).

To conveniently calculate the squeezing parameter ξ^2 (6.21), we use the average total occupation number $\langle \hat{n} \rangle$ for each type of interactions to label the different phases instead of relying on the total number of atoms N (per site). This implicitly assumes that the squeezing parameter (6.21) remains a valid criterion of quantum entanglement even for non-integer occupation numbers such as in the superfluid phase. This assumption does not introduce any inconvenience in a Mott phase since the ground state consists of Fock states with equal total number of particles, *i.e.*, definite spin and thus $\langle \hat{n} \rangle$ becomes an integer. In the superfluid phase, we justify the use of a non-integer $\langle \hat{n} \rangle$ in the following manner. In this section, we calculate the squeezing parameter in two different ways for each case. The first method uses $\langle \hat{n} \rangle$ directly for the entanglement measure. The second method is analogous in form, but only uses integer values of $\langle \hat{n} \rangle$. For the superfluid phase, instead of talking about separability for states with different total number of particles, we focus on the subspace $n_0 + n_\Lambda = n$ block and investigate its correlation. This becomes a meaningful measure when the block we use is the one with the nearest integer total number of particles to $\langle \hat{n} \rangle$. This method has a similar nature as the superselection rules mentioned in Ref. [109] and in Ref. [144] since the projection of the Hilbert space onto a subspace of fixed particle number is considered. Both methods are found to give similar behaviors for the superfluid and the Mott insulator phases. We provide results from the first method in our discussion because they respect the collective nature of the superfluid state and emphasize particle number fluctuations.

There also exist states for which spin squeezing parameter cannot be readily used to characterize their correlation properties. An example is the maximally entangled states (MES) in Ref. [145], which are not squeezed spin states according to the criterion in (6.21). In this case, it is inadequate to talk about squeezing, since the uncertainty in the perpendicular components to the mean isospin vector are meaningless as the denominator for the squeezing measure (6.21) vanishes for all axes. In addition, there exist other states, although whose averaged mean isospin are nonzero, the expectation values for the two components in the denominator might vanish, also making the spin squeezing parameter ξ_i^2 not well defined. In our studies, we find that these states happen only in certain Mott phases, where exact wave functions are available either analytically in the spin [135] or Fock basis [108]. As such, their quantum entanglement properties can be discussed directly using other criteria.

In order to quantify the pairwise quantum correlations both in the superfluid and Mott-insulator regimes, in addition to the squeezing parameter, we use the well-known criterion concurrence [38, 39] discussed in Section 2.6.2.2. For a given two-party state ρ, this measure was equal to

$$C(\rho) \equiv \max\{0, \lambda_1 - \lambda_2 - \lambda_3 - \lambda_4\}, \tag{6.24}$$

where λ_i's are the square roots of the eigenvalues of $\rho\tilde{\rho}$ in decreasing order where

$$\tilde{\rho} = (\sigma_y \otimes \sigma_y)\rho^*(\sigma_y \otimes \sigma_y). \tag{6.25}$$

For the $n = 1$ Mott-insulator phase, this measure is trivial since there is only one particle present. When it comes to the $n = 2$ Mott phase, concurrence clearly quantifies pairwise correlations between the two atoms at the same lattice site. In the superfluid phase, the ground state is a superposition of Fock states with different number of atoms or isospin states with different isospins, we again focus on the subspace with the nearest integer total number of particles $n_0 + n_\Lambda = n$. If the nearest integer is smaller than two, then concurrence is zero. If it is equal to two, the concurrence is simply calculated. When it is equal to three, the three-particle ground state is symmetrized in the first quantization picture and we use reduced two-body density matrix to calculate concurrence.

We report below our investigation of quantum entanglement in our model system for the two regimes: antiferromagnetic and ferromagnetic interactions.

6.3.2 Ferromagnetic regime

For ferromagnetic interaction with $P < 0$, for $\theta = 0$, and a fixed J/U value, the dependence of the order parameters ψ_0 and ψ_Λ on the quantity μ/U is shown in Figure 6.2. We determine the phase of the system for any μ/U value by looking at the order parameter of each component.

Quantum correlations on a single lattice site is evidenced by evaluating the squeezing

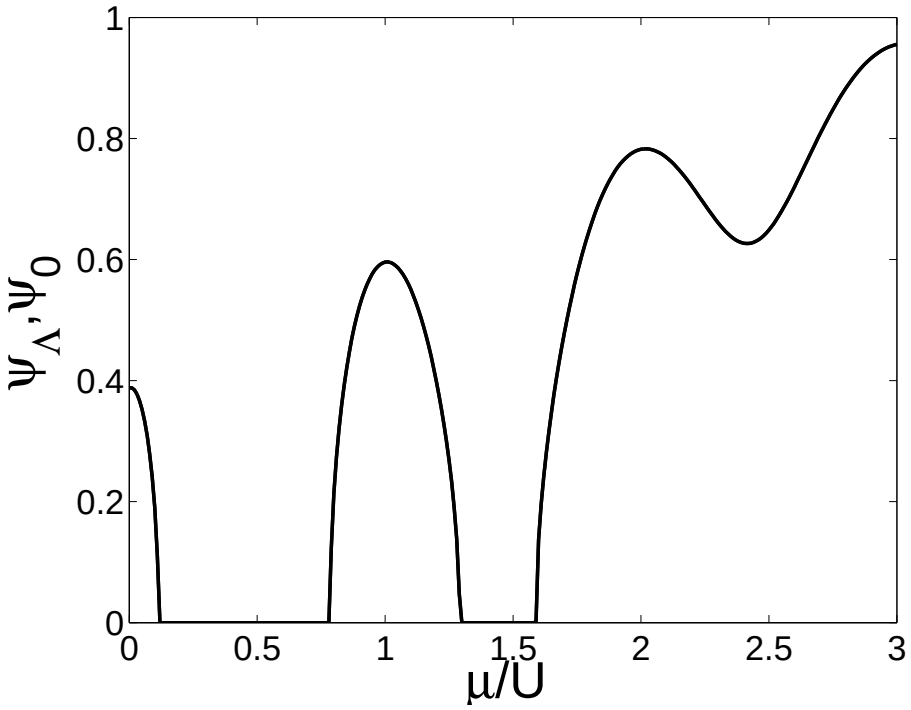

Figure 6.2: The dependence of the order parameters on the value of μ/U for $\theta = 0$, $J/U = 0.455 \times 10^{-1}$, and $P/U = -0.926 \times 10^{-2}$ in the ferromagnetic regime. The vanishing of the order parameters matches closely with the appearance of Mott-insulator phases for the corresponding component.

parameter (6.21). In the superfluid regime, numerical calculations, taking into account the minimization with respect to coordinate rotations, yield $\xi_i^2 > 1$. So there is no particle entanglement in the superfluid phase of a ferromagnetically interacting system when $\theta = 0$. Although, this situation deserves to be more carefully analyzed for those values of μ/U that correspond to Mott-insulator phases.

The spin squeezing parameter is not defined for the zero particle ($n = 0$) ground state $|0, 0\rangle$, the trivial case of no particle entanglement without any particles. When $\theta = 0$, the single particle ($n = 1$) ground states $|10\rangle$ and $|01\rangle$ are degenerate [108] and can be written as $|g\rangle = \cos x|01\rangle + \sin x \exp(\mathrm{iy})|10\rangle$, where $x, y \in [0, 2\pi]$ are arbitrary angles, parameterizing the manifold of the ground state family. We find $\langle T_1\rangle = (1/2)\sin 2x \cos y$, $\langle T_2\rangle = (-1/2)\sin 2x \sin y$, and $\langle T_3\rangle = (-1/2)\cos 2x$. The spin fluctuations are $\langle \Delta T_1^2\rangle = (1/4)(1 - \sin^2 2x \cos^2 y)$, $\langle \Delta T_2^2\rangle = (1/4)(1 - \sin^2 2x \sin^2 y)$, and $\langle \Delta T_3^2\rangle = (1/4)(\sin^2 2x)$. Thus we obtain $\xi_i^2 = 1$ in any direction $i = 1, 2, 3$, for any member of the ground state manifold. The ground state, expressed in the spin representation [135], could be written as an arbitrary superposition of $|T = 1/2, T_1 = \pm 1/2\rangle$ spin states. We write $|g\rangle = |x, y\rangle = \cos(x/2)|1/2, 1/2\rangle + \sin(x/2)\exp(iy)|1/2, -1/2\rangle$ for the ground state in spin representation. Projection of the total spin onto the (x, y) direction gives the spin component $S_{x,y} = \sin x \cos y T_2 + \sin x \sin y T_3 + \cos x T_1$, whose eigenstate is $|x, y\rangle$ with eigenvalue $1/2$, such that $S_{x,y}|x, y\rangle = (1/2)|x, y\rangle$. Such a state is called a coherent spin state (CSS) [110].

The ground state $|g\rangle$ is identified as a pure state of a spin-1/2 system, and as such is a CSS. There exists no other spin to be correlated with, so that $|g\rangle$ cannot be a squeezed spin state (SSS). Particles in a CSS are correlated as all spin 1/2 constituents atoms are pointing along the same direction; although they remain separable, *i.e.*, they are not entangled.

On the other hand, the $n = 1$ Mott state could become *mode entangled* [146] for some α and β. Mode entanglement is a different concept from particle entanglement considered here and could be useful for different applications [146]. It corresponds to entanglement in the second quantization picture, while particle entanglement is associated with the inseparability of the wave function, or density matrix, in the first quantization.

Similarly, the ground states for the $n = 2$ Mott phase are also degenerate for $\theta = 0$. As such they form a manifold represented by $|g\rangle = \cos x|11\rangle + \sin x \exp(\mathrm{i}y)|b\rangle$, where $|b\rangle = (|02\rangle+|20\rangle)/\sqrt{2}$. In this case, $\langle T_1\rangle = \sin 2x \cos y$ and $\langle T_{2,3}\rangle = 0$. The variances are calculated to be $\langle \Delta T_1^2\rangle = 1 - \sin^2 2x \cos^2 y$, $\langle \Delta T_2^2\rangle = \cos^2 x$, and $\langle \Delta T_3^2\rangle = \sin^2 x$. ξ_1^2 becomes either undetermined (a 0/0 form) or ∞ due to vanishing denominators. If we calculate ξ_1^2 after a coordinate rotation by ϕ about the axis-3, we find $\xi_{1'}^2$. Minimizing it with respect to ϕ, we finally get $(\xi_{1'}^2)_{\min} = 1/(2\sin^2 x \cos^2 y)$ with its minimum value at $\phi = \pm\pi/2$. We find $\xi_3^2 = 1/(2\cos^2 x \cos^2 y)$ and $\xi_2^2 = 1/(2\sin^2 x \cos^2 y)$. For some values of x and y, $\xi_{2,3}^2 < 1$ is satisfied. Hence, particle entanglement exists for some members of the ground state manifold. This is consistent with the fact that each degenerate ground state $|11\rangle$ and $|b\rangle$ is particle entangled. For parameters x and y specifying a dominant contribution from a particular degenerate component in $|g\rangle$, particle entanglement is expected. In the spin representation, the ground state is an arbitrary superposition of $|T = 1, T_1 = \pm 1, 0\rangle$. In contrast to the spin-1/2 case of the $n = 1$ Mott phase, now SSS (squeezed spin state), where all particles are entangled, can be found in the ground state family.

When we analyze ferromagnetic regime by calculating the concurrence in light of the discussion in Section 6.3.1, it is found to be zero for all μ/U values except those for the $n = 2$ Mott phase. In this case, the ground state is an arbitrary superposition of two degenerate maximally entangled states, with the concurrence for each state being equal to one. But the concurrence for the ground state manifold mentioned above becomes $C(|g\rangle) = [1 - (1/2)\sin^2(2x)\cos(2y)]^{1/2}$, which is larger than zero for some values of x and y. And this indicates the possibility of pairwise entanglement for certain ground states.

Now we look at the situation when θ takes a small but nonzero value. In this case the relations $J_0 \approx J_\Lambda = J$, $U_0 \approx U_\Lambda = U$, and $K = U + P$ remain valid. However, the parameter δ becomes nonzero, due to the splitting between the two ground state modes: $\sigma = 0$ and $\sigma = \Lambda$. This causes the dependence of the order parameters on μ/U to change as illustrated in Figure 6.3. Note the difference between the order parameters for the two modes.

For the general case with $\theta \neq 0$, performing minimization over the axis rotations shows that the optimal squeezing occurs for the unrotated coordinate axes. By examining the

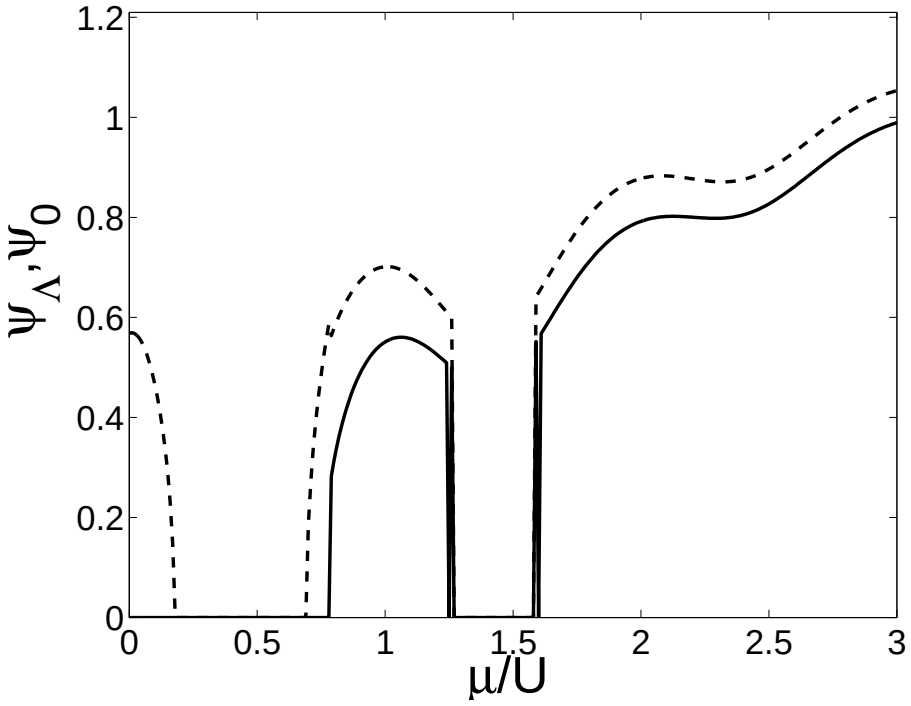

Figure 6.3: The dependence of order parameters for the two modes vs μ/U for a small nonzero θ in the ferromagnetic regime with $J/U = 0.625 \times 10^{-1}$, $P/U = -0.926 \times 10^{-2}$, and $\delta/U = 0.327 \times 10^{-2}$. The solid line denotes ψ_Λ while the dashed line refers to ψ_0.

spin squeezing parameter as a function of μ/U numerically, we find that particles are not entangled in the superfluid regime. We thus look for particle entanglement in the Mott phases.

With a small θ, the degeneracy in the ground states in the Mott phase is removed. In the $n = 1$ Mott-phase, the ground state becomes $|g\rangle = |n_0 = 1, n_\lambda = 0\rangle$. For this state, the mean spin is along the direction of the axis-3 with $\langle T_3 \rangle = 1/2$ and $T_{1,2} = 0$. The spin fluctuations are given by $\langle \Delta T_{1,2}^2 \rangle = 1/4$ and $\langle \Delta T_3^2 \rangle = 0$. Employing a rotation by ϕ about the axis-3, we find that $\xi_{1',2'}^2 = 1$, *i.e.*, the ground state is a CSS.

For the $n = 2$ Mott-phase, we have a non-degenerate ground state of the form $|g\rangle = a|02\rangle + b|20\rangle$ [108] with

$$a = \left\{ \frac{1}{2} \left[1 - \frac{\Delta U - 2\delta}{\sqrt{(\Delta U - 2\delta)^2 + 4P^2}} \right] \right\}^{1/2},$$

$$b = \left\{ \frac{1}{2} \left[1 + \frac{\Delta U - 2\delta}{\sqrt{(\Delta U - 2\delta)^2 + 4P^2}} \right] \right\}^{1/2}. \tag{6.26}$$

For such a state, as in the $n = 1$ Mott phase, the mean spin is pointed along the axis-3 with $\langle T_{1,2} \rangle = 0$ and $\langle T_3 \rangle = b^2 - a^2$. Their corresponding fluctuations are found to be

$\langle \Delta T_1^2 \rangle = (a+b)^2/2$, $\langle \Delta T_2^2 \rangle = (a-b)^2/2$, and $\langle \Delta T_3^2 \rangle = 1-(b^2-a^2)^2$. To determine the optimum noise reduction and spin squeezing, we minimize over rotations about the mean spin (axis-3) direction by an angle ϕ. It is sufficient to consider either one of the rotated $1'$ or $2'$ axes so that a single rotation angle dependent spin squeezing parameter ξ_ϕ^2 can be found as

$$\xi_\phi^2 = \frac{1+2ab\cos 2\phi}{(b^2-a^2)^2}. \tag{6.27}$$

Its minimum occurs at $\phi = \pm\pi/2$ such that $\xi_{\pm\pi/2}^2 = (1-2ab)/(b^2-a^2)^2$. Assuming a small δ/P, we find $\xi_{\pm\pi/2}^2 \sim 1/2 + \mathrm{O}((\delta/P)^2)$, in agreement with numerical calculation reported in Figure 6.3. Thus, the ground state is particle entangled and spin squeezed.

We again calculate the concurrence values for the phases under consideration. It becomes zero everywhere except $n=2$ Mott phase. In this situation $C(|g\rangle) = 2|ab|$ and for small δ/P values $C(|g\rangle) \sim 1 - \mathrm{O}((\delta/P)^2)$. So that the results are in complete agreement with those of squeezing parameter.

6.3.3 Antiferromagnetic regime

In this case, the atomic interaction parameter P is positive. In Figure 6.4, the order parameters are plotted as a function of μ/U at $\theta = 0$.

Similar to the ferromagnetic regime, we first test the existence of spin squeezing for $\theta = 0$. The corresponding minimum squeezing parameter, ξ_2^2 for the fixed axes is shown in Figure 6.5. In contrast to the ferromagnetic case, squeezing is observed for the superfluid phase as well. In numerical calculations, we also rotate the coordinate system to see whether correlations can be enhanced for some angles. The optimum squeezing is found to occur for the fixed axes configurations.

In the $n=1$ Mott-phase, the ground state is a coherent superposition of $|10\rangle$ and $|01\rangle$, which identifies a manifold of any pure state for spin-1/2. The only difference being the quantization axis, it lies along the axis-2, instead of the axis-1. Hence our conclusions for the ferromagnetic case remain applicable. The ground state family is a general CSS and exhibits no squeezing, although mode entanglement can be present.

The $n=2$ Mott insulator state in the antiferromagnetic case, however, is significantly different from the ferromagnetic case considered earlier. It is no longer degenerate as before, and becomes uniquely determined as

$$|g\rangle = \frac{1}{\sqrt{2}}(|20\rangle + |02\rangle), \tag{6.28}$$

instead. For this special superposition state, the mean isospin vector becomes zero, with $\langle T_{1,2,3} \rangle = 0$. Spin fluctuations are found to be $\langle \Delta T_{1,3}^2 \rangle = 1$ and $\langle \Delta T_2^2 \rangle = 0$. Given in the

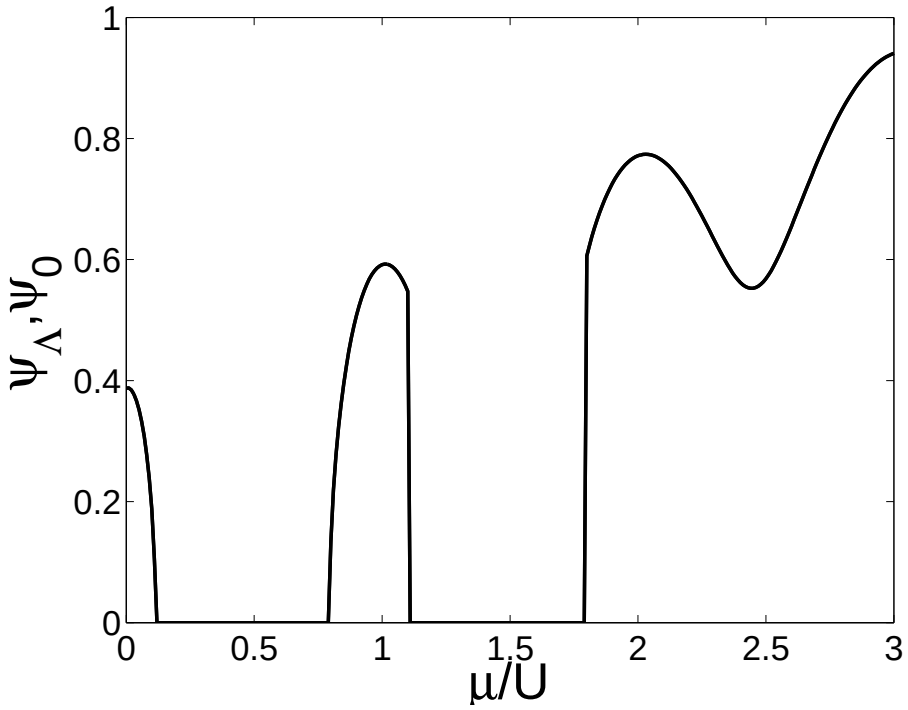

Figure 6.4: The dependence of the order parameters on the values of μ/U for $\theta = 0$ in the antiferromagnetic regime with $J/U = 0.455 \times 10^{-1}$ and $P/U = 0.926 \times 10^{-2}$. The nonzero valued order parameters indicate superfluid phases for the corresponding components.

second quantization form and in the occupation number representation, the mean number of particles in each mode $(0, \Lambda)$ is 1 and the state is mode entangled. In the first quantization, denoting single particle wave functions as $\Psi_{i\sigma}$ for particles $i = 1, 2$ in modes $\sigma = 0, \Lambda$, $|g\rangle$ is found to become $|g\rangle = (1/\sqrt{2})(\Psi_{10}\Psi_{20} + \Psi_{1\Lambda}\Psi_{2\Lambda})$. This state has maximum quantum correlation among the particles and can be identified as a MES [145].

In order to compare the results measured in terms of the calculated concurrence, we show in Figure 6.6 the dependence of concurrence as a function of μ/U.

The presence of particle entanglement in the superfluid phase is reflected by the nonzero values of concurrence for the corresponding μ/U values as shown in Figure 6.6. Having a concurrence of one in the $n = 2$ Mott phase corresponds to the presence of a maximally entangled ground state.

As is done previously for the ferromagnetic case, a small nonzero θ value can be introduced and the system parameters are changed accordingly. The corresponding graph for the order parameters as functions of μ/U are shown in Figure 6.7.

Following the earlier procedure, the minimum squeezing parameter ξ_2^2 is also plotted against μ/U, with the optimized values, corresponding to the fixed coordinate system shown in Figure 6.8.

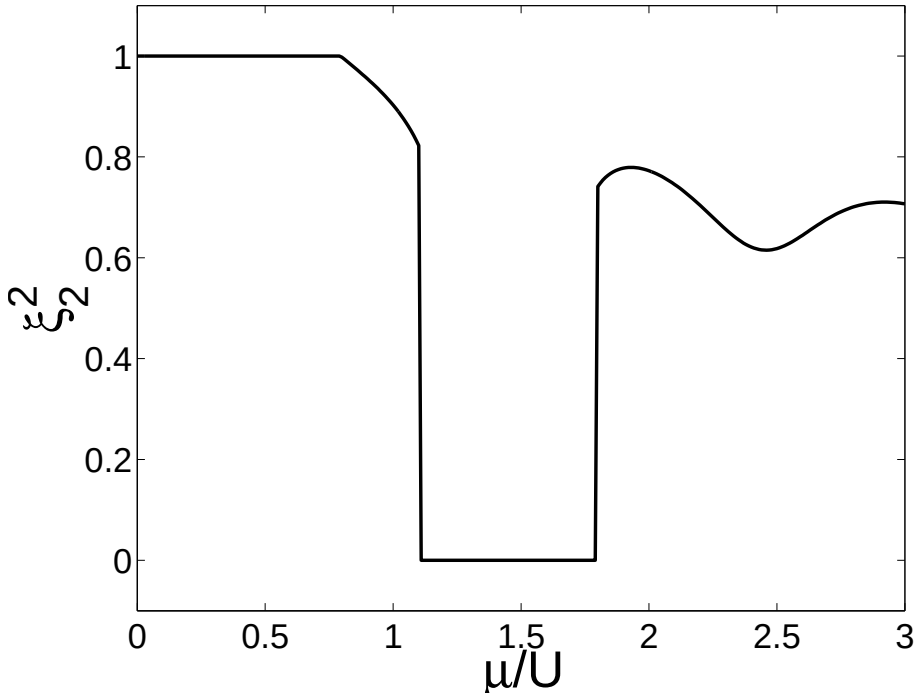

Figure 6.5: The minimum squeezing parameter ξ_2^2 for the fixed axes configuration in the antiferromagnetic regime with $\theta = 0$, $J/U = 0.455 \times 10^{-1}$, and $P/U = 0.926 \times 10^{-2}$. $\xi_2^2 < 1$ denotes spin squeezing for the axis-2.

As in the case of $\theta = 0$, spin squeezing is found to exist for the superfluid phase almost with the same strength. On the other hand, although spin squeezing is detected in the $n = 2$ Mott phase, it is reduced with a nonzero θ. The corresponding ground state for the $n = 2$ Mott phase is the same as in the ferromagnetic case. The MES of the $\theta = 0$ case for the antiferromagnetic interaction becomes a partially entangled state when a small nonzero θ is introduced.

The results from the calculated concurrence as shown in Figure 6.9 are in complete agreement with those from the squeezing parameter. Squeezing is present in the superfluid phase and the maximal entanglement in the $n = 2$ Mott phase becomes partially entangled with the introduction of a small but nonzero θ.

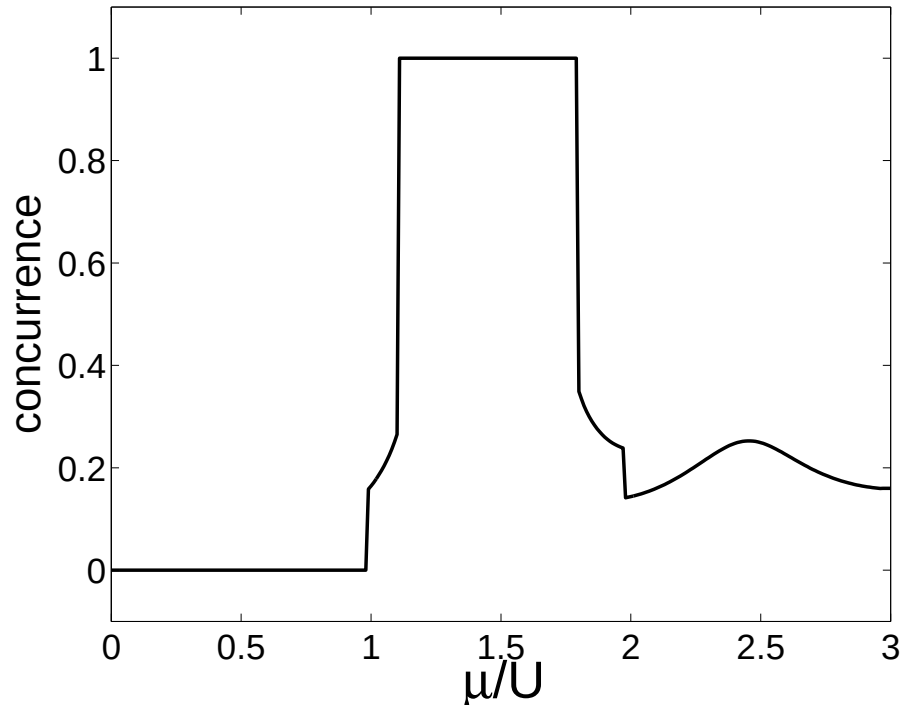

Figure 6.6: Concurrence vs μ/U in the antiferromagnetic regime with $\theta = 0$. The presence of pairwise entanglement is assured if the value of concurrence becomes larger than zero.

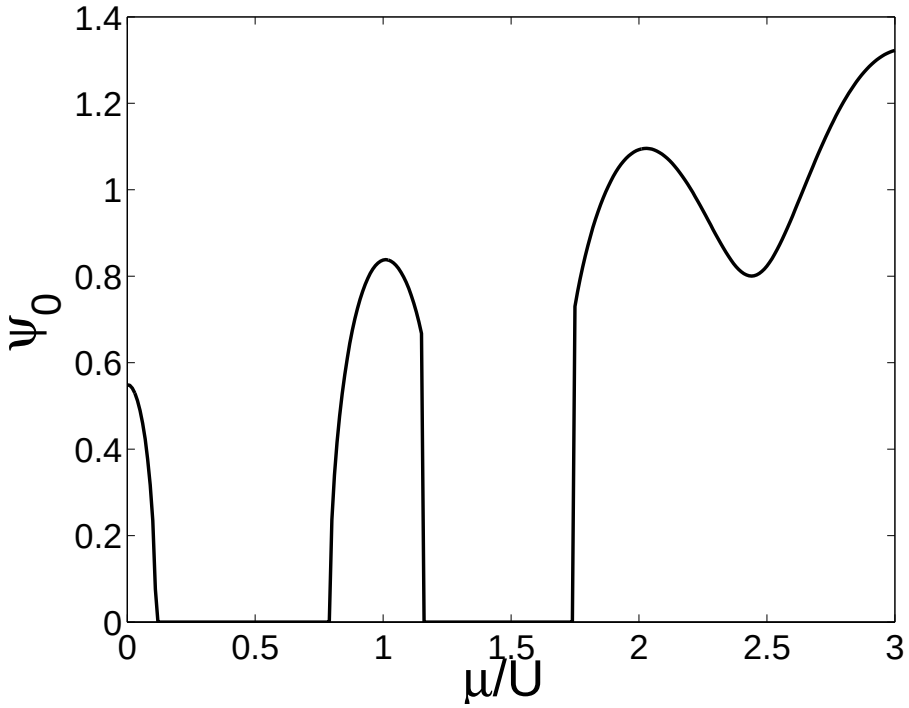

Figure 6.7: The order parameter ψ_0 for the antiferromagnetic regime at a small θ with $J/U = 0.455 \times 10^{-1}$, $P/U = 0.926 \times 10^{-2}$, and $\delta/U = 0.327 \times 10^{-2}$. $\psi_\Lambda = 0$ for these values of interaction parameters.

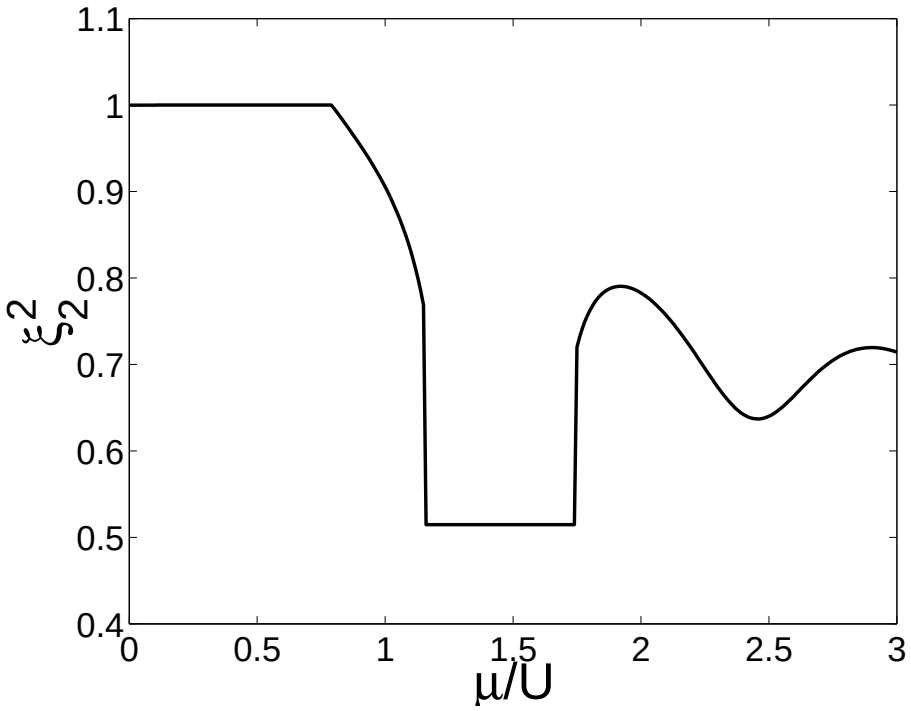

Figure 6.8: The minimum squeezing parameter ξ_2^2 in the antiferromagnetic regime at a small θ in the fixed coordinate system with $J/U = 0.455 \times 10^{-1}$, $P/U = 0.926 \times 10^{-2}$, and $\delta/U = 0.327 \times 10^{-2}$.

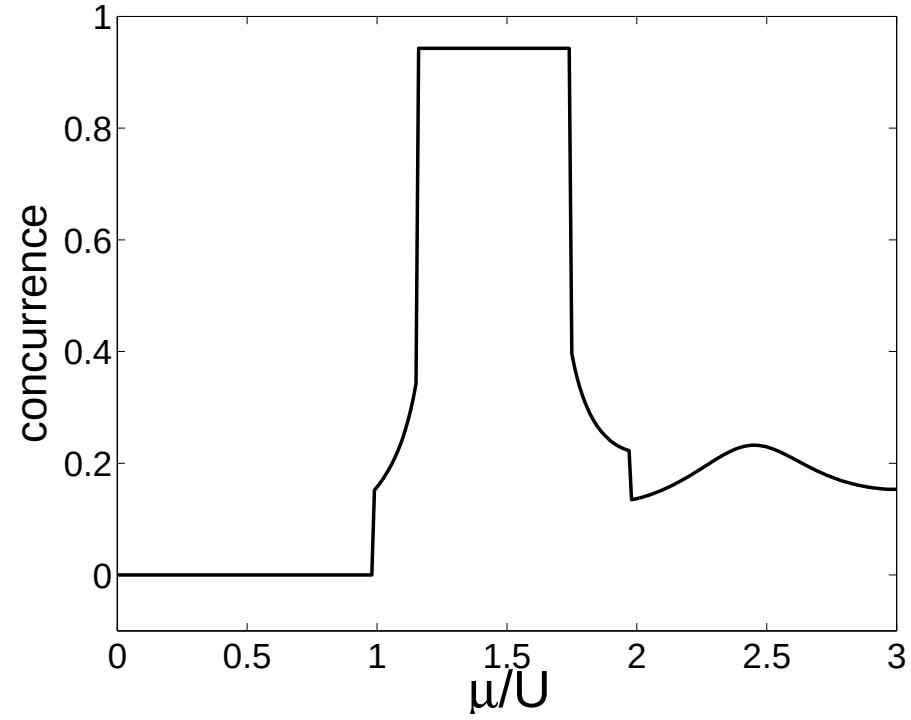

Figure 6.9: Concurrence at a small but nonzero θ in the antiferromagnetic regime. It is seen that part of the superfluid phase contains entangled particles.

Chapter 7

Conclusion

Entanglement, apart from being a scientific curiosity as it was in the early days of quantum theory, is now an indispensable resource for quantum information processing technology. This character of entanglement alone makes it an important subject of research, both in the field of mathematics in its abstract form and in physics through the possible physical applications. One of the most important research area for both fields (mostly for the former one) is to find a reliable and general measure of entanglement. In this regard the present Thesis, in its first part, considers some (and probably most) of the entanglement measures in the available scientific literature. For the last decade, this area of research has been living its most active era and become an industry. As a result there is a large number of proposed measures covering various needs. We first focus on measures for bipartite pure states of finite dimensional systems. Then we summarized the possible extensions and other measures for the more general case of mixed states and multipartite systems. After discussing presumably the most important or widely used ones, we propose a new measure of entanglement by considering dynamical symmetry group approach. According to this approach, for a quantum system under consideration, postulation of a Lie algebra of observables and a representation of this algebra by skew-Hermitian operators is necessary. The corresponding Lie group is called the dynamic symmetry group and a unitary representation of the dynamical group in the state space is quantum dynamical system. By using this construction, we have shown that description of entanglement in a given system requires pre-definition of basic observables and that the entanglement of pure states can be adequately quantified in terms of total variance of all basic observables. The motivation in doing this is to use the quantum fluctuations (strictly nonclassical ones) to quantify the *degree of quantumness*. Our proposed measure can be written as

$$\mu(\psi) = \sqrt{\frac{\mathbb{V}(\psi) - \mathbb{V}_{\text{coh}}}{\mathbb{V}_{\text{ent}} - \mathbb{V}_{\text{coh}}}} \tag{7.1}$$

with $\mathbb{V}(\psi)$ being the total variance of basic observables for state $|\psi\rangle$. Unlike conventional bipartite measure concurrence and three-partite measure 3-tangle, that measure the amount

of entanglement of different groups of correlated parties, our measure gives the total amount of multipartite entanglement, carried by a given state. Other evident virtues of the measure (7.1) are its simple physical meaning, its applicability beyond bipartite systems, and its operational character caused by measurement of quantum uncertainties of well-defined physical observables.

At the same time, this measure cannot be directly applied to calculation of entanglement in mixed states. However, it may be used in the way that has been discussed in Ref. [87] as follows

$$\mu(\rho) = \inf \sum_i p_i \mu(\psi_i).$$

where minimization is calculated over all possible pure state realizations $\{p_i, |\psi_i\rangle\}$.

The physical application part of entanglement research mentioned above is the topic of the second part of the Thesis. In that part, we have investigated quantum correlations between spin-1 bosons with coupled ground states in optical lattices. Both ferromagnetic and antiferromagnetic interactions are considered based on a model, initially developed in Ref. [108], that we believe can be readily adopted to current experimental systems. In addition to characterizing quantum correlations in various quantum phases in terms of coherent and squeezed spin states, and addressing both particle and mode entanglement, the role of lattice parameter in the familiar lin-θ-lin configuration is examined.

We have shown that for ferromagnetic interactions, isospin squeezing (or multi-particle entanglement) is absent in the lattice model of spin-1 bosons in the superfluid phase. The one particle Mott phase is in fact in a CSS, which is not particle entangled, although it displays significant mode entanglement. The two particle Mott state may contain SSS and entangled particles, if one of the degenerate component in the ground state manifold is made dominant. It can be steered into a particle entangled state by introducing a nonzero θ to lift the degeneracy, while the CSS of the $n = 1$ Mott phase or the superfluid phase remains unentangled. The path to quantum entanglement is through the well known single axis twisting type nonlinear interaction [110] for the degenerate ($\theta = 0$) case. With a nonzero θ, quantum entanglement is generated from a generalized LMG interaction, which includes a two-axis twisting type of spin-spin nonlinear interaction.

For antiferromagnetic interactions, spin squeezing and particle entanglement is found in both the $n = 2$ Mott and superfluid phases. In the $n = 2$ Mott state we find maximally entangled particles. Introducing a nonzero θ reduces this to a partially entangled state, and thus decreases particle correlations.

We compared the results of the squeezing parameter (6.21) with those of the concurrence (6.24) for each type of interaction and lattice configuration. They are in complete agreement in demonstrating the presence or absence of entanglement for the different phases.

For the system under consideration, we have investigated the potential ground states and the corresponding quantum correlations via examining entanglement/squeezing properties. Depending on the interaction parameters of the system, abrupt changes may occur if one considers the behavior of entanglement properties. One can introduce symmetry breaking perturbations to the Hamiltonian (6.19) to remove the degeneracy present in the various ground states. This can be done via including magnetic fields and Raman pulses with which adjustments to the ground state populations in any particular spin components can be made [147]. As a specific example, generation of a coherent superposition of degenerate states (in this case Zeeman sublevels $M_F = \pm 1$) by stimulated Raman adiabatic passage scheme is demonstrated experimentally in Ref. [148].

Bibliography

[1] A. Einstein, B. Podolsky and N. Rosen, Phys. Rev. **47**, 777 (1935).

[2] E. Schrödinger, Naturwissenschaften **23**, 807; 823; 844 (1935).

[3] J. S. Bell, Physics **1**, 195 (1964)

[4] A. Aspect, J. Dalibard and G. Roger, Phys. Rev. Lett. **49**, 1804 (1982).

[5] A. K. Ekert, Phys. Rev. Lett. **67**, 661 (1991).

[6] C. H. Bennett and S. J. Wiesner, Phys. Rev. Lett. **69**, 2881 (1992).

[7] C. H. Bennett, G. Brassard, C. Crépeau, R. Jozsa, A. Peres and W. K. Wootters, Phys. Rev. Lett. **70**, 1895 (1993).

[8] P. W. Shor, in *Proceedings of the 35th Annual Symposium on the Foundations of Computer Science*, Ed. by S. Goldwasser (IEEE Computer Society, Los Alamitos, 1994).

[9] P. W. Shor, SIAM J. Comput. **26**, 1484 (1997).

[10] L. K. Grover, in *Proceedings of the 28th Annual ACM Symposium on the Theory of Computation*, (ACM Press, New York, 1996).

[11] L. K. Grover, Phys. Rev Lett. **79**, 325 (1997).

[12] J. Schlientz and G. Mahler, Phys. Rev. A **52**, 4396 (1995).

[13] C. H. Bennett, G. Brassard, S. Popescu, B. Schumacher, J. Smolin and W. K. Wootters, Phys. Rev. Lett. **76**, 722 (1996).

[14] C. H. Bennett, H. Bernstein, S. Popescu and B. Schumacher, Phys. Rev. A **53**, 2046 (1996).

[15] C. H. Bennett, D. DiVincenzo, J. Smolin and W. K. Wootters, Phys. Rev. A **54**, 3824 (1996).

[16] A. A. Klyachko, E-print arXiv quant-ph/0206012.

[17] A. A. Klyachko and A. S. Shumovsky, J. Opt. B: Quant. Semiclas. Opt. **5**, S322 (2003).

[18] A. A. Klyachko and A. S. Shumovsky, J. Opt. B: Quant. Semiclas. Opt. **6**, S29 (2004).

[19] A. A. Klyachko and A. S. Shumovsky, J. Phys: Conf. Series **36**, 87 (2006).

[20] M. A. Nielsen and L. L. Chuang, in *Quantum Computation and Quantum Information*, (Cambridge University Press, Cambridge, 2000).

[21] M. B. Plenio and S. Virmani, Quant. Inf. Comp. **7**, 1 (2007).

[22] R. F. Werner, Phys. Rev. A **40**, 4277 (1989).

[23] V. Vedral, M. B. Plenio, M. A. Rippin and P. L. Knight, Phys. Rev. Lett. **78**, 2275 (1997).

[24] M. B. Plenio and V. Vedral, Contemp. Phys. **39**, 431 (1998).

[25] V. Vedral and M. B. Plenio, Phys. Rev. A **57**, 1619 (1998).

[26] J. von Neumann, Mathematische Grundlagen der Quantenmechanik, Number XXXVIII in *Die Grundlehren der Mathematischen Wissenschaften in Einzeldarstellungen*, (Springer, 1932).

[27] S. Popescu and D. Rohrlich, Phys. Rev. A **56**, R3319 (1997).

[28] G. Vidal, J. Mod. Opt. **47**, 355 (2000).

[29] M. Horodecki, P. Horodecki and R. Horodecki, Phys. Rev. Lett. **84**, 2014 (2000).

[30] M. J. Donald, M. Horodecki and O. Rudolph, J. Math. Phys. **43**, 4252 (2002).

[31] E. M. Rains, E-print arXiv quant-ph/9707002.

[32] K. Audenaert, M. B. Plenio and J. Eisert, Phys. Rev. Lett. **90**, 027901 (2003).

[33] P. M. Hayden, M. Horodecki and B. Terhal, J. Phys. A: Math. Gen. **34**, 6891 (2001).

[34] K. Audenaert, F. Verstraete and B. De Moor, Phys. Rev. A **64**, 052304 (2001).

[35] J. Eisert, T. Felbinger, P. Papadopoulos, M. B. Plenio and M. Wilkens, Phys. Rev. Lett. **84**, 1611 (2000).

[36] B. Terhal and K. G. H. Vollbrecht, Phys. Rev. Lett. **85**, 2625 (2000).

[37] K. G. H. Vollbrecht and R. F. Werner, Phys. Rev. A **64**, 062307 (2001).

[38] S. Hill and W. K. Wootters, Phys. Rev. Lett. **78**, 5022 (1997).

[39] W. K. Wootters, Phys. Rev. Lett. **80**, 2245 (1998).

[40] W. K. Wootters, Quant. Inf. Comp. **1**, 27 (2001).

[41] D. Bures, Trans. Am. Math. Soc. **135**, 199 (1969).

[42] M. Hübner, Phys. Lett. A **163**, 239 (1992).

[43] A. Uhlmann, Rep. Math. Phys. **9**, 273 (1976).

[44] J. Eisert, K. Audenaert and M. B. Plenio, J. Phys. A: Math. Gen. **36**, 5605 (2003).

[45] A. Peres, Phys. Rev. Lett. **77**, 1413 (1996).

[46] M. Horodecki, P. Horodecki and R. Horodecki, Phys. Lett. A **223**, 1 (1996).

[47] K. Zyczkowski, P. Horodecki, A. Sanpera and M. Lewenstein, Phys. Rev. A **58**, 883 (1998).

[48] J. Eisert and M. B. Plenio, J. Mod. Opt. **46**, 145 (1999).

[49] M. B. Plenio, Phys. Rev. Lett. **95**, 090503 (2005).

[50] M. Christandl and A. Winter, J. Math. Phys. **45**, 829 (2004).

[51] F. G. S. L. Brandão and R. O. Vianna, Phys. Rev. Lett. **93**, 220503 (2004).

[52] K. Horodecki, M. Horodecki, P. Horodecki and J. Oppenheim, Phys. Rev. Lett. **94**, 160502 (2005).

[53] E. M. Rains, IEEE Trans. Inf. Theory **47**, 2921 (2001).

[54] A. Harrow and M. A. Nielsen, Phys. Rev. A **68**, 012308 (2003).

[55] O. Cohen, Phys. Rev. Lett. **80**, 2493 (1998).

[56] D. DiVincenzo, C. Fuchs, H. Mabuchi, J. Smolin, A. Thapliyal and A. Uhlmann, in *Quantum Computing and Quantum Communications: First NASA International Conference*, Ed. by C. P. Williams (Springer-Verlag, 1999).

[57] F. Verstraete, M. Popp and J. I. Cirac, Phys. Rev. Lett. **92**, 027901 (2004).

[58] M. A. Nielsen, J. Phys. A: Math. Gen. **34**, 6987 (2001).

[59] V. Coffman, J. Kundu and W. K. Wootters, Phys. Rev. A **61**, 052306 (2000).

[60] T. J. Osborne and F. Verstraete, Phys. Rev. Lett. **96**, 220503 (2006).

[61] M. A. Can, A. A. Klyachko and A. S. Shumovsky, Phys. Rev. A **66**, 022111 (2002).

[62] J. S. Bell, Rev. Mod. Phys. **38**, 447 (1966).

[63] J. von Neumann, in *Mathematical Foundations of Quantum Mechanics*, (Princeton University Press, Princeton, 1996).

[64] G. C. Wick, A. S. Wightman and E. P. Wigner, Phys. Rev. **88**, 101 (1952).

[65] E. P. Wigner, in *Gruppentheorie und ihre Anwendungen auf die Quantummechanik der Atomspectren*, (Vieweg, Braunschweig, 1931).

[66] E. P. Wigner, Ann. Math. Phys. **40**, 149 (1939).

[67] R. Hermann, in *Lie Groups for Physicists*, (Benjamin, New York, 1966).

[68] G. G. Emch, in *Mathematical and Conceptual Foundations of 20th Century Physics*, (North Holland, Amsterdam, 1984).

[69] A. L. Onishchik and E. B. Vinberg, in *Lie groups and Lie algebras III, Encyclopedia of Math. Science*, (Springer, Berlin, 1994).

[70] R. Delbourgo and J. R. Fox, J. Phys. A **10**, L233 (1977).

[71] A. Perelomov, in *Generalized coherent states and their applications*, (Springer, New York, 1986).

[72] H. Barnum, E. Knill, G. Ortiz and L. Viola, Phys. Rev. A **68**, 032308 (2003).

[73] A. A. Klyachko, B. Öztop and A. S. Shumovsky, Appl. Phys. Lett. **88**, 124102 (2006).

[74] A. A. Klyachko, B. Öztop and A. S. Shumovsky, Phys. Rev. A **75**, 032315 (2007).

[75] F. Mintert and A. Buchleitner, Phys. Rev. A **72**, 012336 (2005).

[76] P. Rungta, V. Bužek, C.M. Caves, M. Hillery and G.J. Milburn, Phys. Rev. A **64**, 042315 (2001).

[77] J. M. G. Sancho and S. F. Huelga, Phys. Rev. A **61**, 042303 (2000).

[78] A. F. Abouraddy, B. E. A. Saleh, A. V. Sergienko and M. C. Teich, Phys. Rev. A **64**, 050101(R) (2001).

[79] J. Řeháček, B. G. Englert and D. Kaszlikowski, Phys. Rev. A **70**, 052321 (2004).

[80] E. Schrödinger, Proc. Prussian Acad. Sci. **19**, 296 (1930).

[81] V. V. Dodonov, E. V. Kurmushev, and V. I. Man'ko, Phys. Lett. A **79**, 150 (1980).

[82] A. Miyake, Phys. Rev. A **67**, 012108 (2003).

[83] W. Dür, G. Vidal and J. I. Cirac, Phys. Rev. A **62**, 062314 (2000).

[84] F. Verstraete, J. Dehaene, B. De Moor and H. Verschelde, Phys. Rev A **65**, 052112 (2002).

[85] A. Ać in, D. Bruß, M. Lewenstein and A. Sanpera, Phys. Rev. Lett. **87**, 040401 (2001).

[86] W. J. Munro, D. F. V. James, A. G. White and P. G. Kwiat, Phys. Rev. A **64**, 030302(R) (2001).

[87] F. Mintert, M. Kuś and A. Buchleitner, Phys. Rev. Lett. **92**, 167902 (2004).

[88] M. H. Anderson, J. R. Ensher, M. R. Matthews, C. E. Wieman and E. A. Cornell, Science **269**, 198 (1995).

[89] C. C. Bradley, C. A. Sackett, J. J. Tollett and R. G. Hulet, Phys. Rev. Lett. **75**, 1687 (1995).

[90] K. B. Davis, M. O. Mewes, M. R. Andrews, N. J. van Druten, D. S. Durfee, D. M. Kurn and W. Ketterle, Phys. Rev. Lett. **75**, 3969 (1995).

[91] M. R. Andrews, C. G. Townsend, H. J. Miesner, D. S. Durfee, D. M. Kurn and W. Ketterle, Science **275**, 637 (1997).

[92] I. Bloch, T. W. Hänsch and T. Esslinger, Nature **403**, 166 (2000).

[93] J. R. Abo-Shaeer, C. Raman, J. M. Vogels and W. Ketterle, Science **292**, 476 (2001).

[94] K. W. Madison, F. Chevy, W. Wohlleben and J. Dalibard, Phys. Rev. Lett. **84** 806 (2000).

[95] M. Greiner, C. A. Regal and D. S. Jin, Nature **426**, 537 (2003).

[96] S. Jochim, M. Bartenstein, A. Altmeyer, G. Hendl, S. Riedl, C. Chin, J. Hecker-Denschlag and R. Grimm, Science **302**, 2101 (2003).

[97] M. W. Zwierlein, C. A. Stan, C. H. Schunk, S. M. F. Raupach, S. Gupta, Z. Hadzibabic and W. Ketterle, Phys. Rev. Lett. **91**, 250401 (2003).

[98] E. P. Gross, Il Nuovo Cimento **20**, 454 (1961).

[99] L. P. Pitaevskii, Sov. Phys. JETP **13**, 451 (1961).

[100] N. Bogoliubov, J. Phys. **11**, 23 (1947).

[101] D. Jaksch, C. Bruder, J. I. Cirac, C. W. Gardiner and P. Zoller, Phys. Rev. Lett. **81**, 3108 (1998).

[102] M. Greiner, O. Mandel, T. Esslinger, T. W. Hänsch and I. Bloch, Nature **415**, 39 (2002).

[103] M. P. A. Fisher, P. B. Weichman, G. Grinstein and D. S. Fisher, Phys. Rev. B **40**, 546 (1989).

[104] R. B. Diener, Q. Zhou, H. Zhai and T. -L. Ho, Phys. Rev. Lett. **98**, 180404 (2007).

[105] G. -H. Chen and Y. -S. Wu, Phys. Rev. A **67**, 013606 (2003).

[106] J. -M. Hou and M. -L. Ge, Phys. Rev. A **67**, 063607 (2003).

[107] K. V. Krutitsky and R. Graham, Phys. Rev. Lett. **91**, 240406 (2003).

[108] K. V. Krutitsky and R. Graham, Phys. Rev. A **70**, 063610 (2004).

[109] L. Amico, R. Fazio, A. Osterloh and V. Vedral, Rev. Mod. Phys. **80**, 517 (2008).

[110] M. Kitagawa and M. Ueda, Phys. Rev. A **47**, 5138 (1993).

[111] A. Sørensen, L. -M. Duan, J. I. Cirac and P. Zoller, Nature **409**, 63 (2001).

[112] K. Helmerson and L. You, Phys. Rev. Lett. **87**, 170402 (2001).

[113] M. Zhang, K. Helmerson and L. You, Phys. Rev. A **68**, 043622 (2003).

[114] S. Yi and H. Pu, Phys. Rev. A **73**, 023602 (2006).

[115] A. Sørensen and K. Mølmer, Phys. Rev. Lett. **83**, 2274 (1999).

[116] A. Einstein, Sitzungber. K. Preuss. Akad. Wiss. **1925**, 3 (1925).

[117] S. N. Bose, Zeitschrift für Physik **26**, 178 (1924).

[118] F. London, Phys. Rev. **54**, 947 (1938).

[119] F. London, Nature **141**, 643 (1938).

[120] O. Penrose and L. Onsager, Phys. Rev. **104**, 576 (1956).

[121] J. D. Jackson, in *Classical Electrodynamics*, (Wiley, New York, 1962).

[122] C. J. Pethick and H. Smith, in *Bose-Einstein Condensation in Dilute Gases*, (Cambridge University Press, Cambridge, 2002).

[123] D. J. Griffiths, in *Introduction to Electrodynamics*, (Prentice-Hall, New Jersey, 1999).

[124] M. Greiner, *Ph.D. Thesis*, `http://www.physics.harvard.edu/~greiner/publications/PhD_greiner.pdf`.

[125] A. E. Siegman, in *Lasers*, (University Science Books, Sausalito, 1986).

[126] N. W. Ashcroft and N. D. Mermin, in *Solid State Physics*, (Saunders College Publishing, Fort Worth, 1976).

[127] P. Jessen and I. H. Deutsch, Adv. At. Mol. Opt. Phys. **37**, 95 (1996).

[128] G. Brennen, C. Caves, P. Jessen and I. H. Deutsch, Phys. Rev. Lett. **82**, 1060 (1999).

[129] D. Jaksch, H. J. Briegel, J. I. Cirac, C. W. Gardiner and P. Zoller, Phys. Rev. Lett. **82**, 1975 (1999).

[130] O. Mandel, M. Greiner, A. Widera, T. Rom, T. W. Hänsch and I. Bloch, Phys. Rev. Lett **91**, 010407 (2003).

[131] G. H. Wannier, Phys. Rev. **52**, 191 (1937).

[132] I. Bloch, J. Dalibard and W. Zwerger, Rev. Mod. Phys. **80**, 885 (2008).

[133] K. Sheshadri, H. R. Krishnamurthy, R. Pandit and T. V. Ramakrishnan, Europhys. Lett. **22**, 257 (1993).

[134] W. Zwerger, J. Opt. B: Quant. Semiclass. Opt. **5**, S9 (2003).

[135] K. V. Krutitsky, M. Timmer and R. Graham, Phys. Rev. A **71**, 033623 (2005).

[136] T. -L. Ho, Phys. Rev. Lett. **81**, 742 (1998).

[137] B. Öztop, M. Ö. Oktel, Ö. E. Müstecaplıoğlu and L. You, J. Phys. B: At. Mol. Opt. Phys. **42**, 145505 (2009).

[138] H. L. Lipkin, N. Meshkov and A. J. Glick, Nucl. Phys. **62**, 188 (1965).

[139] R. G. Unanyan and M. Fleischhauer, Phys. Rev. Lett. **90**, 133601 (2003).

[140] K. Helmerson and L. You, Phys. Rev. Lett. **87**, 170402 (2001).

[141] M. Zhang, K. Helmerson and L. You, Phys. Rev. A **68**, 043622 (2003).

[142] X. G. Wang and B. C. Sanders, Phys. Rev. A **68**, 012101 (2003).

[143] A. R. Usha Devi, X. G. Wang and B. C. Sanders, Quant. Inf. Proc. **2**, 207 (2003).

[144] H. M. Wiseman and J. A. Vaccaro, Phys. Rev. Lett. **91**, 097902 (2003).

[145] A. Micheli, D. Jaksch, J. I. Cirac and P. Zoller, Phys. Rev. A **67**, 013607 (2003).

[146] L. -M. Duan, J. I. Cirac and P. Zoller, Phys. Rev. A **65**, 033619 (2002).

[147] N. V. Vitanov, T. Halfmann, B. W. Shore and K. Bergmann, Annu. Rev. Phys. Chem. **52**, 763 (2001).

[148] F. Vewinger, M. Heinz, R. Garcia Fernandez, N. V. Vitanov and K. Bergmann, Phys. Rev. Lett. **91**, 213001 (2003).

Appendix A

Calculation of entanglement measure $\mu(\psi)$

Here we calculate the total variance $\mathbb{V}(\psi)$ and the entanglement measure $\mu(\psi)$.

Let $\mathrm{Herm}(\mathcal{H})$ be space of all Hermitian operators acting in Hilbert space $\mathcal{H}$ with trace metric $\mathrm{tr}_{\mathcal{H}}(\mathrm{XY})$. For *simple algebra* $\mathcal{L}$ restriction of the trace metric onto $\mathcal{L}$ is proportional to the Cartan-Killing form

$$\mathrm{tr}_{\mathcal{H}}(\mathrm{XY}) = \mathrm{D}_{\mathcal{H}} \cdot (\mathrm{X},\mathrm{Y})_{\mathrm{K}}, \quad \mathrm{X},\mathrm{Y} \in \mathcal{L}$$

with the coefficient $D_{\mathcal{H}}$ known as *Dynkin index* [69]. Consider now orthogonal projection $\rho_{\mathcal{L}}$ of $\rho := |\psi\rangle\langle\psi| \in \mathrm{Herm}(\mathcal{H})$ into subalgebra $\mathcal{L} \subset \mathrm{Herm}(\mathcal{H})$, so that $\mathrm{tr}_{\mathcal{H}}(\rho \mathrm{X}) = \mathrm{tr}_{\mathcal{H}}(\rho_{\mathcal{L}}\mathrm{X})$, $\forall X \in \mathcal{L}$. The projection $\rho_{\mathcal{L}}$ is closely related to the mean operator (3.4)

$$\begin{aligned} X_\psi &= \sum_\alpha \mathrm{tr}_{\mathcal{H}}(\rho \mathrm{X}_\alpha)\mathrm{X}_\alpha = \sum_\alpha \mathrm{tr}_{\mathcal{H}}(\rho_{\mathcal{L}}\mathrm{X}_\alpha)\mathrm{X}_\alpha \\ &= D_{\mathcal{H}} \sum_\alpha (\rho_{\mathcal{L}}, X_\alpha)_K X_\alpha = D_{\mathcal{H}} \cdot \rho_{\mathcal{L}}. \end{aligned}$$

Therefore

$$\langle\psi|X_\psi|\psi\rangle = \mathrm{tr}_{\mathcal{H}}(\rho \mathrm{X}_\psi) = \mathrm{tr}_{\mathcal{H}}(\rho_{\mathcal{L}}\mathrm{X}_\psi) = \mathrm{D}_{\mathcal{H}}\mathrm{tr}_{\mathcal{H}}(\rho_{\mathcal{L}}^2)$$

and the total variance (3.2) can be written in the form

$$\mathbb{V}(\psi) = C_{\mathcal{H}} - \langle\psi|X_\psi|\psi\rangle = C_{\mathcal{H}} - D_{\mathcal{H}} \cdot \mathrm{tr}_{\mathcal{H}}(\rho_{\mathcal{L}}^2). \tag{A.1}$$

For simple algebra the Casimir $C_{\mathcal{H}}$ and Dynkin index $D_{\mathcal{H}}$ are given by equations

$$C_{\mathcal{H}} = (\lambda, \lambda + 2\delta), \quad D_{\mathcal{H}} = \frac{\dim \mathcal{H}}{\dim \mathcal{L}}(\lambda, \lambda + 2\delta), \tag{A.2}$$

where λ denotes the highest weight of irreducible representation $\mathcal{H}$ and 2δ is the sum of positive roots of $\mathcal{L}$. For example, for full algebra of traceless Hermitian operators $\mathcal{L} = \mathfrak{su}(\mathcal{H})$

we have

$$C_{\mathcal{H}} = \dim \mathcal{H} - \frac{1}{\dim \mathcal{H}}, \quad D_{\mathcal{H}} = 1. \tag{A.3}$$

In general, algebra $\mathcal{L}$ splits into simple components $\mathcal{L} = \bigoplus_A \mathcal{L}_A$ and its irreducible representation $\mathcal{H}$ into tensor product $\mathcal{H} = \bigotimes_A \mathcal{H}_A$. In this case equation (A.1) should be modified as follows

$$\mathbb{V}(\psi) = \sum_A \left[C_{\mathcal{H}_A} - D_{\mathcal{H}_A} \cdot \mathrm{tr}_{\mathcal{H}_\mathrm{A}}(\nu_\mathrm{A}^2 \rho_{\mathcal{L}_\mathrm{A}}^2) \right], \tag{A.4}$$

where $\nu_A = \dim \mathcal{H} / \dim \mathcal{H}_A$.

In quantum information setting $\mathcal{L}_A$ is the full algebra of traceless Hermitian operators $X_A : \mathcal{H}_A \to \mathcal{H}_A$. In this case everything can be done explicitly.

By definition of reduced states ρ_A we have

$$\mathrm{tr}_{\mathcal{H}}(\rho \mathrm{X_A}) = \mathrm{tr}_{\mathcal{H}_\mathrm{A}}(\rho_\mathrm{A} \mathrm{X_A}) = \nu_\mathrm{A}^{-1} \mathrm{tr}_{\mathcal{H}}(\rho_\mathrm{A} \mathrm{X_A}).$$

Comparing this with equation $\mathrm{tr}_{\mathcal{H}}(\rho \mathrm{X_A}) = \mathrm{tr}_{\mathcal{H}}(\rho_{\mathcal{L}_\mathrm{A}} \mathrm{X_A})$, $\forall X_A \in \mathcal{L}_A$ characterizing the projection $\rho_{\mathcal{L}_A} \in \mathcal{L}_A$ we infer

$$\rho_{\mathcal{L}_A} = \nu_A^{-1} \rho_A^0,$$

where $\rho_A^0 = \rho_A - (1/\dim \mathcal{H}_A)\mathbf{I}$ is traceless part of ρ_A. This allows to calculate the trace

$$\mathrm{tr}_{\mathcal{H}_\mathrm{A}}(\rho_{\mathcal{L}_\mathrm{A}}^2) = \nu^{-2} \left[\mathrm{tr}_{\mathcal{H}_\mathrm{A}}(\rho_\mathrm{A}^2) - \frac{1}{\dim \mathcal{H}_\mathrm{A}} \right].$$

Plugging this into equation (A.4) and using (A.3) we finally get

$$\mathbb{V}(\psi) = \sum_A \left[\dim \mathcal{H}_A - \mathrm{tr}_{\mathcal{H}_\mathrm{A}}(\rho_\mathrm{A}^2) \right]. \tag{A.5}$$

As an example, consider completely entangled state ψ for which $\rho_A = (1/\dim \mathcal{H}_A)\mathbf{I}$. This gives the maximum of the total variance

$$\mathbb{V}_{\max} = \mathbb{V}_{\mathrm{ent}} = \sum_A \left(\dim \mathcal{H}_A - \frac{1}{\dim \mathcal{H}_A} \right).$$

The minimum of the total variance is attained for coherent (=separable) state ψ, for which reduced states ρ_A are pure. Hence

$$\mathbb{V}_{\min} = \mathbb{V}_{\mathrm{coh}} = \sum_A (\dim \mathcal{H}_A - 1).$$

Combining these equations we can write down our measure of entanglement (7.1) explicitly for a multicomponent system $\mathcal{H} = \bigotimes_A \mathcal{H}_A$ of arbitrary format

$$\mu^2(\psi) = \frac{\sum_A [1 - \mathrm{tr}(\rho_\mathrm{A}^2)]}{\sum_A \left(1 - \frac{1}{\dim \mathcal{H}_A}\right)}. \tag{A.6}$$

Appendix B

3-tangle

For an arbitrary normalized state of three qubits

$$|\psi\rangle = \sum_{\ell,m,n=0}^{1} \psi_{\ell mn}|\ell mn\rangle$$

the 3-tangle has the form [59, 82]

$$\begin{aligned}\tau(\psi) &= 4|\psi_{000}^2\psi_{111}^2 + \psi_{001}^2\psi_{110}^2 + \psi_{010}^2\psi_{101}^2 + \psi_{100}^2\psi_{011}^2 - 2(\psi_{000}\psi_{001}\psi_{110}\psi_{111} \\ &+ \psi_{000}\psi_{010}\psi_{101}\psi_{111} + \psi_{000}\psi_{100}\psi_{011}\psi_{111} + \psi_{001}\psi_{010}\psi_{101}\psi_{110} + \psi_{001}\psi_{100}\psi_{011}\psi_{110} \\ &+ \psi_{010}\psi_{100}\psi_{011}\psi_{101}) + 4(\psi_{000}\psi_{011}\psi_{101}\psi_{110} + \psi_{001}\psi_{010}\psi_{100}\psi_{111})|.\end{aligned}$$

Appendix C

Completely entangled four-qubit states

A general pure state of four qubits can be written in the form

$$|\psi\rangle = \sum_{k,\ell,m,n=0}^{1} \psi_{k\ell mn}|k,\ell,m,n\rangle \tag{C.1}$$

with the normalization condition $\sum_{k,\ell,m,n=0}^{1} |\psi_{k\ell mn}|^2 = 1$. Thus, there are 31 real parameters, defining any state. Condition (3.9) gives twelve equations for the coefficients $\psi_{k\ell mn}$ in (C.1)

$$\begin{aligned}
\langle\sigma_x^{(A)}\rangle &= (\psi^*_{0000}\psi_{1000} + \psi^*_{0100}\psi_{1100} + \psi^*_{0010}\psi_{1010} + \psi^*_{0001}\psi_{1001} + \psi^*_{0110}\psi_{1110} + \psi^*_{0101}\psi_{1101} \\
&\quad + \psi^*_{0011}\psi_{1011} + \psi^*_{0111}\psi_{1111}) + (c.c.) = 0, \\
\langle\sigma_x^{(B)}\rangle &= (\psi^*_{0000}\psi_{0100} + \psi^*_{1000}\psi_{1100} + \psi^*_{0010}\psi_{0110} + \psi^*_{0001}\psi_{0101} + \psi^*_{1010}\psi_{1110} + \psi^*_{1001}\psi_{1101} \\
&\quad + \psi^*_{0011}\psi_{0111} + \psi^*_{1011}\psi_{1111}) + (c.c.) = 0, \\
\langle\sigma_x^{(C)}\rangle &= (\psi^*_{0000}\psi_{0010} + \psi^*_{1000}\psi_{1010} + \psi^*_{0100}\psi_{0110} + \psi^*_{0001}\psi_{0011} + \psi^*_{1100}\psi_{1110} + \psi^*_{1001}\psi_{1011} \\
&\quad + \psi^*_{0101}\psi_{0111} + \psi^*_{1101}\psi_{1111}) + (c.c.) = 0, \\
\langle\sigma_x^{(D)}\rangle &= (\psi^*_{0000}\psi_{0001} + \psi^*_{1000}\psi_{1001} + \psi^*_{0100}\psi_{0101} + \psi^*_{0010}\psi_{0011} + \psi^*_{1100}\psi_{1101} + \psi^*_{1010}\psi_{1011} \\
&\quad + \psi^*_{0110}\psi_{0111} + \psi^*_{1110}\psi_{1111}) + (c.c.) = 0, \\
\langle\sigma_y^{(A)}\rangle &= i(\psi^*_{1000}\psi_{0000} + \psi^*_{1100}\psi_{0100} + \psi^*_{1010}\psi_{0010} + \psi^*_{1001}\psi_{0001} + \psi^*_{1110}\psi_{0110} + \psi^*_{1101}\psi_{0101}
\end{aligned}$$

$$
\begin{aligned}
& +\psi^*_{1011}\psi_{0011} + \psi^*_{1111}\psi_{0111}) + (c.c.) = 0, \\
\langle\sigma_y^{(B)}\rangle &= i(\psi^*_{0100}\psi_{0000} + \psi^*_{1100}\psi_{1000} + \psi^*_{0110}\psi_{0010} + \psi^*_{0101}\psi_{0001} + \psi^*_{1110}\psi_{1010} + \psi^*_{1101}\psi_{1001} \\
& +\psi^*_{0111}\psi_{0011} + \psi^*_{1111}\psi_{1011}) + (c.c.) = 0, \\
\langle\sigma_y^{(C)}\rangle &= i(\psi^*_{0010}\psi_{0000} + \psi^*_{1010}\psi_{1000} + \psi^*_{0110}\psi_{0100} + \psi^*_{0011}\psi_{0001} + \psi^*_{1110}\psi_{1100} + \psi^*_{1011}\psi_{1001} \\
& +\psi^*_{0111}\psi_{0101} + \psi^*_{1111}\psi_{1101}) + (c.c.) = 0, \\
\langle\sigma_y^{(D)}\rangle &= i(\psi^*_{0001}\psi_{0000} + \psi^*_{1001}\psi_{1000} + \psi^*_{0101}\psi_{0100} + \psi^*_{0011}\psi_{0010} + \psi^*_{1101}\psi_{1100} + \psi^*_{1011}\psi_{1010} \\
& +\psi^*_{0111}\psi_{0110} + \psi^*_{1111}\psi_{1110}) + (c.c.) = 0, \\
\langle\sigma_z^{(A)}\rangle &= |\psi_{0000}|^2 - |\psi_{1000}|^2 + |\psi_{0100}|^2 + |\psi_{0010}|^2 + |\psi_{0001}|^2 - |\psi_{1100}|^2 - |\psi_{1010}|^2 \\
& -|\psi_{1001}|^2 + |\psi_{0110}|^2 + |\psi_{0101}|^2 + |\psi_{0011}|^2 - |\psi_{1011}|^2 - |\psi_{1101}|^2 - |\psi_{1110}|^2 \\
& +|\psi_{0111}|^2 - |\psi_{1111}|^2 = 0, \\
\langle\sigma_z^{(B)}\rangle &= |\psi_{0000}|^2 + |\psi_{1000}|^2 - |\psi_{0100}|^2 + |\psi_{0010}|^2 + |\psi_{0001}|^2 - |\psi_{1100}|^2 + |\psi_{1010}|^2 \\
& +|\psi_{1001}|^2 - |\psi_{0110}|^2 - |\psi_{0101}|^2 + |\psi_{0011}|^2 + |\psi_{1011}|^2 - |\psi_{1101}|^2 - |\psi_{1110}|^2 \\
& -|\psi_{0111}|^2 - |\psi_{1111}|^2 = 0, \\
\langle\sigma_z^{(C)}\rangle &= |\psi_{0000}|^2 + |\psi_{1000}|^2 + |\psi_{0100}|^2 - |\psi_{0010}|^2 + |\psi_{0001}|^2 + |\psi_{1100}|^2 - |\psi_{1010}|^2 \\
& +|\psi_{1001}|^2 - |\psi_{0110}|^2 + |\psi_{0101}|^2 - |\psi_{0011}|^2 - |\psi_{1011}|^2 + |\psi_{1101}|^2 - |\psi_{1110}|^2 \\
& -|\psi_{0111}|^2 - |\psi_{1111}|^2 = 0, \\
\langle\sigma_z^{(D)}\rangle &= |\psi_{0000}|^2 + |\psi_{1000}|^2 + |\psi_{0100}|^2 + |\psi_{0010}|^2 - |\psi_{0001}|^2 + |\psi_{1100}|^2 + |\psi_{1010}|^2 \\
& -|\psi_{1001}|^2 + |\psi_{0110}|^2 - |\psi_{0101}|^2 - |\psi_{0011}|^2 - |\psi_{1011}|^2 - |\psi_{1101}|^2 + |\psi_{1110}|^2 \\
& -|\psi_{0111}|^2 - |\psi_{1111}|^2 = 0,
\end{aligned}
$$

where $\langle\sigma_\alpha^{(i)}\rangle = \langle\psi_{\rm ent}|\sigma_\alpha^{(i)}|\psi_{\rm ent}\rangle$ and *c.c.* denotes complex conjugate. Thus, there are infinitely many completely entangled states and the state (3.26) at $|x| = 1/\sqrt{2}$ is among them.